UNIVERSITY OF NAPLES FEDERICO II

School of Polytechnic and Basic Sciences

Department of Chemical, Materials and Industrial Production Engineering

XXXVI PhD Programme in
Industrial Products and Processes Engineering

Design and development of furan-based epoxy resins and their applications as advanced materials

PhD COURSE COORDINATOR
Ch.mo Prof. Andrea D'Anna

PhD CANDIDATE
Noemi Faggio

PhD SUPERVISOR
Ch.mo Prof. Veronica Ambrogi
CO-SUPERVISORS
Dr. Gennaro Gentile
Dr. Pierfrancesco Cerruti

Table of contents

Abstract

Nowadays, environmental concerns on the use of polymeric materials, related to a plastic waste reduction, lead to a responsible use of these materials and a forecast on the end-life workpieces disposal. Moreover, in the perspective of environmental impact reduction, the use of non-renewable materials is highly discouraged. For this reason, the scientific and industrial community is focused on the development of new bio-based polymers.

In this framework, this research work is aimed to investigate the products and the potential applications of different renewable furan based epoxy resins cured with bio-based hardeners. First, a deep discussion on the state of art, regarding the current synthesis of bio-based epoxy monomers and curing agents, is proposed. Then the synthesis of a new furan based epoxy monomer, identified with name 2,5-bis[oxiran-2-ylmethoxy)methyl]furan (BOMF), provided by the extraction from polysaccharides is carried out. It was then cross-linked through the appropriate choice of green crosslinking agents, the first case study regards the use of maleic anhydride (MA) as curing agent in order to generate a resin with enhanced adhesive properties for carbon fiber reinforced plastic joints. The same combination is investigated for nanofibers production through electrospinning with the aim to assembly bilayer filters for fluids. In the second case study, another curing agent, isophorone diamine (IPD), was used to produce nanocomposites with different contents of carbon nanotubes, which have the objective to improve the electro-thermal properties of nonconductive commercial fabrics. The discussion on the choice of curing agents is crucial regarding the environmental impact of these resins. Maleic anhydride (MA), which is not impacting on the environment and isophorone diamine (IPD) which gives excellent mechanical properties and reaction kinetics, has been selected.

The epoxy resins obtained have been characterized from the thermal, mechanical, rheological and morphological point of view and used in different fields of application such as adhesives for composites, protective nanofibers for commercial membranes, nanocomposites and conductive and thermoresponsive textiles.

The various tested epoxy and hardener combinations has proven to preserve an high renewable content. In comparison with a commercial epoxy resin, the mechanical properties of the system BOMF/MA are lower, especially which regards tensile strength and stiffness, but there was obtain an exceptional improvement in to use as adhesive for composites due to more flexible behavior. The same system was used to obtain electrospun nanofibers and they exhibited uniformity, lack of defects and high resistance to chloroform washing, which made them very suitable for the employ in bilayer membranes for fluid filtering. The latter system, BOMF/IPD in combination with carbon nanotubes, has proven to have outstanding and repetable electrothermal properties to be used in fabric coating with the aim to potentially introduce this production in biomedical devices.

This thesis work reports the following structure:

In Chapter 1 there will be an introduction on epoxy resins and an exposition of the main problems related to the use of epoxy monomers of petrochemical derivation. It was reported the state of the art on bio-based epoxy monomers, specifically derived from vegetable oils, lignocellulosic compounds and polysaccharides with a focus on furan-based ones; followed by a brief review on bio-based curing agents, specifically carboxylic acids, anhydrides, amino acids and amines.

Chapter 2 shows all the materials, the procedures and characterization techniques used.

In Chapter 3 are reported synthesis, formulation, characterization and application of the BOMF/MA system. The characterized system has been used as adhesive for carbon fiber composites (CFRP). Thermal, mechanical and adhesive properties of polymerized samples have been evaluated and compared with those of a BPA based system. The results have shown that BOMF/MA resin has outstanding adhesive properties against carbon fiber reinforced composite (CFRP) joints, exceeding the BPA-based counterpart by 3 times. This result is due to the strong hydrogen bonding interaction of the resin with the epoxy substrate CFRP, mediated by the hydroxyl groups formed on the polymerization BOMF/MA.

In Chapter 4 the same system has been used as a material for the realization of epoxy nanofibers obtained by electrospinning for the realization of protective layers of membranes in application such as fluid filters. Epoxy nanofibers were obtained by the core-shell method, using PLA as the 'sacrificial polymer'.

Chapter 5, will show the realization of a different epoxy system BOMF/IPD. The resin was characterized thermally and mechanically and DSC analysis showed T_g performance at 70 °C, This has allowed to identify the most performant epoxy/curing agent formulation for the realization of conductive nanocomposites by adding suitable quantities of carbon nanotubes (CNT). CNT/epoxy nanocomposites were then used to impregnate a natural cotton fabric, used as thermo-responsive wearable textiles. The temperatures achieved (around 37 °C) demonstrate the high potential for use as wearable textiles and for biomedical devices, being comfortable temperatures for humans.

In the last section are summarized the most remarkable results and are depicted the following developments which lead to further improvements of the activities about the investigation of the potential applications of BOMF and different curing agents in green perspective.

List of acronyms

2-MI 2-Methyl imidazole

2,4-EMI 2-ethyl-4-methylimidazole

AA acrylic acid

AESO soybean oil acrylate

Arg arginine

ATR Attenuated total reflection

BHMF bisfuran diepoxide (2,5-bis(hydroxymethyl)furan

BOF or **BOMF** monofuran diepoxide (2,5-bis[(2-oxiranylmethoxy) methyl]-furan

BPA Bisphenol A

CA contact angles

CAc citric acid

CAGR Compound Annual Growth Rate

CATA carboxylic acid-modified tannic acid

CeA cellulose acetate

CFRP carbon fiber composites or carbon fiber reinforced polymers

ChNF chitin nanofiber

CMMY cured myrcene with maleic anhydride

CNC cellulose nanocrystals

CNT carbon nanotubes

CO castor oil

CPI cationic polymerization catalyst

CsNF chitosan nanofiber

CSO cottonseed oil

Cys cysteine

DCPD dicyclopentadiene

DDE diamine diphenyl ether

DDM 4,4′-diaminodiphenyl methane

DDS diamonodiphenylsulfone

DETA diethylenetriamine

DFA discriminant function analysis

DGEBA diglycidyl ether of bisphenol A

DGEBF diglycidyl ether of bisphenol F

DGEI diglycidyl isosorbide ethers

DGF diglycidyl ester of 2,5-furandicarboxylic acid

DGT diglycidyl ester of terephthalic acid

DMA dynamic mechanical analysis

DMF dimethylformamide

DMS dynamic mechanical spectrometer

DMPK dimaleopimaryl ketone

DSC Differential scanning calometry

DTA diethylenetriamine

DW distilled water

EA ethyl acetate

ECH epichlorohydrin

ECO epoxidized castor oil

ECSO epoxidized cottonseed oil

EDA ethylene diamine

EEW epoxy equivalent weight

EIA epoxy monomer from itaconic acid

ELO epoxidized lineseed oil

ELO/FA epoxidized lineseed oil + furfuryl alcohol

EMETCO epoxidized methacrylate castor oil

EP epoxy resin

ERRγ oestrogen receptor-γ

ESO or **ESBO** epoxidized soybean oil

ESS epoxidized sucrose soyate

EVO epoxidized vegetable oils

FA furfuryl alcohol

FDCA furandicarboxylic acid or 2,5-furandicarboxylic acid

FT-IR - **FTIR** Fourier transform infrared spectroscopy

GA-EP epoxy resin polymerization system consisting of gallic acid

HCCP hyper-crosslinked carbohydrate polymer

HCPVC polybasic carboxylic acid

HHPA Hexahydrophthalic anhydride

HMF 5-hydroxymethylfurfural

HMDA 1,6-hexamethylene diamine

HMF 5-hydroxymethylfurfural

HMF-DDDS-EP epoxy monomer 5-hydroxymethylfurfural, 4,4'-diaminodiphenyldisulfide

HP hydrogen peroxide

HPAn hexahydrophthalic anhydride

IA itaconic acid

IAEDK bio-based imidoamine curing agent

ICP inductively coupled plasma

IDAE isosorbide diallyl ether

IDGE isosorbide diglycidyl ether

IMA two amine-imidazole salt complexes

IPD or **IPDA** isophorone diamine

IR infrared

ISA isosorbide-based diamine

ISE Isosorbide diglycidyl ether

IsMA isosorbide monoacrylate

KPS potassium persulphate

LOAn maleated linseed oil

LOI Limiting oxygen index

Lys lysine

LYS L-lysine methyl ester hydrochloride

m-CPBA meta-Chloroperbenzoic acid

M-XDA m-Xylylenediamine

MA maleic anhydride

MAc maleic acid

MDA methylenedianiline

MEK methyl ethyl ketone

MetA methacrylic acid

MFC microfibrillated cellulose

MFE-DETA glycidylated product of 4-methilcatechol-furfural

MHE-DETA glycidylated product of 4-methilcatechol-HMF

MHHPA Methylhexahydrophthalic anhydride

MMY myrcene with maleic anhydride

MNA methyl nadic anhydride

MPA maleopimaric acid

MTHPA methyltetrahydrophthalic anhydride

MTS-1-40 mesoporous TS-1-40

MWCNTs multi walled carbon nanotubes

NMR nuclear magnetic resonance

PAHs polycyclic aromatic hydrocarbons

PAN polyacrylonitrile

PBS Polybutylene succinate

PDMS-NH2 poly amino (dimethylsiloxane)

PE polyethylene

PEF poly(2,5-ethylene furandicarboxylate)

PEMA pentaerythritol with maleic anhydride

PEMPAE multifunctional Bio-based Epoxy Resin

PET polyethylene terephthalate

PFA polyfurfurylalcohol

PIMA Poly(isobutylene-alt-maleic anhydride)

PLA Polylactic acid

PLA/r core shell fiber PLA + resin

PMCs polymer matrix composites

PMDA pyromellitic dianhydride

PP polypropylene

PSAs pressure sensitive adhesives

PVP polyvinylpyrrolidone

RAC risk assessment committee

RCS refrigerator cooling system

RMA rosin maleic anhydride

SA salicylic acid

SE epoxy monomer based on sorbitol

SEM Scanning electron microscopy

SiNP silica nanoparticles

SLJ single lap joints

SPE polyglycidyl ether sorbitol

St styrene

TA tannic acid

TAc tartaric acid

TBBr tetrabutylammonium bromide

TCHMDA trans-1,4-cyclohexylamine

TEM transmission electron microscopy

TETA triethylenetetramine

TGA thermogravimetric analysis

THF tetrahydrofuran

THPA tetrahydrophtalic anhydride

TMAC Total Material Appearance Capture

TMP trimethylolpropane triglycidyl ether

TPAn terpene-based acid anhydride

TS-1 titanium silicalite-1

UV-Vis Ultraviolet–visible spectroscopy

WCA water contact angle

XRD x-ray diffraction

Xyl xylitol

Chapter

1 Introduction and objectives

1.1 Epoxy resins

Epoxy resins constitute a class of thermosetting polymers derived from monomers containing two or more oxirane groups. The high reactivity of the epoxide ring is the result of sp^3 hybridization of the two carbons, so that the bonding atoms prefer to orient 109° to each other, but the ring is highly distorted because it is fixed in a 60° planar structure. (**Fig. 1.1**).

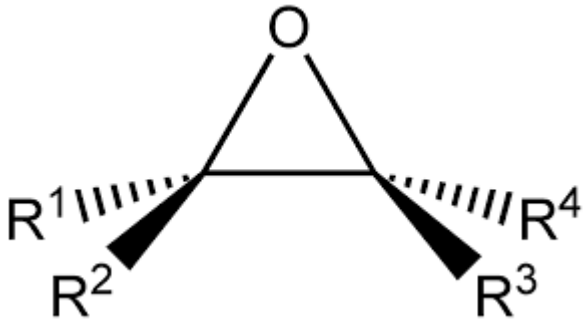

Fig. 1.1 Epoxide ring structure

Thanks to their versatility, they are used as reinforced composites, adhesives, high performance coatings and encapsulating materials. Epoxy thermosets have excellent electrical and mechanical properties, good adhesion to many metals and resistance to moisture and thermal and environment exposure. The widespread use of epoxies is due to the easy processing before curing, excellent wetting properties with reinforcements, good weathering resistance, excellent dimensional stability and high chemical and corrosion resistance [1,2].

Epoxy resins are obtained starting from a liquid form, which irreversibly solidifies through a cure process; very rigid materials are generated, in which the motion of the chains is limited due to the high number of crosslinks. To produce a thermosetting resin, it is essential that the initial monomers possess two or more reactive groups per molecule. This is crucial for forming a three-dimensional crosslinked structure that fills the entire reaction volume [3].

The initial phase of the curing process between resin and curing agent involves the formation of larger molecules. When all the branched structures grow, the sample reaches a critical point known as the gelation point. After this point, the hardened

resin will no longer dissolve in the solvents, but will only swell due to absorption [4].

It is very important to identify the curing conditions, considering the degree of polymerization, which refers to the rate at which the epoxy and reactive groups of the crosslinking agents are consumed [5].

Generally, the cross-linking of epoxy systems requires an initial curing step at low temperatures to promote the formation of linear chains, followed by a post-cure at high temperatures that promotes cross-linking.

The synthesis of epoxy resins originated in the United States in 1927, using epichlorohydrin as a precursor to form the epoxy group. In 1936, pioneering research on epoxy resins based on bisphenol-A was conducted by Castan at the Swiss chemical company Giba AG, and simultaneously by Greenlee at the American company Devoe and Reynolds Co. These companies secured the first patents in 1943 (Castan) and 1950 (Greenlee) respectively, establishing themselves as global leaders in the manufacturing of adhesives and epoxy-based surface coatings [6].

According to the latest findings from SNS Insider Research, the market size of Epoxy Resins reached US$ 24.61 billion in 2022. It is anticipated to achieve US$ 42.28 billion by 2030, exhibiting a robust Compound Annual Growth Rate (CAGR) of 7% during the forecast period spanning from 2023 to 2030 (**Fig. 1.2**) [7].

Fig. 1.2 Epoxy Resins Market Performance Forecast 2023-2030

The first and still the most important class of commercial epoxy resins is the reaction

product of bisphenol A (BPA) and epichlorohydrin in the presence of sodium hydroxide. It is called diglycidyl ether of bisphenol A (DGEBA). It has the general structure shown in **Fig. 1.3**. High molecular weight resins are prepared by reducing the excess of epichlorohydrin and reacting under strongly alkaline conditions [8].

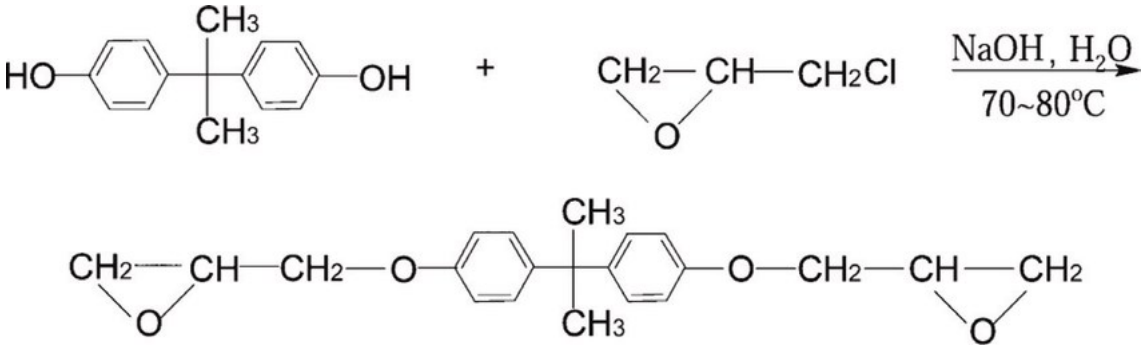

Fig. 1.3 DGEBA chemical structure

1.2 BPA issue

Bisphenol A (BPA), used as a monomer or as a plasticizer, is one of the most chemicals with the largest production volume in the world and is so called because it is obtained by the reaction of two moles of phenol with one mole of acetone (**Fig. 1.4**).

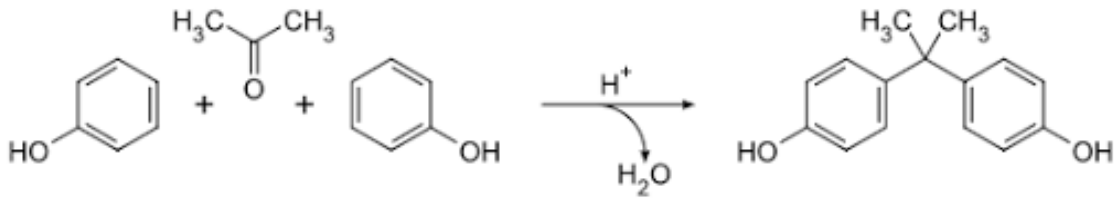

Fig. 1.4 Chemical structure of BPA

It is, therefore, a product entirely derived from the petrochemical industry.

However, most commercially available epoxy resins are made from bisphenol A (BPA), which has been classified as toxic to human health, especially the endocrine system. BPA, if in fact, can mimic certain hormones and be recognized by the body as such, causing immune and reproductive system problems along with changes in brain chemistry [9,10,11].

The two methyl and phenolic groups of BPA have been shown to interact with and bind oestrogen receptor-γ (ERRγ), so the body detects the presence of oestrogen [12].

Governments in the European Union and North America have implemented regulations to eliminate the harmful effects of BPA on citizens. For example, in 2014, in line with the opinion adopted by the RAC (Risk Assessment Committee), BPA has classified in the hazard class reproductive toxicity category 1B "may damage fertility". European legislation on BPA provides for limiting the contact of infants and children with this substance, through toys, feeding bottles, etc [8,13,14,15]. In cosmetic products, Bisphenol A has also been identified as a prohibited substance [16].

The most widely used epoxy monomer in the epoxy resin industry is diglycidyl ether of Bisphenol A (DGEBA, **Fig. 1.5**).

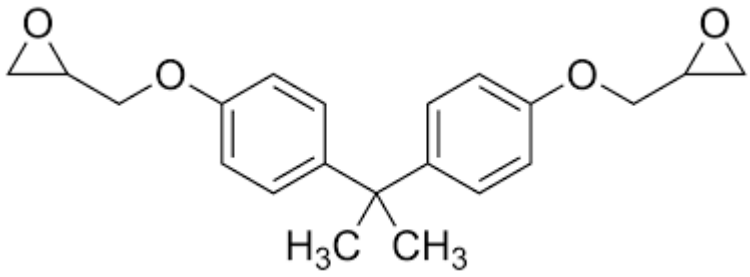

Fig. 1.5 Chemical structure of DGEBA

DGEBA is prepared from the liquid reaction between epichlorohydrin (ECH) and bisphenol A, the reaction occurs in the presence of an alkylammonium halide, such as tetrabutylammonium bromide or benzyltriethylammonium chloride, so that the BPA is deprotonated to the corresponding phenol.

In the first part of the reaction, the oxygen of the phenol attacks the chlorine atom or the epoxy ring according to an SN2 mechanism, then a strong base (NaOH) leads to the closure of the chlorinated derivative according to an SN1 mechanism (**Fig. 1.6**).

This compound is capable of self-condensation reaction and the number of units of the two reactants in its condensed form depends on the stoichiometry of the reaction.

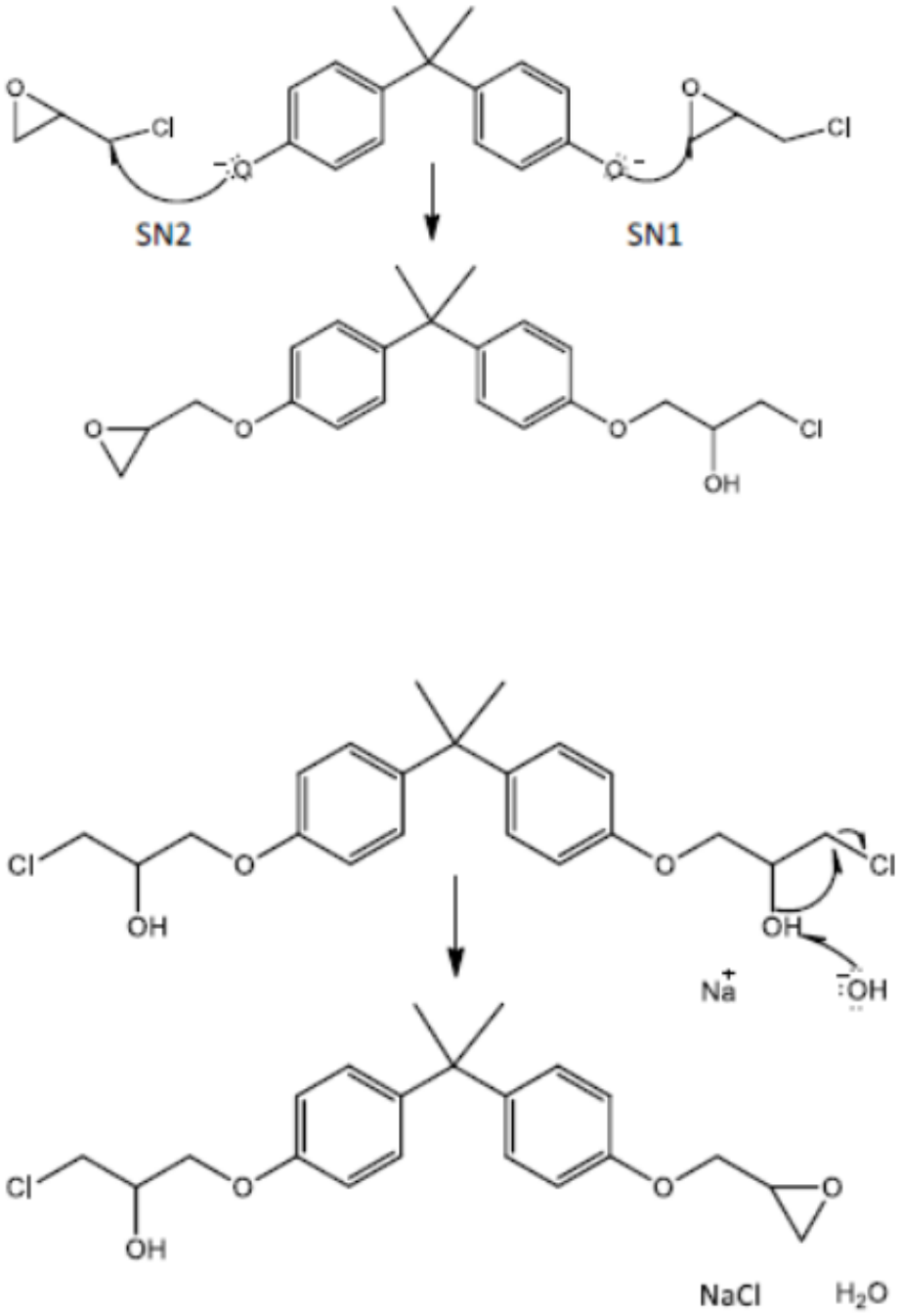

Fig. 1.6 Intramolecular cyclization of chlorohydrin intermediate

The synthesis of epoxy resins from BPA is an efficient process that has been optimized over the years to achieve the lowest possible cost.

To replace BPA as a precursor for epoxy resins, the main challenge was to create a simple, efficient synthetic route that produces a competitive material; Considering that thermosets containing the core of the BPA structure in the polymer network exhibit excellent mechanical properties and provide robust materials for use in the construction, transportation and furniture industries, the focus was on creating resins that have some value-added properties, such as lower viscosity or increased flame retardant property.

1.3 Bio-based epoxy monomers

In recent years, there has been increasing development of epoxy resins prepared from monomers obtained from renewable sources.

In recent years, there has been an increasing development of epoxy resins prepared from monomers obtained from renewable sources. Particular attention has been paid to the use of epoxidized vegetable oils (EVO) such as soybean oil [17], linseed oil [18], castor oil [19], hemp oil [20] and cottonseed oil [21], which are widely used as the main material for the manufacture of various biobased products and have many advantages over petroleum-derived materials, such as low cost and biodegradability.

Another viable alternative to Bisphenol A in the synthesis of bio-based epoxy resins concerns the use of lignin.

Lignin is the second most abundant and interesting of all natural polymers, after cellulose. The three main components present in the cell wall of natural lignocellulosic materials are lignin, hemicelluloses and cellulose.

Lignin is low in weight, non-polluting and biodegradable; it also has an aromatic structure with the presence of hydroxyl, carboxyl and phenolic groups that can very easily react with epichlorohydrin to form biobased epoxy resins [22].

Another interesting class of raw materials that lend themselves to the production of bio-based epoxy resins are polysaccharides.

Many monomers derived from carbohydrates, such as sorbitol, maltitol and isosorbide lead to epoxy networks with interesting properties [23].

1.3.1 Epoxidized vegetable oils

Vegetable oils are extracted from plant seeds and serve as an energy source for the germination process. Vegetable oils are ester derivatives of fatty acids and glycerol; these molecules are also known as triglycerides or triacylglycerols [24], as the name suggests, vegetable oils are extracted from plant seeds, and they function as the energetic source for the germination process.

Vegetable oils are used for many purposes, such as cooking food, oil colours production, soap production, environmental heating and biofuels.

The triglyceride harbors several reactive sites marked by C=C double bonds, which act as reactive sites for the alteration of fatty acids in vegetable oils. Among these, epoxidation emerges as the most notable functionalization reaction involving the C=C bonds of fatty acids. Double bonds can be involved in many reactions such as oxidation, halogenation, reduction and epoxidation. Furthermore, epoxidized vegetable oils are widely used in the polymer industry due to their high availability, non-toxicity, renewability and low cost.

Bio-based epoxidized vegetable oils are a viable alternative to petroleum-based polymers.

Unfortunately, resins based on epoxidized vegetable oils have low thermal and mechanical properties due to their long and flexible aliphatic chains, making them uncompetitive with current commercially available DGEBA-based resins. To improve properties, some strategies involve the use of rigid cross-linking molecules.

For example, Gaina et al. [25] made new epoxy resins prepared from epoxidized castor oil cross-linked with 3-hexahydro-4-methylphthalic anhydride (MHHPA) in the presence or absence of trimethylolpropane triglycidyl ether (TMP). Epoxidized castor oil (ECO) was obtained by in situ epoxidation with peroxyacetic acid. Compared to petroleum-based resins, ECO-based resins have a lower T_g, however, the introduction of TMP increases the T_g of ECO-containing resins. The water absorption test showed that as the T_g increased, the percentage mass of water input decreased.

Pin et al. [26] earlier reported MHHPA cured epoxidized linseed oil (ELO) catalyzed by 2-methylimidazole with good thermal stability and higher damping factor. Anhydride is a high temperature curing-agent. The used of the catalyst reduced the curing temperature of the reaction. It also increased the mechanical and thermal properties.

Also in 2015, a new procedure was developed to obtain fully bio-based epoxy resins from epoxidized linseed oil (ELO), using polyfurfurylalcohol (PFA) as a copolymer, in the presence of boron trifluoride ethylamine as a catalyst [27]. The decision to use both polymers was due to the different properties of the two materials. PFA, in fact, is a polymer with high T_g and thermal stability, but very brittle, unlike vegetable oils, which instead have low mechanical properties but high flexibility. Copolymerization was confirmed by FTIR, 1D and 2D NMR and DSC analysis; the latter was also used to determine the optimal amount of catalyst and the ELO/FA ratio, which were set at 1% catalyst and 50/50 molar ratio. Analysis of the mechanical behaviour revealed the ductility of the ELO50/FA50 resin, while the thermal stability was lower than that of PFA (364°C ELO/FA versus 402°C PFA), but still better than that of DGEBA.

Reinhardt et al. [28] have realized a fully biobased epoxy thermoset based on epoxidized linseed oil (ELO) and tannic acid (TA). The tannic acid has a high degree of functionality and its aromatic structure makes it possible to create a fully biobased polymer network, imparting high stiffness and strength. A maximum T_g of 146 °C, a flexural modulus of 2986 MPa and a flexural strength of 72 MPa were obtained. The good thermal and mechanical properties of TA/ELO resin expose its potential as a biobased replacement for petrochemical-based epoxy resins for high performance applications.

Another strategy to improve the mechanical properties of epoxidized vegetable oil resins is to use different crosslinking agents simultaneously. For example, Thiele et al. [29] synthesized an epoxy resin based on ELO cross-linked with different amounts of methyltetrahydrophthalic anhydride (MTHPA), pyromellitic dianhydride (PMDA) and maleic acid (MA). In order to study the effect of ELO

mass on gel time and hardness, different ELO masses (8, 10, 12, 14 and 16 g) were used, while keeping the amount of the curing system (4 g) (MTHPA, PMDA and MA) constant. As the mass of ELO increased, the gelling time increased, while the hardness of the samples did not change. It was seen that replacing petroleum-based PMDA with biogenic compounds, in particular oxalic acid and citric acid, resulted in new biobased epoxy resins with shorter gel times while maintaining hardness.

Albarran-Preza et al. [30] also synthesized a new xylitol functionalized epoxidized linseed oil (ELO). Epoxidation of the oil was achieved by a chemoenzymatic method with hydrogen peroxide and novoenzyme and was subsequently reacted with xylitol by a nucleophilic opening of the epoxy rings. The reaction temperature, reaction time and amount of catalyst were evaluated by preparing five reactions with different temperatures. The final monomers obtained are ELO-Xyl-50% and ELO-Xyl-100%; the cross-linking conditions for the production of the resins were 180°C for 60 minutes for ELO-Xyl-50% and 200°C for 120 minutes for ELO-Xyl-100% + ELO. The viscosity of the fully functionalized monomer ELO-Xyl-100% was 3 times higher than that of the partially functionalized monomer ELO-Xyl-50%.

Furthermore, the hydroxyl groups were highly reactive to the opening of the epoxy rings in the presence of even moderate amounts of catalyst, thus increasing the cost-effectiveness of the synthesis procedure. Among the vegetable oils that are best suited for epoxidation is cottonseed oil (CSO). Recently, bio-based thermosetting polymers have been synthesized from epoxidized cottonseed oil (ECSO) cross-linked with maleic anhydride [31]. The 95% of the C=C bonds present in CSO were converted into epoxy groups. Furthermore, it was shown that the physical and mechanical properties of the resulting polymer can be changed by changing the density of the cross-links, in particular viscous and sticky semi-solid materials were obtained for the lowest ECSO:mal 2:3 molar ratio, while rigid mesh materials were obtained for the highest ECSO:mal molar ratios (2:4, 2:5 and 2:6).

In recent work, the effects of microwave irradiation on the epoxidation process of soybean oil (ESO) were studied [32]. The epoxidation of the oil occurred by reaction

with peracetic acid generated in situ by the reaction between hydrogen peroxide (HP) and acetic acid at 35 wt%. Formic acid and HP at 60% by weight are commonly used, but to avoid detonation, it was decided to replace formic acid with acetic acid. Selective microwave heating increased the process speed by 50% compared to the conventional process and favoured the formation of a uniform suspension between the phases. While in the case of conventional heating the optimum stirring speed was found to be 450 rpm, in the case of microwave heating the stirring speed is an order of magnitude lower, 45 rpm, which translates into energy savings. The optimum temperature was chosen in a range between 60 and 70 °C, a good compromise between low reaction time and slow degradation of the product.

When it comes to epoxidation, one of the main objectives is to develop alternative, environmentally friendly methods. In this regard, Chen et al. [33] in 2019 developed a green approach for the epoxidation of soybean oil (ESO) by preparing a series of hetero-catalysts, titanium silicalite-1 (TS-1) with different Si/Ti ratios (TS-1-x, x = 40, 70, 80), mesoporous TS-1-40 (MTS-1-40) and anatase TiO_2. After being characterized by XRD, IR, UV-Vis, TGA, ICP, SEM, TEM and N2 adsorption, hydrogen peroxide (H_2O_2) was used as an oxidant and the catalytic reactions of SO epoxidation were studied. The results reveal that TS-1-x catalysts exhibit higher epoxidation catalytic activity and lower H_2O_2 consumption than anatase TiO_2, due to the unique nature and coordination geometry of the Ti sites in the TS-1 structure. Furthermore, an efficient high-temperature calcination regeneration method for spent TS-1 was proposed, which could be very useful for scaling up this clean, non-acidic epoxidation process for ESO production.

Vegetable oils can often also be used to synthesize green hardeners. Frias et al. [34] reported a simple method for the preparation of amine derivatives based on soya oil. The hardeners were synthesized via the Michael addition reaction of soybean oil acrylate (AESO) with different diamines, namely 1,6-hexamethylene diamine (HMDA), trans-1,4-cyclohexylamine (TCHMDA) and L-lysine methyl ester hydrochloride (LYS). The hardeners were subsequently cross-linked with

epoxidized soybean oil (ESO). The soy-based thermosets proved to have a very low water absorption capacity and a very low degradation capacity in PBS (37 °C, pH = 7.4).

Vegetable oils can be used as a raw material for the production of pressure sensitive adhesives (PSAs) that can compete with those derived from petrochemical sources, but with the environmental advantage of being sustainable. Cinnamea et al. [35] have synthesized PSA from mixtures of epoxidized soybean oil and sebacic acid in a one-step, solvent-free, catalyst-free reaction. Curing conditions, pot-life, and gel content were determined. The rheological profile and gel content of the obtained PSA was strongly dependent on the curing conditions (temperature and time). Stoichiometric ESO-SA mixtures polymerized at 170 °C between 65 and 75 minutes showed the best balance between tack and cohesion. It can be concluded that the viscoelastic profile, cohesion and adhesive properties of ESO-SA-based PSAs can be controlled by varying the curing parameters according to the desired application (permanent or removable PSA).

In addition to epoxidation, various functional groups can be added during synthesis to improve the thermal and mechanical properties of the material. Cayli et al. [36] synthesized epoxidized methacrylate castor oil (EMETCO). The synthesis took place in 2 steps, in the first step, castor oil (CO) is methacrylate with methacrylate chloride, then it was epoxidized by means of the Prilezhaev reaction. This reaction takes place between an olefin and a peroxyacid with the formation of an epoxide and a carboxylic acid. EMETCO was copolymerized with acrylic acid (AA), styrene (ST) and methacrylic acid (MetA). The EMETCO-ST-MA polymer has the highest storage modulus of 2.25 GPa. On the other hand, the EMETCO-AA copolymer showed the lowest build-up modulus at 350 MPa. In addition, the EMETCO-ST copolymer showed the lowest weight loss temperature of 5%, while EMETCO-MA showed the highest weight loss temperature of 5%, at 280 °C. The final product has a low viscosity and could be used in the future as a substitute material for many industrial monomers such as styrene, acrylate epoxide or prepolymers.

Kousaalya et al. [37] used oil extracted from the inedible seeds of Perilla frutescens to synthesize sustainable green epoxides through the Prilezhaev epoxidation reaction at 40, 50 and 60 °C for 8 h. The epoxidation of the oil took place in two steps: formation of the performic acid in the presence of H_2SO_4 as catalyst and conversion of the double bond to epoxide. A high content of epoxy groups was observed due to the high unsaturation content in perilla oil, as confirmed by its high iodine value (196 g/100 g). Reaction kinetics for epoxidation and ring opening reactions showed activation energy of 20.10 kJ/mol and 43.11 kJ/mol, indicating higher stability of epoxy groups and lower probability of α-glycol formation. This was further confirmed by results from α-glycol content test, which showed its molar concentration at less than 20% of epoxy molar concentration.

1.3.2 Epoxidized lignocellulosic compounds

Bioplastics are sustainable alternatives to plastic products for use in everyday lives, textile industry, health care, electronics and packaging applications [38]. In recent years, bioplastics materials are emerging as possible alternatives to complement and gradually replace petroleum-based plastics. Compared to petrochemical-based plastics, bioplastics are synthetically produced from lignocellulosic biomass, which is biodegradable and reduces the adverse environmental impacts. Petrochemical plastics contain dioxins and polycyclic aromatic hydrocarbons (PAHs) that pose severe health issues when released to the environment [39]. Additionally, for every 1 kg of plastic burnt, 2.8 kg of CO_2 is released into the atmosphere [40]. Mekonnen et al. [39] reported that 34 million tons of plastic wastes are produced annually of which 93% is disposed of in landfills and oceans. Some petrochemical plastics are non-biodegradable and pose effective disposal issues as they accumulate in landfills and oceans for hundreds to thousands of years hampering many natural ecosystems. These environmental constraints have stimulated interest in bioplastics, which could help in overcoming the sustainability and environmental challenges caused during the production, usage and disposal of synthetic plastics.

The main purpose of this section is to show the state of art, regarding the different strategies and methodologies adopted to replace the petroleum based process with

lignocellulosic derived epoxy resins. Green synthesis strategies, advanced processing methods, and life-cycle management approaches are highlighted to demonstrate the unique performance and sustainability characteristics of bioderivable thermosets. Structure–property and structure-activity relationships also are discussed in the context of maximizing performance and safety. For comparative purposes, bioderivable and biobased materials are benchmarked against appropriate commercial thermosets with emphasis on suitability for potential applications. Some future opportunities for the development of safer, higher-performance, biobased thermosets are provided. In **Fig. 1.7** are reported the key aspects related to the production of bio-based thermosets.

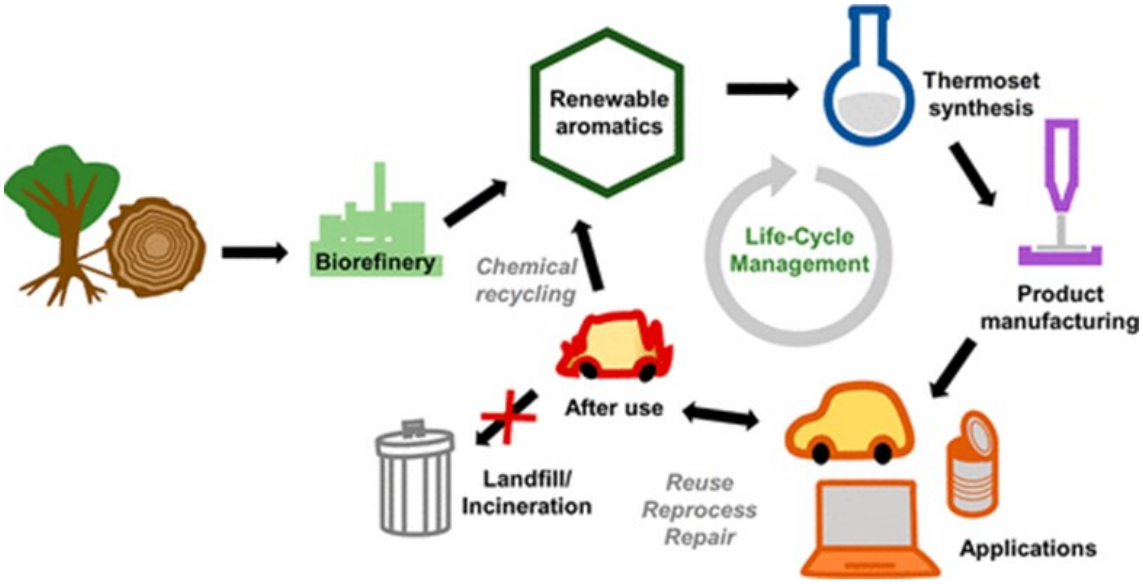

Fig. 1.7 Key aspects of LCB-derived thermosets. The generation of renewable aromatic chemicals, monomer and thermoset synthesis, material processing, product applications/performance, recyclability, and life-cycle management are all crucial in the development of next-generation, sustainable materials [41]

The catalytic conversion of (ligno)cellulose is currently subject of intense research. Isosorbide is one of the interesting products that can be produced from (ligno)cellulose as it can be used for the synthesis of a wide range of pharmaceuticals, chemicals, and polymers. Isosorbide is obtained after the hydrolysis of cellulose to glucose, followed by the hydrogenation of glucose to sorbitol that is then dehydrated to isosorbide

Cellulose, a homopolymer of D-glucose, is the most abundant component of lignocellulosic biomass. Cellulose is a crystalline polymer due to its intra- and intermolecular hydrogen bond network. The conversion of cellulose to added value chemicals has received a lot of interest due to the rarefaction of fossil oil and environmental concerns. One of the interesting reactions is the conversion of cellulose to isosorbide, a 1,4:3,6-dianhydrohexitol. This reaction occurs in several steps: 1) hydrolysis of cellulose to glucose 2) hydrogenation of glucose to sorbitol and 3) dehydration of sorbitol to isosorbide [42].

Isosorbide, a molecule obtained from biomass can find many applications such as additives, pharmaceuticals and monomers for polymer industries [43,44,45]. For instance, one polymer obtained from isosorbide, poly(ethylene-co-isosorbide) terephthalate, can replace polyethylene terephthalate (PET) [46].

At an industrial level, isosorbide is produced from the double dehydration of D-sorbitol using a strong acid catalyst. D-Sorbitol is produced from the hydrogenation of glucose obtained mostly from the hydrolysis of starch, but also from sucrose or cellulose.

Based on the study of each step reported in the literature, several researchers investigated the direct conversion of cellulose or lignocellulosic biomass to isosorbide. Several strategies were employed such as a combination of homogeneous acid and supported metal catalyst, or a combination of supported metal catalyst and solid acid or a metal on an acid support.

In a review, containing the methods to perform a one-pot synthesis of isosorbide from cellulose or lignocellulosic biomass, Bonnin et al. proposed different processes [42]. Through the combination of homogenous acid catalyst such as hydrochloric acid or sulfuric acid, and metal catalyst based on Pt, Pd and Ru. The main constrains regard the pH which is the key parameter to determine the quantity of biomass converted to isosorbide.

Asada et al. [47] studied the synthesis of epoxy resin from low molecular weight lignin. The lignin was extracted from different biomasses (cedar, eucalyptus and bamboo) by using methanol and then functionalized by the reaction with epichlorohydrin, catalyzed by a water-soluble phase transfer catalyst

tetramethylammonium chloride, which was further reacted with 30 wt% aqueous NaOH for ring closure using methyl ethyl ketone as a solvent.

The extraction and separation of steam-exploded samples were performed in two processes. The pretreated cedar at a steam pressure of 3.5 MPa (243◦C) and a steaming time of 5 min was extracted with DW and methanol as extracting solvents. In the case of Process 1, 100 g (dry weight basis) of steam-exploded cedar was extracted with 6 L of DW at room temperature with stirring, and separated into two fractions: water-soluble material (9.2 g) and water-insoluble residue (90.8 g). Because the water-soluble material contains not only oligosaccharides and monosaccharides derived from hemicellulose but also water-soluble polyphenols derived from lignin, they are expected to be used as functional food compound. The water-insoluble residue was extracted with methanol at 80 °C using a Soxhlet apparatus, which yielded 19.4 g of methanol-soluble lignin with a weight-average molecular weight of 1600. This methanol-soluble lignin can be used as a raw material for epoxy resin synthesis. Furthermore, the methanol-insoluble residue was hydrolyzed enzymatically into glucose (21.9 g), which can be a substrate for the production of alcohol, lactic acid, and others. The water-insoluble residue in the case of Process 2, was extracted with methanol at room temperature, giving 13.6 g of methanol-soluble lignin with a weight-average molecular weight of 1330, whereas the methanol-insoluble residue was hydrolyzed enzymatically into glucose (27.5 g). The decrease in the amount of methanol-soluble lignin during Process 2 was described as a low solubility of high-molecular weight lignin at low temperature. This led to the extraction of low-molecular weight lignin at low temperature.

Conversion process of steam-exploded cedar treated at a steam pressure of 3.5 MPa (243 °C) and a steaming time of 5 min into raw materials of useful products

The high-purity (above 99%) low molecular weight methanol-soluble lignins were extracted from the steam-exploded lignocellulosic samples (cedar, eucalyptus, and bamboo).The methanol-soluble lignins were used as a raw material for the synthesis of bio-based epoxy resins, in epichlorohydrin and TMAC under alkaline conditions, whereas insoluble residues were enzymatically hydrolyzed to produce

glucose. Good yields of biomass-derived epoxy resins (63.4–68.2%) were obtained, which were in accordance with the yield from bisphenol A (70%),suggesting that the biomass-based as well as the bisphenol A-based resins could be synthesized using the same synthetic route. these high bio-based content resins (more than 80% lignin content)derived from different lignocellulosic materials may be desirable candidates in the field of electronics and also could be an excellent substitute for fossil resource-derived bisphenol A.

Epoxy thermosets have gained extensive usage in dental fillings/prostheses, nanocomposites, and superglues due to simplicity, versatility, and robustness of the epoxide cross-linking chemistry [48].

There are other forms of biomass-based plastics known as drop-in bioplastics or (bio-based) drop-in chemicals such as bio-propylene (bio-PP), bio-polyethylene terephthalate (bio-PET) and bio-polyethylene (bio-PE). The term “drop-in” appears for these bioplastics because their manufacturing uses the majority of the pathways, infrastructure and machinery as the petrochemical plastics except for their precursor raw material being plant-based biomass. However, due to lack of technological constraints and economy of scale, the production cost of drop-in bioplastics are comparatively more expensive than petrochemical plastics in the current market [49].

The use of lignin in epoxy resins has been a subject of immense interest with a lot of research developments focused on different lignin-epoxy formulations. The use of lignin in resin formulations requires that the lignin is free from impurities such as moisture, sugars and free salts. This can be achieved by replacing waste lignin such as Kraft and soda lignin with the ones produced from high-purity processes such as organosolv lignin or by post-isolation purification methods (e.g. deionization and precipitation) [50]. Regardless, it should be noted that almost all-waste lignin poses enormous challenges with organic solvent solubility, thereby requiring special solvent mixtures for their formulation [51]. Lignin-epoxy resins with 50% lignin formulation have been reported to fabricate printed wiring boards for use in the electronics industry while exhibiting similar properties to those of common laminate resins [52]. To incorporate lignin as a polyol precursor in epoxy

resins many strategies have been adopted as mentioned below. One approach involves blending lignin for reaction with epoxy polymer [53]. Another approach involves reacting lignin with epichlorohydrin followed by cross-linking while other methods involve chemical modification of lignin (e.g. hydroxypropylation and phenolation), which address the challenges of poor reactivity and solubility of lignin [46].

Mahajan J.S. et al. [41] report the possibility to obtain aromatic monomers from lignin depolymerization in order to constitute the base for the obtainment of thermosets with unique and useful features such as reversible bond formation, self-catalyzed curing, or reduced estrogen receptor binding. They provided an overview of LCB-derived aromatic precursors for thermoset applications, which are divided into two major sections: lignin-derived phenolic building blocks and cellulosic-derived furanic building blocks. Each section is subdivided into the key functional handles that are used to generate thermosets from each precursor. The impact of these functionalities on materials synthesis and performance is described, and the properties of the bioderivable materials are compared to those of commercial analogues. Reprocessable and recyclable materials with reversible chemistries also are examined to emphasize a holistic approach to life-cycle management that accounts for the beginning (i.e., feedstock choice), middle (i.e., processing), and end (i.e., recycling or disposal) of the polymer life cycle (**Fig. 1.8**).

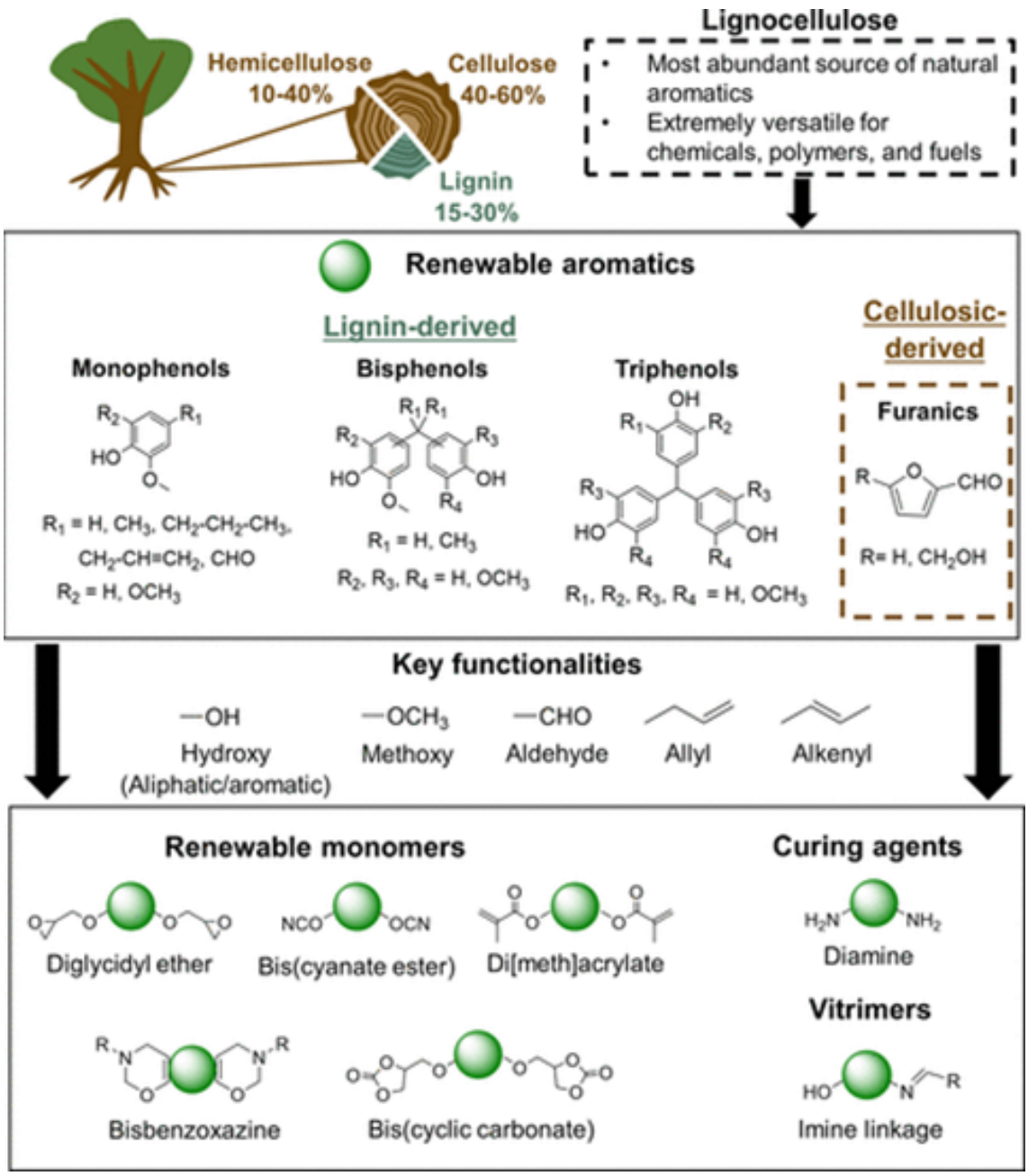

Fig. 1.8 Overview of LCB-derivable building blocks for thermoset applications, along with key characteristics and functionalities, and general structures of monomers and curing agents [41]

Cellulose is the most abundant natural polymer, and hemicellulose is the third most prevalent macromolecule, behind lignin. The high abundance and straightforward depolymerization of cellulosics present many opportunities for the production of renewable platform chemicals for polymer applications. Cellulosics also are versatile, as both aromatic and nonaromatic monomers can be obtained from depolymerization. For example, isosorbide, a chiral diol with a unique bicyclic

ring structure, has been studied extensively in biobased polymers, including as an alternative to BPA, and dilactones are being investigated for thermoset applications. The reader is directed to a review by Klemm et al. [54] for additional information on other nonaromatic, cellulosic-derived building blocks. The remainder of this section focuses on aromatic furans because of their unique reactivity that enables the synthesis of high-T_g compounds with utility as monomers, aminic curing agents, and reprocessable thermosets.

Furans are the most promising aromatic chemicals from cellulosics. They are versatile building blocks for renewable polymer development because they possess numerous functional handles that easily can be converted into amines, diols, acrylates, and epoxies. The two most common furanic chemicals are HMF and furfuryl alcohol, which are produced through continued dehydration of cellulose- and hemicellulose-derived monosaccharides, respectively. Recently, another furanic compound, furandicarboxylic acid (FDCA), has been recognized as a valuable precursor for biobased alternatives to polyesters like poly(ethylene terephthalate) (PET). In particular, poly(2,5-ethylene furandicarboxylate) (PEF) is gaining commercial traction because of its improved barrier properties in comparison to PET. The remainder of this section highlights how furanic building blocks can be used to design monomers, curing agents, and vitrimers for thermosets.

Asada C. et al. [55] studied a process to synthesize a bio-based cured epoxy resin using acetone-soluble lignin, a low-molecular-weight lignin, obtained from steam-exploded wheat straw. Steam explosion was used as a pretreatment to obtain low-molecular-weight lignin as a raw material for the epoxy resin and curing agent.

The solid and liquid materials were separated by filtration, and the residue was extracted at room temperature for 3 h using 150 mL acetone to dissolve the acetone-soluble lignin. Since acetone can extract more low-molecular-weight lignin than methanol, acetone extraction was used in this work. Acetone-soluble lignin was obtained and used as a raw material for synthesis of epoxy resin and curing agent after concentration and drying of the acetone extract.

They synthetized epoxy resin from lignin and from ligno-p-cresol and used the curing agent obtained from acetone soluble lignin and also from ligno-p-cresol.
A high yield of acetone-soluble lignin, a low-molecular-weight lignin, can be extracted from wheat straw using steam explosion followed by water and acetone extraction, which is a novel extraction method of organosolv lignin that has low environmental load and does not use corrosive substances such as sulfur. Acetone-soluble lignin is useful as a raw material for epoxy resin and as a curing agent for the synthesis of bio-based cured epoxy resin. The additional positive effects of p-cresol into the acetone-soluble lignin on cured epoxy resin's thermal and mechanical properties were observed. The current study demonstrated the possibility of using acetone-soluble lignin as an alternative fossil-derived raw material for the synthesis of cured epoxy resin that can be used in the electronic substrate field.

1.3.3 Epoxidized polysaccharides

Natural sugars, also called saccharides or carbohydrates, are polyhydroxylated aldehydes or ketones with the brute chemical formula $C_n(H_2O)_m$ where n and m can be different. There are two families in particular: ketoses and aldoses, containing between 3 and 7 carbon atoms for the natural oxides. The carbon atom carrying the aldehyde functional group is located at position 1 in the carbon skeleton, while the carbon atom defining the ketone functional group is located at position 2. The orientation of the carbon atom at the n-1 position defines the D or L series. In nature, D sugars (D-glucose and D-fructose) are preponderant.

Saccharides or carbohydrates called sugars are divided into simple (monosaccharides and oligosaccharides) called sugars and complex (polysaccharides). Sugars are often used for the production of bio-based epoxy resins. Monomers derived from carbohydrates such as sucrose, maltitol, sorbitol and isosorbide lead to the formation of epoxy resins with good properties.

The most important polysaccharide, especially in the production of bio-based materials, is the cellulose, composed of D-glucose units, which constitutes, together with hemicellulose and lignin, the structural component of the plant cell.

Isosorbide is considered as a viable candidate to replace BPA in thermoset materials, the most convenient way to produce diglycidyl ether from an isosorbide precursor is to graft epoxy groups to isosorbide by mixing it with epichlorohydrin in basic medium [56].

Musa et al. [57] developed a new fully biobased lino-epoxy composite by means of a one-pot ultrasound-assisted heterogeneous synthesis with sodium hydroxide microspheres, producing a fully epoxidized prepolymer with an excellent epoxy equivalent weight (EEW) of 269 g/eq compared to 284 g/eq of the silent method. The ratio of the epoxy ring to the isosorbide part was above 1.5, confirming a high degree of functionalization, which should ensure high reactivity for a subsequent polymerization operation.

In subsequent work, diglycidyl isosorbide ethers (DGEI) were cross-linked with isophorone diamine (IPD) with different epoxy equivalent weights (EEW). A specific epoxy formulation exhibits high reactivity with the amine hardener, inducing a high glass transition from 46 to 78 °C and stiffness to indentation [58]. Mechanical tensile investigations on unidirectional composites have validated their use for structural applications, with a Young's modulus and ultimate tensile strength comparable to petroleum-based epoxy/linen fibre materials.

Another interesting work on an entirely isosorbide-based cross-linked material was proposed by Li et al. [59] who synthesized both a diamine and an epoxy monomer from isosorbide. The isosorbide-based diamine (ISA) was synthesized through the thiol-ene coupling reaction in an aqueous environment. Isosorbide diglycidyl ether (ISE) was obtained through the epoxidation of diallyl isosorbide. After cross-linking, a fully bio-based epoxy resin was obtained with good shape memory properties in terms of near 100% shape recovery ratio, 97% shape fixity ratio, constant thermomechanical cyclic behaviour and shape recovery rate.

Nonque et al. [60] prepared sustainable polyacrylates and thermosets from isosorbide monoacrylate (IsMA), completely bio-based. In order to obtain different chain sizes of PIMA with programmable T_g, the Mayo synthesis method was used. The higher molecular weight PIMA showed interesting T_g above 100 °C, comparable

to those of polyacrylates used in industry. Treatment of the high T_g PIMA with succinic anhydride resulted in a high-performance thermoset with thermomechanical properties close to those of commercial epoxy resins, such as those based on DGEBA (T_g = 116 °C and E' = 4 GPa).

In a recent work, an epoxy resin was synthesized from an isosorbide-based monomer to make bio-based resins that can be used in coating applications [61]. The isosorbide was functionalized in a two-step reaction to introduce epoxy groups that were subsequently activated by UV radiation to trigger cross-linking and obtain dry films. The first step involved the synthesis of isosorbide diallyl ether (IDAE), then isosorbide diglycidyl ehter (IDGE) was obtained by the addition of 3-chloroperbenzoic acid (m-CPBA). The resin was polymerized by UV-cationic procedure, achieving a conversion of more than 85%, and a filler made from macadamia nut shell was added to increase the final hardness of the coating. With 30% filler, a hardness of up to 72 Shore D was achieved, compared to 19 Shore D of unfilled biobased epoxy resin. The addition of the filler also led to an increase in the glass transition temperature from 24 to 39 °C.

Wu et al. [62] made an epoxy resin from an epoxy monomer based on sorbitol (SE), branched poly amino (dimethylsiloxane) (PDMS-NH2) as a liquid repellent agent and isophorone diamine as a curing agent. The resin was applied as anti-smudge coatings. The results showed remarkable self-cleaning performance and good repellency to various liquids, including water and oils, with a PDMS-NH2 content of 0.5%. In addition, the coatings showed high transparency and excellent corrosion resistance.

Several bi- and tetrafunctional epoxy components have been obtained from d-glucose, the most promising of these being trifunctional glucopyranoside and glucofuranoside for high-tech applications [63]. A one-step reaction was tried, protecting the hydroxyl groups at positions 4 and 6, bi- and tri-functional epoxy components based on glucopyranoside were synthesized through the allylation of the free OH groups, followed by the epoxidation of the carbon-carbon double bond with m-chloroperbenzoic acid, resulting in a relatively rigid cyclic structure. A

tetrafunctional epoxy component was then synthesized by removing the protective 4,6-O-benzylidene group. In addition, a trifunctional glucofuranoside molecule was also prepared by reacting glucose with acetone and removing the 5,6-O-isopropylidene group. The bioderived epoxy monomers were successfully polymerized with 4,4′-diaminodiphenyl methane (DDM) as a hardener. The thermal stability of the polymerized epoxy resins was evaluated by thermogravimetric analysis (TGA), which showed an onset of degradation starting at 300 °C, furthermore, T_g values up to 175 °C were reached.

1.3.3.1 Furan-based epoxy monomers

Among biomass-based platform chemicals, furan-based compounds are a suitable replacement for petro-sourced chemicals because of their aromatic characteristics and sustainability.

Furan-based substances derived from biomass are obtained from simple sugars (pentoses and hexoses) or from polysaccharides. From here, the units can be transformed into furan biopolymer precursors: 2,5-furandicarboxylic acid (FDCA) and furfuryl alcohol (FA). These precursors are epoxidized and subsequently cross-linked (**Fig. 1.9**).

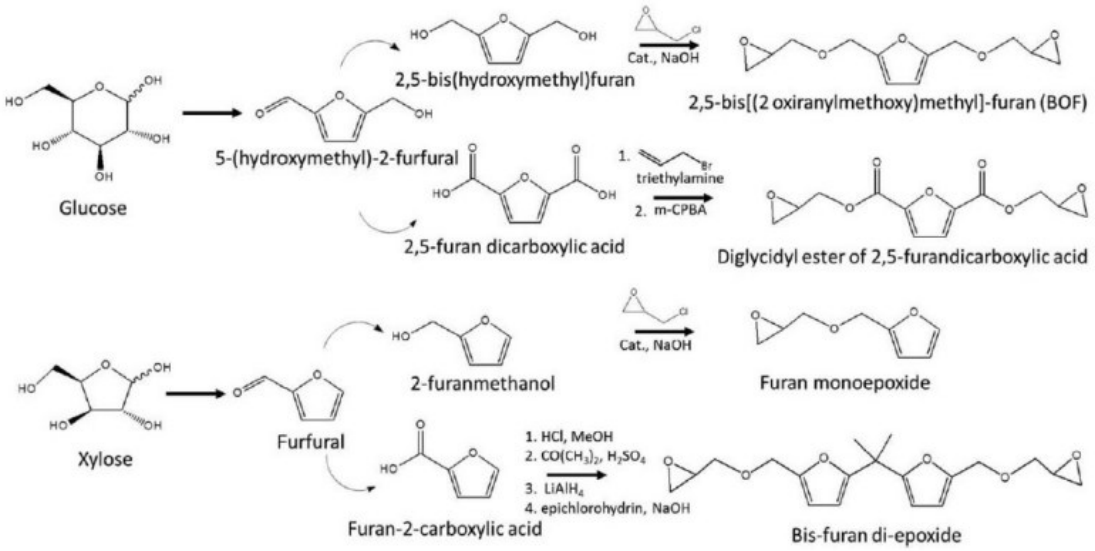

Fig. 1.9 Epoxidation and cross-linking of 2,5-furandicarboxylic acid (FDCA) and furfuryl alcohol (FA)

Some of these furan-based epoxy monomers are: monofuran diepoxide (2,5-bis[(2-oxiranylmethoxy) methyl]-furan, or BOF) and bisfuran diepoxide (2,5-bis(hydroxymethyl)furan, or BHMF).

These epoxides are photo cross-linked with fluoride salt initiators and traditional hardeners [64].

BOF shows promising values of T_g (71-88 °C) and conservative modulus E' at room temperature (3.5 GPa). Thus, compared to similar benzene polymers, BOF possesses lower T_g (approximately 29-44 °C lower), but higher glass modulus E'.

The diglycidyl ester of FDCA (DGF), i.e. epoxidized FDCA, was compared with its terephthalic acid-based petrochemical counterpart (DGT), after cross-linking with two traditional hardeners (MHHPA and D230, anhydridine and amine). DGF has a significantly higher T_g, while thermal stability and mechanical properties are comparable to DGT [65].

This may be due to the presence of carboxyl groups adjacent to the furan ring, which prevent rotation of the ring in the polymeric lattice. Thus, FDCA shows excellent potential to replace terephthalic acid in the preparation of epoxy resins, but also for thermoplastics, if one think of polyethylene terephthalate (PET).

Jiang et al. [66] reported a mild and scalable synthesis of two types of dipoxide monomers (BOF and bBOF), based on furan from 5-hydroxymethylfurfural (HMF) and furfural, the monomers had high yields and purity. The monomers were polymerized with different diamines (D230, IPDA, M-XDA) and were characterized thermally and mechanically. The results of the tensile tests and DMA analyses showed high moduli with the exception of bBOF/D230 and BOF/D230, due to the flexible polymerization agent D230. The T_g was also higher for the systems containing BOF due to its higher stiffness. All epoxy systems showed good thermal stability with $T_{d5\%}$ values between 268 and 310 °C in air.

In 2018, lignin and carbohydrate-derived monomers, including 4-methylcatechol, 5-hydroxymethylfurfural (HMF) and furfural, were used to prepare bisphenol-furan type polyphenols, followed by glycidylation to produce the corresponding epoxides, and then polymerization/curing with DETA to afford MFE-DETA and MHE-DETA epoxy thermosets [67]. The general strategy of this study was to prepare

two mixtures of catechol and furfural compounds obtained from the depolymerization of lignin and carbohydrates. Each mixture of catechol and furan was reacted individually to understand the reactions and properties of the products. products. In detail, bisphenol-furan molecules were designed as precursors for polymerization. The synthesis was developed through a single reaction step. The T_g measured by DMS had a value of 110 °C for MHE-DETA and 100 °C for MFE-DETA. The values of the storage modulus E' of MHE-DETA and MFE-DETA at 45 °C was 9.6 GPa and 6.6 GPa, respectively. These results indicate that MHE-DETA has better thermomechanical properties than MFE-DETA. TGA analysis revealed good thermal stability of both resins, as for both epoxy thermosets the T_{d5} was 174.2 °C for MFE-DETA and 214.0 °C for MHE-DETA, while the temperature at T_{d50} reached 381 °C for MHE-DETA and 362.4 °C for MFE-DETA, almost comparable to the corresponding BPA-based resins.

Cho et al. [68] used carbohydrate biomass to form epoxy-terminated furan compounds with a yield in excess of 70%. The kinetics of cationic photopolymerization of the synthetic compounds was studied in terms of the total heat flux calculated by photo-DSC analysis.

It was shown that the values of the first half-life (t½), which corresponds to the polymerization rate vary from 0.54 to 1.15 minutes when irradiated with UV 40 mW/cm^2. Studies have also shown that in the presence of furan rings there was an increase in tensile strength almost by a factor of twice as high (4.7 MPa) as when polycarbonate was functionalized with phenylglycidyl ether based on petrochemicals with formation of phenyl rings (2.6 MPa). The compound bis-epoxy furan followed a very similar route of synthesis to mono furan diepoxy, but showed lower strength due to its hydrophobic and stiffness properties.

Starting from the synthesis of 2,5-bis[(oxiran-2-ylmethoxy)methyl]furan reported in the work of Cho et al. [68], new carbohydrate-derived epoxy resins were synthesized and characterized. Specifically, 2,5-bis[(oxirane-2-ylmethoxy)methyl]furan was synthesized and polymerized with methyl anhydride. The effect of different initiators was studied in order to identify the most effective polymerizable formulations. A series of resins was then prepared by varying the

epoxide-anhydride ratios [69]. Kinetic evaluation using FTIR was carried out by following the actual consumption of the anhydride group during polymerization together with the formation of carbonyl peaks characteristic of the ester group of the polymerized resin. For the stoichiometric system, the change in rheological properties began after the formation of 85% of the ester groups. The thermal stability of the polymerized resins, tested by TGA, showed results comparable to those of the thermoset DGEBA/MNA: T_{d5} = 256 and 271 °C in nitrogen and air, respectively.

Depending on the epoxy/anhydride ratio, the networks showed T_{gs} and tensile moduli between 29 and 70 °C and between 0.3 and 1.7 GPa, respectively, demonstrating that the BOMF/MNA systems are very versatile with regard to their thermomechanical properties.

Cross-linking agents can also be synthesized from furan compounds. Nabipour et al. [70] produced a fully biobased epoxy thermoset by polymerizing a furan-derived epoxy monomer (HMF-DDDS-EP) with a furan-based hardener (DFA). The monomer synthesis saw the formation of a yellow Schiff base that was washed with cold ethanol, acetone and absolute ether to remove impurities. Finally, the light yellow powder obtained was dried for 12 hours at 60 °C in a vacuum oven in a 92% yield. It was then epoxidized using epichlorohydrin. The polymerized HMF-DDDS-EP/DFA thermoset incorporates a high glass transition temperature (171 °C), high tensile strength (62.9 MPa), inherent anti-flammability (UL-94 V-0 classification and high LOI of 36.0%), degradability and recyclability, representing an advanced thermoset material derived from renewable resources.

1.4 Bio-based curing agents

The curing process of a resin involves changing its properties to form a cross-linked structure. To accomplish the process, crosslinking agents, or hardeners, are added to the resin. There are a variety of commercially available curing agents, and their effect on crosslinking kinetics is always under investigation. However, the most commonly used are of fossil origin, and are often toxic.

Typical curing agents encompass amines, amides, hydroxyls, acid anhydrides, phenols, and polyphenols (**Fig. 1.10**).

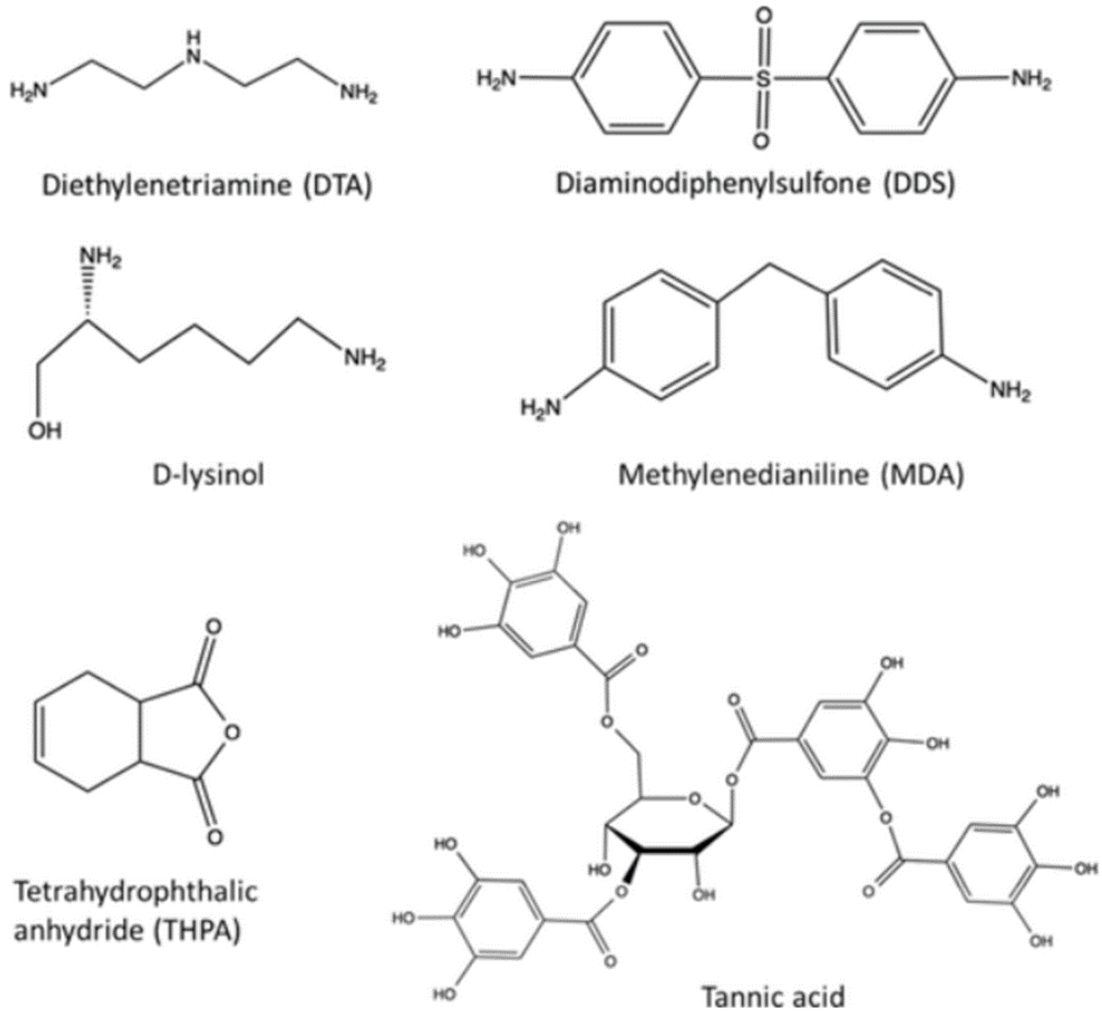

Fig. 1.10 Chemical structures of hardeners: DTA, DDS and MDA are toxic amines; lysinol is a biological amino acid; THPA is a traditional anhydride; tannic acid is a natural polyphenol [71].

In recent years, therefore, there has been a need to develop hardeners from natural and renewable raw materials. Examples are modified vegetable oils, amines from rosin, biological acids and anhydrides and polyphenols [72].

1.4.1 Bio-based carboxylic acids

Epoxy resin curing agents often involve carboxylic acids, typically obtained from petrochemical sources. However, these acids can also be sourced naturally, for example, from fruit juices or fatty acids. Employing carboxylic acid curing agents from natural origins has the potential to enhance the bio-based content of cured epoxy resins.

Barros et al. [73] polymerized epoxidized soybean oil (ESO) with different carboxylic acids such as salicylic (SA), maleic (MA) and citric (CAc). The carboxylic acids were added to the ESO in a stoichiometric ratio of R = 1.2 epoxy groups/acids (or R = 0.8 acids/epoxy). The curing and degradation processes were carried out using FTIR and TG. The FTIR spectra demonstrated the curing through the disappearance of the epoxy group band at 950 and 813 cm^{-1}, with ESO/MA exhibiting a lower degree of absorption of 67.74 wt%, which is reflected in a lower thermal stability and lower degree of cross-linking. ESO/CA and ESO/SA showed a gel content (GC) > 80%, indicating the formation of a 3D network with a higher cross-linking density, compared to ESO/MA. TGA analysis showed similar degradation behaviour for all samples with good thermal stability, with $T_{5\%}$ and T_{max} ranging from 79 to 221 °C and 391 to 401 °C, respectively.

A new polybasic carboxylic acid (HCPVC) consisting of vanillin and hexachlorocyclotriphazene was successfully synthesized via nucleophilic substitution reaction and Pinnick oxidation [74]. First, vanillin and anhydrous potassium carbonate as a deacidification reagent were dissolved in THF. Next, HCCP dissolved in THF was added dropwise into the flask in a steady and slow manner under a nitrogen atmosphere for a period of 1 hour at room temperature (25 °C). Subsequently, the reaction mixture was heated slowly. The filtration bath solution was removed by vacuum distillation and the white solid product, HCPV (12.94 g), was obtained after being recrystallized and purified with ethanol. HCPVC was synthesized by the Pinnick oxidation of HCPV and showed positive polymerization activity and its polymerization condition was applicable to wood. Furthermore, the epoxy resin cross-linked with HCPVC (HCPVC-EP) showed pre-eminent flame resistance with a UL-94 V-0 rating and an LOI value of 30.7%,

compared to resins cross-linked with other hardeners (DDM-EP and MAH-EP), which were found to be flammable without rating and with a low LOI of less than 22.8%.

Recent advances in microbial engineering are paving the way for the commercial availability of additional suites of poly(carboxylic acid) structures that have not been evaluated in epoxy coating systems. Hevus et al. [75] selected 12 biological di- and tricarboxylic acids as curing agents for two multifunctional epoxy resins: biobased sucrose epoxide (ESS) and the petrochemical Araldite MY $_{721}$. The epoxide-acid-solvent polymerization took place in the absence of a catalyst, and since the biobased acid is soluble in water, the use of an ESS-acid system with water as solvent resulted in 100% biobased coatings, achieving complete conversion of the carboxyl groups of the biobased acids. Films made with the developed formulations demonstrated excellent solvent resistance and adhesion to metal substrates. Furthermore, by modifying the chemical structure of the acid and the epoxy resin, the hardness and flexibility of the coatings can be controlled.

Another fully bio-based epoxy resin was obtained by cross-linking polyglycidyl ether (SPE) sorbitol with various bio-based di- and tricarboxylic acids, such as citric acid (CAc), tartaric acid (TAc), maleic acid (MAc) and itaconic acid (IA), in the presence or absence of microfibrillated cellulose (MFC) [76]. For the SPE/IA systems, the cross-linking of the C = C unsaturated bonds in the IA units was investigated with the addition of potassium persulphate (KPS) as an aqueous radical initiator, which also improved the T_g (62.8 °C), tensile strength (15.4 MPa) and tensile modulus (1.08 GPa). The use of MFC improved the storage modulus in the 60-100 °C temperature range.

A bio-derived epoxy resin was produced by combining gallic acid with epichlorohydrin, and a carboxylic acid-modified tannic acid (CATA) was acquired through a simple esterification process [77]. This process utilized the epoxy resin polymerization system consisting of gallic acid (GA-EP), methylnadic anhydride (MNA) and 2-ethyl-4-methylimidazole (2,4-EMI) as a hardening agent. The use of GA-EP/MNA/2,4-EMI with CATA resulted in the formation of a homogenous

system after polymerization, showing a toughness of 74.7 % and a tensile strength of 52.1 MPa.

1.4.2 Bio-based anhydrides

Unlike amine-based agents, anhydride curing agents typically necessitate more rigorous conditions for the curing process. However, they excel in applications related to electricity. There exists several bio-based sources for the production of anhydride curing agents.

Biobased curing agents for epoxy resins can also be derived from terpenes. For instance, a novel curing agent based on terpenes, created by combining myrcene, a monoterpene with three double bonds, including a conjugated diene, with maleic anhydride (MMY), is employed in the polymerization of bisphenol A-based epoxies (E-51) [78]. Epoxy resin cross-linked with MMY was more flexible than pure MMY. By increasing the weight ratio of cured sample (CMMY), the tensile strength and T_g decreased, while the elongation at break increased.

The obtained cured material is characterized by a tensile strength of 48.74 MPa and a storage modulus of 19.06 MPa, but a poor impact property of 8.55 kJ/m^2 and a very low elongation at break (7.54%).

Takahashi et al. [79] polymerized epoxidized soybean oil (ESO) with a terpene-based acid anhydride (TPAn), and the thermal and mechanical properties of the polymerized product were compared to ESO polymerized with hexahydrophthalic anhydride (HPAn), maleated linseed oil (LOAn) or thermally latent cationic polymerisation catalyst (CPI). ESO-TPAn showed a higher glass transition temperature (67.2°C), compared to ESO-HPAn (59.0°C), ESO-LOAn (-41.0°C) and ESO-CPI (10.0°C). The storage modulus at 20°C and the tensile strength were also higher than the other cured ESOs. ESO-TPAn resin was used to obtain biocomposites with regenerated cellulose tissue (lyocell) as filler by compression moulding. The tensile strength and modulus of the ESO-TPAn/lyocell composite with a fibre content of 75 wt% were 65 MPa and 2.3 GPa, three times higher than those of ESO-TPAn.

Another fully bio-based epoxy resin was prepared from a eugenol-based epoxy and a rosin-based anhydride curing agent [80]. The rosin-based systems were compared to those cured with commercially available petroleum-based curing agents such as HHPA. The syntheses of eugenol epoxide and rosin anhydride were investigated, and the chemical structures of the products and intermediates were characterized using ^{1}H NMR and Fourier transform infrared spectroscopies. Moreover, the eugenol epoxy, when cured using a rosin-derived anhydride (MPA), demonstrated a higher glass transition temperature (T_g) compared to the one cured with HHPA, 155.3 °C and 114.2 °C respectively. The findings of this investigation suggest that eugenol and rosin have the potential to serve as feedstocks for epoxy resins, and the cured resins exhibit performance comparable to their petrochemical counterparts.

New polymer thermosets were obtained from epoxidized soybean oil and maleopimaric acid (MPA), catalyzed by 2-ethyl-4-methylimidazole [81]. Maleopimaric acid was synthesized with abietic acid and maleic anhydride using sulfonic acid p-toluene as a catalyst. In particular, the synthesis of the MPA included two reactions, an isomerization reaction followed by a Diels-Alder reaction. The Diels-Alder reaction is a concerted reaction with only one step from raw materials to the product. No intermediate is formed but the reaction proceeds through a transitional state. The results showed that the total heat release for ring opening polymerization of epoxy soybean oil and maleopimaric acid was only 31.7 kJ/mol epoxy group. The tensile strength and the T_g were comparable with the corresponding petrochemical-based materials, while the elongation at break (61.5%), the storage module (1268 MPa) and thermal stability with $T_{10\%}$ of 349 C were improved.

Zhang et al. [82] have developed a new bio-based thermohardening system from epoxy resin (EP), with rosin anhydride (maleopimaric acid, RAM) as a curing agent and latent catalyst type of imidazole (two amine-imidazole salt complexes, IMA), to be used as a matrix for prepreg hot-melt polymerization at medium temperature. For comparison a petrochemical-based cross-linking agent methylhexahydrophthalic anhydride (MHHPA) was used. The reaction energy

(86.5 kJ mol^{-1}) related to the carbonyl group of RAM is larger than that of MHHPA reaction with oxirane (81.04 kJ mol^{-1}) and IMA reaction with oxirane (77.9 kJ mol^{-1}), according to the Kissinger Method. As regards the mechanical properties, the results showed that the bending strength, the bending modulus and the glass transition temperature of the cross-linked laminates with increased by 44%, 73% and 70°C respectively.

In 2018, a cardanol-based di-anhydride was synthesized and used as a hardener in the preparation of anti-corrosive epoxy coatings [83]. Cardanol and glycidil methacrylate were initially reacted and maleic anhydride was added to form a di-anhydride compound. The coatings obtained showed excellent hardness and flexibility, it was also observed that T_g increases with the hardening agent content. Finally, corrosion tests were carried out, the anti-corrosive properties were evaluated by salt spray tests, exposing the coated panels to the 5% NaCl solution for 500 h. The results showed that coatings treated with the compound dianhydride effectively limited the permeation of corrosive species through the coating and provided better protection to the underlying substrate.

1.4.3 Bio-based amines and amino acids

Amines and their derivatives comprise a broad spectrum of hardeners. Amines are widely used in resins for their nucleophilia, which allows them to be reactive at room temperature [84].

Cycloaliphatic diamines in the cross-linking of epoxy resins are the most widely used and performing. The cycloaliphate structure and the mean reactive amino groups offer the following advantages:

- Good machinability of the liquid matrix;
- High performance composites with high glass transition temperatures;
- High mechanical strength;
- Improvement of mechanical properties;
- Good temperature performance;
- Resistance to impact stress;

- Resistance to moisture and hot water;
- Good chemical resistance.

Among the most widely used amino acids as crosslinking agents for epoxy resins are L-tryptophan, lysine, cysteine and arginine (**Fig. 1.11**).

Industrially, they are prepared via fermentation or enzymatic methods. For example, the hydrogenation of lysine - produced by fermentation of sugars - generates the modified amino acid lysol, which can act as an excellent hardener for epoxy resins.

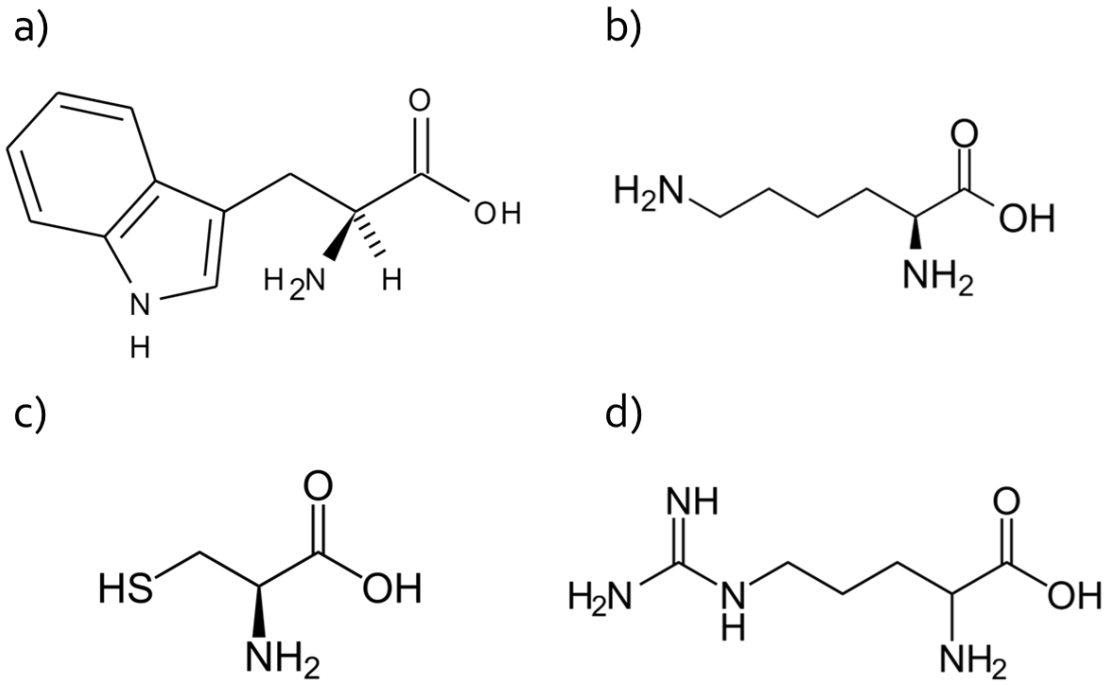

Fig. 1.11 (a) L-triptophan, (b) lysine, (c) cysteine and (d) arginine chemical structures

In order to obtain a low toxicity epoxy resin, L-tryptophan was combined with the two commercial late polymerization agents 2-Undecyl-1H-imidazole and 3,3'-(4-Methyl-1,3-phenylene)bis(1,1-dimethylurea) as cross-linking agents for bisphenol A ether diglicidyl (DGEBA) [85]. The DSC results showed that glass transition temperatures of about 100 °C are reached. In the presence of late hardening agents, DGEBA and L-Triptophan react together showing a clear exothermic transition ΔH = 376 J/g for the system with 2-Undecyl-1H-imidazole and 310 J/g for that

with 3,3'-(4-Methyl-1,3-phenylene)bis(1,1-dimethylurea, in the first scan. Therefore, in the second heating, no residual reaction heat is recorded and both the resins obtained show high T_g.

In a subsequent work L-tryptophan and guanine were studied as new green polymerization agents for the cross-link of bisphenol diglycidyl ether A (DGEBA) [86]. In particular, L-tryptophan has been combined with other bio-based molecules such as urea, theobromine, theophylline, and melamine to increase the thermal properties of epoxy resin and reduce the crosslinking reaction temperature. While guanine, a totally heterocyclic molecule showing amino functional groups, has been tested as a single hardener. The use of melamine allows a reaction temperature (206 ºC) similar to that of normal L-tryptophan, higher than those of the sample in which commercial fossil-based late polymerization agents were used and leads to the highest final T_g (118 ºC). The cross-linked system with guanine, on the other hand, showed too high reaction temperatures for industrial purposes (260-280)However, even in this case, very high T_g values of more than 100 °C are achieved which represent a very promising result for a biocompatible, non-toxic and environmentally friendly molecule.

Motahari et al. [87] used L-tryptophan as an ecofriendly treating agent for the production of epoxy-based nanocomposites. Specifically, a study was done on the cure kinetics of the epoxy resin DGEBA treated with tryptophan in the presence of 2,4,5-triphenylimidazole as a catalyst. The nanocomposite was obtained by adding silica nanoparticles (SiNP). Comparing the glass transition temperatures, T_g (101.9 °C) and the heat of the reaction, ΔH (214.4 J/g), the optimal molar ratio for DGEBA/Trp was found to be 2:1 and the optimal content of SiNP was determined to be 5 phr.

Lysine (Lys) and arginine (Arg) and cysteine (Cys) have been used as bio cross-linking agents of a water-soluble epoxy resin bio-based, sorbitol polyglycidyl ether (SPE) with chitin nanofiber (ChNF) not higher than 10 wt% and chitosan nanofiber (CsNF) not higher than 2 wt% as fillers to prepare biocomposites obtained by compression molding and casting methods [88]. Dynamic mechanical analysis

revealed that a higher order of the peak temperature of the loss module (T_α) was SPE-Lys (39 °C) > SPE-Arg (33 °C) > SPE-Cys (21 °C). The 50-100 ºC storage modules for SPE-Lys/ChNF, SPE-Cys/ChNF and biocomposite SPE-Cys/CsNF were much higher than for the corresponding polymerized resins.

Yu et al. [89] synthesized a new type of latent 1,5-pentanediamine and maleic anhydride curing agent used in conjunction with a bio-based epoxy monomer from itaconic acid (EIA) to achieve a fully bio-based one-component epoxy system. Thanks to the hydrogen bond from amide bonds, the PDA-MAH-EIA network obtained showed a very high glass transition temperature 87 °C measured by DSC analysis, a tensile strength of 98 MPa and Young's modulus of 1930 MPa. In addition, the ester bonds in the network give PDA-MAH-EIA a favorable degradability with a maximum degradation rate of 24.64 $mgml^{-1}h^{-1}$.

Recently, lignin-based epoxy polymerization agents with equivalent weight of hydroxyl amine up to 68 g/eq have been obtained by ring-opening reactions of cyclic Aza-silane species (A2-DL) [90]. These lignin aminated species have shown good compatibility in traditional epoxy resins of bisphenol F (DGEBF) and epoxy soybean oil (ESBO) and could be easily homogenized without the need for solvents. The kinetic parameters of curing were obtained using the method of Borchardt and Daniels. The results showed for DGEBF/A2-DL, a activation energy of 101 kJ/mol and pre-exponential factor ln(Z) of 27.6 s^{-1} were observed, while ESBO/A2-DL displayed an activation energy of 71 kJ/mol and ln(Z) of 13.3 s^{-1}. The heightened pre-exponential factor demonstrated by DGEBF/A2-DL leads to accelerated curing at lower temperatures, attributed to an increased likelihood of collision between epoxy and amine groups facilitated by π-π stacking interactions. Utilizing A2-DL, stand-alone DGEBF thermosets were successfully fabricated, exhibiting commendable thermomechanical properties, a glass transition temperature of 85 °C, and a Young modulus of 1.67 GPa.

Ortiz et al. [91] produced fully biobased epoxy resins combining epoxidized linseed oil, lignin and a bio-based diamine (Priamine 1074®) derived from dimers of fatty acids. Lignin, being rich in aromatic structures, gives hardness and strength. With

a content of 12.5% by weight of lignin, both the glass transition temperature and Young's modulus increased, and the increase was even more pronounced at 22% by weight, rising from -12 to 0 °C, respectively. The fact that all resin components are bulk chemicals opens the door to the production of fully biobased resins at an industrial level.

A photourable thermosetting biocomposite has been successfully created in just two steps using four components, using a solvent-free process based on an epoxy/amine reaction of epoxy linseed oil and a dynamic molecule (4,4 - diaminodiphenyl disulfide), by UV irradiation [92]. Compared to a similar material without disulfide bond, this coating has a lower cross-linking density and a greater elongation at rupture (66%). A significant repair of a scratch depth of 100 μm has been achieved: a 42% increase in tensile strength was observed in 3 h of UV irradiation at 100 °C. However prolonged exposure to UV rays leads to photooxidation of the material surface.

BPA-based epoxy resins, GY-2600 Araldite and GY-240 have been cross-linked with bio-based phenalkamines Cardolite. NX-6019, Cardolite Lite-2002 and Cardolite instead GX-6004 and compared with cross-linked systems with low molecular weight amines such as EDA, TETA and Jeffamine D-230 [93]. It was shown that DSC polymerization of epoxy resins by phenalkamines began at lower temperatures, and cross-linking rates were slightly lower than those treated by low molecular weight amino hardeners. The T_gs are also comparable for the 2 classes of systems, however they are slightly lower for systems treated with phenalkamine, but using the more reactive phenalkamine GX-6004 you can reach T_gs DI 80-85 % C. One of the biggest advantages of using bio-based phenalkamines is the lowest enthalpy of crosslinking, the cure from phenalkamine begins later, but proceeds faster.

Thakur et al. [94] synthesized the Multifunctional Biological Based Epoxy Resin (PEMPAE), from the Diels-Alder reaction between gum rosin and maleic anhydride (MA) with pentaerythritol to obtain the esterified product (PEMA) which was further epoxidized with epichlorohydrin and potassium hydroxide. In

addition, a bio-based imidoamine (IAEDK) was synthesized by the reaction between diamine diphenyl ether (DDE) with dimaleopimaryl ketone (DMPK), a MA dehydrodecarboxylate derivative. The results revealed that the system cured with imidoamina exhibits the lowest curing temperature, high reactivity and high thermal performance compared to those of its corresponding synthetic precursor. The bio-based cured system showed improved chemical resistance after immersion of 30, 60 and 90 days in NaOH, NaCl and HCl, weight loss of cured resin coatings on steel specimens was evaluated. The high chemical resistance in the case of imidoamine cured sample indicates the high degree of crosslinking of imidoamine curing agent with pentaerythritol based epoxy resin.

1.5 Polymeric nano-fibers through electrospinning process

Electrospinning of thermoplastic polymers is widely used in applications such as filters and coatings, but has only recently been applied to thermosetting polymers due to their chemical structure and reactivity [95].

Nanofibers synthesized by electrospinning thermoplastic polymers such as polyaniline, polyvinylpyrrolidone, polyvinyl alcohol, polycaprolactone [96], have been studied for the development of thermoset and thermoplastic blends and sheaths for the manufacture of such fibers, however, the presence of thermoplastic content in the resulting fibers can deteriorate their mechanical properties, especially under high thermal conditions.

Obtaining epoxy resin nanofibers is still a challenge today due to the reactivity of the epoxy, low viscosity of the solution, lack of plasticity and the brittleness of the fibers. In a recent work, these difficulties were overcome by dissolving the epoxy in methyl ethyl ketone solvent and obtaining suitable electrospinning conditions by controlling the degree of cross-linking of the epoxy in the solvent [97]. Similarly, submicron filaments of a CNT/epoxy composite were produced by developing a partial polymerization strategy through a heat treatment process. In this case, the addition of CNT to the epoxy improved the mechanical modulus of the fibers by 49% and reduced the porosity of the manufactured filaments by up to 25% [98].

However, the degree of cross-linking is difficult to control due to the high reactivity of epoxy groups. A more efficient method to obtain epoxy nanofibers consists of a core-shell process.

Fast self-repairing carbon fiber/epoxy composites based on a thermosetting thermoplastic core-shell nanofiber were produced to improve the healing efficiency and reactivity of self-repairing composites. The core-shell nanofiber was prepared by coaxial electrospinning under the assumption that the melting temperature of the thermoplastic copolyimide corresponds to the curing temperature of the encapsulated epoxy curing agent. The thermal expansion of the PA provided an additional driving force for healing. Therefore, the core-shell acted together as a healing agent and rapidly filled the damaged region, realizing the full healing potential [99].

Furthermore, in order to obtain epoxy nanofibers, a core-shell process was devised in which a 'sacrificial' thermoplastic polymer was used as a mould to allow the epoxy nanofibers to polymerize internally. After cross-linking of the epoxy resin, the polymer used as a mould was subsequently removed by washing in a solvent. This methodology appears to be particularly promising to be used in epoxy system, in which becomes difficult to control the crosslinking degree.

1.6 Lack of knowledge

The literature review, reported in this chapter, is aimed to introduce the main topics and the current issues which will lead to the experimental study, carried out during the PhD course. It clearly appears that the main problem to be solved, in the environmental reduction perspective, is the removal of petroleum-based precursor BPA from conventional epoxy resins. So, in order to identify the lack of knowledge, it is necessary to depicts the state of art regarding the synthesis of the biobased epoxy resins, in particular those derived from polysaccharides. Similarly, it is worthy to take into account the availability of different environmental friendly curing agents, which could improve the bio content of the polymerized mixture and also could offer different application opportunities. The main part of this study

is focused on the investigation of thermal and mechanical properties of diverse epoxy resins, which conduct to the exploration of the various applications.

Particular attention is addressed to electrospinning process which could enlarge the range of applicability of these epoxy systems, it is considered very difficult to be performed on the thermoset resins, but it represents a huge gap in the research studies and also an highly promising development.

References

1. Shundo A, Yamamoto S, Tanaka K. Network Formation and Physical Properties of Epoxy Resins for Future Practical Applications. *JACS Au* 2022; 2: 1522–1542.

2. Rahman MM, Akhtarul Islam M. Application of epoxy resins in building materials: progress and prospects. *Polym Bull* 2022; 79: 1949–1975.

3. Auvergne R, Caillol S, David G, et al. Biobased thermosetting epoxy: Present and future. *Chem Rev* 2014; 114: 1082–1115.

4. Riemenschneider W, Bolt HM. Esters, Organic. *Ullmann's Encycl Ind Chem*. Epub ahead of print 2005. DOI: 10.1002/14356007.a09_565.pub2.

5. Duemichen E, Javdanitehran M, Erdmann M, et al. Analyzing the network formation and curing kinetics of epoxy resins by in situ near-infrared measurements with variable heating rates. *Thermochim Acta* 2015; 616: 49–60.

6. John Wiley & Sons. Vol. 9 EPOXY RESINS. *Encycl Polym Sci Technol*; 9.

7. Paulet A. Epoxy Resins Market Size 2023-2030 (US $ in Bn).

8. Jackson R. European developments. *Debates Relig Educ* 2011; 24: 168–179.

9. Mg R, Girigoswami A. file:///C:/Users/Haneen/Downloads/263-Article Text-1963-2-10-20190530.pdf. *Biointerface Res Appl Chem* 2021; 12: 105–119.

10. Vandenberg LN, Hauser R, Marcus M, et al. Human exposure to bisphenol A (BPA). *Reprod Toxicol* 2007; 24: 139–177.

11. Vandenberg LN, Ehrlich S, Belcher SM, et al. Low dose effects of bisphenol A. *Endocr Disruptors* 2013; 1: e26490.

12. Okada H, Tokunaga T, Liu X, et al. Direct evidence revealing structural elements essential for the high binding ability of bisphenol a to human estrogen-related receptor-γ. *Environ Health Perspect* 2008; 116: 32–38.

13. Beausoleil C, Emond C, Cravedi JP, et al. Regulatory identification of BPA as an endocrine disruptor: Context and methodology. *Mol Cell Endocrinol* 2018; 475: 4–9.

14. Health A, Parliament E. Regulation (EU) No 321/2011. *Off J Eur Union* 2011; 3–4.

15. Commission TE. COMMISSION DIRECTIVE 2014/81/EU of 23 June 2014. *Off J Eur Union* 2014; 2014: 23–25.

16. Michałowicz J. Bisphenol A - Sources, toxicity and biotransformation. *Environ Toxicol Pharmacol* 2014; 37: 738–758.

17. Olivieri G V., De Quadros J V., Giudici R. Epoxidation Reaction of Soybean Oil: Experimental Study and Comprehensive Kinetic Modeling. *Ind Eng Chem Res* 2020; 59: 18808–18823.

18. Turco R, Tesser R, Russo V, et al. Epoxidation of Linseed Oil by Performic Acid Produced in Situ. *Ind Eng Chem Res* 2021; 60: 16607–16618.

19. Fu Q, Tan J, Han C, et al. Synthesis and curing properties of castor oil-based triglycidyl ether epoxy resin. *Polym Adv Technol* 2020; 31: 2552–2560.

20. Omonov TS, Patel V, Curtis JM. The Development of Epoxidized Hemp Oil Prepolymers for the Preparation of Thermoset Networks. *JAOCS, J Am Oil Chem Soc* 2019; 96: 1389–1403.

21. Meng Y, Kebir N, Leveneur S. Reactivity and structure: epoxidation of cottonseed oil and the corresponding fatty acid methyl ester. *Biomass Convers Biorefinery*. Epub ahead of print 2023. DOI: 10.1007/s13399-023-04985-1.

22. Ralph J, Lapierre C, Boerjan W. Lignin structure and its engineering. *Curr Opin Biotechnol* 2019; 56: 240–249.

23. Chrysanthos M, Galy J, Pascault JP. Preparation and properties of bio-based epoxy networks derived from isosorbide diglycidyl ether. *Polymer (Guildf)*

2011; 52: 3611–3620.

24. Kaikade DS, Sabnis AS. Polyurethane foams from vegetable oil-based polyols: a review. *Polym Bull* 2023; 80: 2239–2261.

25. Gaina C, Ursache O, Gaina V, et al. Novel Bio-Based Materials: From Castor Oil to Epoxy Resins for Engineering Applications. *Materials (Basel)*; 16. Epub ahead of print 2023. DOI: 10.3390/ma16165649.

26. Pin JM, Sbirrazzuoli N, Mija A. From epoxidized linseed oil to bioresin: An overall approach of epoxy/anhydride cross-linking. *ChemSusChem* 2015; 8: 1232–1243.

27. Pin JM, Guigo N, Vincent L, et al. Copolymerization as a Strategy to Combine Epoxidized Linseed Oil and Furfuryl Alcohol: The Design of a Fully Bio-Based Thermoset. *ChemSusChem* 2015; 8: 4149–4161.

28. Reinhardt N, Breitsameter JM, Drechsler K, et al. Fully Bio-Based Epoxy Thermoset Based on Epoxidized Linseed Oil and Tannic Acid. *Macromol Mater Eng* 2022; 307: 1–10.

29. Thiele K, Eversmann N, Krombholz A, et al. Bio-based epoxy resins based on linseed oil cured with naturally occurring acids. *Polymers (Basel)* 2019; 11: 1–8.

30. Albarrán-Preza E, Corona-Becerril D, Vigueras-Santiago E, et al. Sweet polymers: Synthesis and characterization of xylitol-based epoxidized linseed oil resins. *Eur Polym J* 2016; 75: 539–551.

31. Wijayapala R, Mishra S, Elmore B, et al. Synthesis and characterization of crosslinked polymers from cottonseed oil. *J Appl Polym Sci* 2019; 136: 1–7.

32. Piccolo D, Vianello C, Lorenzetti A, et al. Epoxidation of soybean oil enhanced by microwave radiation. *Chem Eng J* 2019; 377: 120113.

33. Chen C, Cai L, Li L, et al. Heterogeneous and non-acid process for production of epoxidized soybean oil from soybean oil using hydrogen

peroxide as clean oxidant over TS-1 catalysts. *Microporous Mesoporous Mater* 2019; 276: 89–97.

34. Frias CF, Serra AC, Ramalho A, et al. Preparation of fully biobased epoxy resins from soybean oil based amine hardeners. *Ind Crops Prod* 2017; 109: 434–444.

35. Ciannamea EM, Ruseckaite RA. Pressure Sensitive Adhesives Based on Epoxidized Soybean Oil: Correlation Between Curing Conditions and Rheological Properties. *JAOCS, J Am Oil Chem Soc* 2018; 95: 525–532.

36. Çayli G, Gürbüz D, Çınarli A. Characterization and Polymerization of Epoxidized Methacrylated Castor Oil. *Eur J Lipid Sci Technol* 2019; 121: 1–5.

37. Kousaalya AB, Beyene SD, Gopal V, et al. Green epoxy synthesized from Perilla frutescens: A study on epoxidation and oxirane cleavage kinetics of high-linolenic oil. *Ind Crops Prod* 2018; 123: 25–34.

38. Thakur S, Chaudhary J, Sharma B, et al. Sustainability of bioplastics: Opportunities and challenges. *Curr Opin Green Sustain Chem* 2018; 13: 68–75.

39. Mekonnen T, Mussone P, Khalil H, et al. Progress in bio-based plastics and plasticizing modifications. *J Mater Chem A* 2013; 1: 13379–13398.

40. Burgos N, Valdés A, Jiménez A. Valorization of agricultural wastes for the production of protein-based biopolymers. *J Renew Mater* 2016; 4: 165–177.

41. Mahajan JS, O'Dea RM, Norris JB, et al. Aromatics from Lignocellulosic Biomass: A Platform for High-Performance Thermosets. *ACS Sustain Chem Eng* 2020; 8: 15072–15096.

42. Bonnin I, Mereau R, Tassaing T, et al. One-pot synthesis of isosorbide from cellulose or lignocellulosic biomass: a challenge? *Beilstein J Org Chem* 2020; 16: 1713–1721.

43. Zhu Y, Durand M, Molinier V, et al. Isosorbide as a novel polar head derived from renewable resources. Application to the design of short-chain amphiphiles with hydrotropic properties. *Green Chem* 2008; 10: 532–54.

44. Tundo P, Aricò F, Gauthier G, et al. Green synthesis of dimethyl isosorbide. *ChemSusChem* 2010; 3: 566–570.

45. Flewitt P. Word-processing systems. *Beyond Word Process* 1984; 174: 33–42.

46. Diani J, Gall K. Finite Strain 3D Thermoviscoelastic Constitutive Model. *Society* 2006; 1–10.

47. Asada C, Basnet S, Otsuka M, et al. Epoxy resin synthesis using low molecular weight lignin separated from various lignocellulosic materials. *Int J Biol Macromol* 2015; 74: 413–419.

48. Brooks C. Molecular Dynamics Simulations of Epoxy Resin Systems to Study Physical Properties. 2018; 1–9.

49. Okolie JA, Nanda S, Dalai AK, et al. Chemistry and Specialty Industrial Applications of Lignocellulosic Biomass. *Waste and Biomass Valorization* 2021; 12: 2145–2169.

50. Stewart D. Lignin as a base material for materials applications: Chemistry, application and economics. *Ind Crops Prod* 2008; 27: 202–207.

51. Lora JH, Glasser WG. Recent industrial applications of lignin: A sustainable alternative to nonrenewable materials. *J Polym Environ* 2002; 10: 39–48.

52. Kosbar LL, Gelorme JD, Japp RM, et al. Introducing biobased materials into the electronics industry: Developing a lignin-based resin for printed wiring boards. *J Ind Ecol* 2000; 4: 93–105.

53. Upton BM, Kasko AM. Strategies for the conversion of lignin to high-value polymeric materials: Review and perspective. *Chem Rev* 2016; 116: 2275–2306.

54. Klemm D, Heublein B, Fink HP, et al. Cellulose: Fascinating biopolymer and sustainable raw material. *Angew Chemie - Int Ed* 2005; 44: 3358–3393.

55. Asada C, Fujii M, Suzuki A, et al. Cured epoxy resin synthesized using acetone-soluble lignin and ligno-p-cresol obtained from steam-exploded wheat straw. *Biomass Convers Biorefinery* 2023; 13: 10495–10504.

56. Fenouillot F, Rousseau A, Colomines G, et al. Polymers from renewable 1,4:3,6-dianhydrohexitols (isosorbide, isomannide and isoidide): A review. *Prog Polym Sci* 2010; 35: 578–622.

57. Ethers BOG. Towards Greener Epoxy Precursors.

58. Musa C, Kervoëlen A, Danjou PE, et al. Bio-based unidirectional composite made of flax fibre and isosorbide-based epoxy resin. *Mater Lett* 2020; 258: 126818.

59. Li C, Dai J, Liu X, et al. Green Synthesis of a Bio-Based Epoxy Curing Agent from Isosorbide in Aqueous Condition and Shape Memory Properties Investigation of the Cured Resin. *Macromol Chem Phys* 2016; 217: 1439–1447.

60. Nonque F, Sahut A, Jacquel N, et al. Isosorbide monoacrylate: A sustainable monomer for the production of fully bio-based polyacrylates and thermosets. *Polym Chem* 2020; 11: 6903–6909.

61. Pezzana L, Emanuele A, Sesana R, et al. Cationic UV-curing of isosorbide-based epoxy coating reinforced with macadamia nut shell powder. *Prog Org Coatings*; 185. Epub ahead of print 2023. DOI: 10.1016/j.porgcoat.2023.107949.

62. Wu Z, Lin Y, Yuan X, et al. Sorbitol-based epoxy anti-smudge coatings with liquid repellency for various applications. *J Appl Polym Sci* 2023; 140: 1–11.

63. Rapi Z, Szolnoki B, Bakó P, et al. Synthesis and characterization of biobased epoxy monomers derived from d-glucose. *Eur Polym J* 2015; 67: 375–382.

64. Hu F, La Scala JJ, Sadler JM, et al. Synthesis and characterization of thermosetting furan-based epoxy systems. *Macromolecules* 2014; 47: 3332–3342.

65. Deng J, Liu X, Li C, et al. Synthesis and properties of a bio-based epoxy resin from 2,5-furandicarboxylic acid (FDCA). *RSC Adv* 2015; 5: 15930–15939.

66. Jiang Y, Yun J, Pan X. Renewable Furan-Based Epoxy Resins Derived from 5-Hydroxymethylfurfural and Furfural. *ACS Sustain Chem Eng* 2022; 10: 16555–16562.

67. Jiang Y, Ding D, Zhao S, et al. Renewable thermoset polymers based on lignin and carbohydrate derived monomers. *Green Chem* 2018; 20: 1131–1138.

68. Cho JK, Lee JS, Jeong J, et al. Synthesis of carbohydrate biomass-based furanic compounds bearing epoxide end group(s) and evaluation of their feasibility as adhesives. *J Adhes Sci Technol* 2013; 27: 2127–2138.

69. Marotta A, Faggio N, Ambrogi V, et al. Curing Behavior and Properties of Sustainable Furan-Based Epoxy/Anhydride Resins. *Biomacromolecules* 2019; 20: 3831–3841.

70. Nabipour H, Wang X, Song L, et al. A furan-derived epoxy thermoset with inherent anti-flammability, degradability, and raw material recycling. *Mater Today Chem*; 27. Epub ahead of print 2023. DOI: 10.1016/j.mtchem.2022.101315.

71. Stanzione J, La Scala J. Sustainable polymers and polymer science: Dedicated to the life and work of Richard P. Wool. *J Appl Polym Sci*; 133. Epub ahead of print 2016. DOI: 10.1002/app.44212.

72. Ding C, Matharu AS. Recent developments on biobased curing agents: A review of their preparation and use. *ACS Sustain Chem Eng* 2014; 2: 2217–2236.

73. Barros A, Nepomuceno N, Nicácio P, et al. Enhancement of Biobased Epoxy Through the Curing and Thermal Stability Control with Carboxylic Acids. *J Polym Environ*. Epub ahead of print 2023. DOI: 10.1007/s10924-023-03136-x.

74. Huang Y, Ma T, Wang Q, et al. Synthesis of Biobased Flame-Retardant Carboxylic Acid Curing Agent and Application in Wood Surface Coating. *ACS Sustain Chem Eng* 2019; 7: 14727–14738.

75. Hevus I, Ricapito NG, Tymoshenko S, et al. Biobased Carboxylic Acids as Components of Sustainable and High-Performance Coating Systems. *ACS Sustain Chem Eng* 2020; 8: 5750–5762.

76. Sugane K, Mishima T, Shibata M. Biobased epoxy nanocomposites composed of sorbitol polyglycidyl ether, biobased carboxylic acids and microfibrillated cellulose. *J Polym Res* 2021; 28: 1–11.

77. Xu J, Liu X, Fu S. Bio-based epoxy resin from gallic acid and its thermosets toughened with renewable tannic acid derivatives. *J Mater Sci* 2022; 57: 9493–9507.

78. Yang X, Wang C, Li S, et al. Study on the synthesis of bio-based epoxy curing agent derived from myrcene and castor oil and the properties of the cured products. *RSC Adv* 2017; 7: 238–247.

79. Yang Z, Peng H, Wang W, et al. Crystallization behavior of poly(ε-caprolactone)/layered double hydroxide nanocomposites. *J Appl Polym Sci* 2010; 116: 2658–2667.

80. Qin J, Liu H, Zhang P, et al. Use of eugenol and rosin as feedstocks for biobased epoxy resins and study of curing and performance properties. *Polym Int* 2014; 63: 760–765.

81. Chen Y, Xi Z, Zhao L. New bio-based polymeric thermosets synthesized by ring-opening polymerization of epoxidized soybean oil with a green curing agent. *Eur Polym J* 2016; 84: 435–447.

82. Zhang XF, Wu YQQG, Wei JH, et al. Curing kinetics and mechanical properties of bio-based composite using rosin-sourced anhydrides as curing agent for hot-melt prepreg. *Sci China Technol Sci* 2017; 60: 1318–1331.

83. Wazarkar K, Sabnis A. Cardanol based anhydride curing agent for epoxy coatings. *Prog Org Coatings* 2018; 118: 9–21.

84. Stemmelen M, Pessel F, Lapinte V, et al. A fully biobased epoxy resin from vegetable oils: From the synthesis of the precursors by thiol-ene reaction to the study of the final material. *J Polym Sci Part A Polym Chem* 2011; 49: 2434–2444.

85. Mazzocchetti L, Merighi S, Benelli T, et al. Evaluation of Tryptophan - Late curing agent systems as hardener for epoxy resin. *AIP Conf Proc*; 1981. Epub ahead of print 2018. DOI: 10.1063/1.5046032.

86. Merighi S, Mazzocchetti L, Benelli T, et al. Evaluation of novel bio-based amino curing agent systems for epoxy resins: Effect of tryptophan and guanine. *Processes* 2021; 9: 1–13.

87. Motahari A, Omrani A, Rostami AA, et al. Preparation and characterization of a novel epoxy based nanocomposite using tryptophan as an eco-friendly curing agent. *Thermochim Acta* 2013; 574: 38–46.

88. Shibata M, Fujigasaki J, Enjoji M, et al. Amino acid-cured bio-based epoxy resins and their biocomposites with chitin- and chitosan-nanofibers. *Eur Polym J* 2018; 98: 216–225.

89. Yu Z, Ma S, Tang Z, et al. Amino acids as latent curing agents and their application in fully bio-based epoxy resins. *Green Chem* 2021; 23: 6566–6575.

90. Silau H, Melas A, Dam-Johansen K, et al. Bio-based amine curing agents prepared from lignin by ring-opening functionalization with cyclic aza-silanes and their curing kinetics investigated for aliphatic and aromatic epoxy species. *Prog Org Coatings* 2023; 184: 107822.

91. Ortiz P, Vendamme R, Eevers W. Fully biobased epoxy resins from fatty acids and lignin. *Molecules* 2020; 25: 1–11.

92. Geelhand de Merxem L, Vuluga D, Lecamp L. A biobased self-healing thermoset coating with a dynamic photosensitive molecule. *Polymer (Guildf)* 2021; 217: 123454.

93. Jonikaitė-Švėgždienė J, Pastarnokienė L, Juknevičiūtė V, et al. Curing of epoxy resins by bio-based phenalkamines vs low-molecular-weight amines: study by DSC. *Chemija* 2022; 33: 54–63.

94. Thakur T, Jaswal S, Parihar S, et al. Bio-based epoxy thermosets with rosin derived imidoamine curing agents and their structure-property relationships. *Express Polym Lett* 2020; 14: 512–529.

95. Shneider M, Zattelman R, Kaestner A, et al. Electrospinning of epoxy fibers: Effect of curing conditions on solution rheological behavior. *J Appl Polym Sci*; 140. Epub ahead of print 2023. DOI: 10.1002/app.54437.

96. Megahed AA, Zoalfakar SH, Hassan AEA, et al. A novel polystyrene/epoxy ultra-fine hybrid fabric by electrospinning. *Polym Adv Technol* 2018; 29: 517–527.

97. Shneider M, Sui XM, Greenfeld I, et al. Electrospinning of epoxy fibers. *Polymer (Guildf)* 2021; 235: 124307.

98. Aliahmad N, Biswas PK, Wable V, et al. Electrospun Thermosetting Carbon Nanotube-Epoxy Nanofibers. *ACS Appl Polym Mater* 2021; 3: 610–619.

99. Chen B, Zhang Y, Mao C, et al. Research on electrospinning thermosetting-thermoplastic core-shell nanofiber for rapid self-healing of carbon fiber/epoxy composites. *Compos Sci Technol* 2022; 227: 109577.

Chapter

2 Experimental section

2.1 Materials

The commercially available bio-based epoxy precursor, namely 2,5-bis(hydroxymethyl)furan (BHMF, 97%) was purchased from Apollo Scientific. Maleic anhydride (MA, powder, 95%) was provided by Sigma Aldrich and used as a curing agent. Bisphenol A diglycidyl ether (DGEBA, epoxy equivalent weight EEW = 172−176) was purchased from Sigma-Aldrich. 2-methylimidazole (2-MI, 99%), (±) epichlorohydrin (ECH, ≥99%), tetrabutylammonium bromide (TBBr, ≥99%) and ethanol (96%) were purchased from Acros Organics. Anhydrous sodium hydroxide pellets (NaOH, ≥97%), ethyl acetate (EA, 99%), hexane (HX, 99%), tetrahydrofuran (THF, 99.9%) and magnesium sulphate (MgSO4) were purchased from Carlo Erba. All chemicals were used as received, without further purification. Glacial acetic acid was purchased from Romil.

A carbon fiber-reinforced tetraglycidyl diaminodiphenylmethane-based thermosetting polymer (CFRP) was provided by Alenia Aermacchi (Pomigliano d'Arco, Italy). The CFRP was made of two superposed prepreg layers (Prepreg Fabric 934-41-3KT400HN-P-193-C, and Prepreg Tape 934-37-6KT400HB-145, Fiberite Europe, Germany).

Polylactic acid (PLA) was obtained from Sigma-Aldrich.

Isophorone diamine (IPD) was purchased from Sigma-Aldrich. Multiwall carbon nanotubes (CNT) NC7000^{TM} were purchased by Nanocyl. Cotton fabric (cotton, plain wave, weight 230 g/m^2, thickness about 1 mm, thread density 730 yarns/m), purchased by a local distributor, was employed as substrate for the application epoxy-based nanocomposite coatings.

2.2 Synthesis of 2,5-bis[oxiran-2-ylmethoxy)methyl]furan (BOMF)

BOMF was synthesized slightly modifying the procedure described by Cho et al.[1]. A 50 wt % aqueous solution of NaOH (1.44 mol, 57.7 g), TBBr (1.68 mol, 3.86 g) and ECH (1.68 mol, 132 mL) was added to a double-necked round-bottomed flask equipped with a magnetic stirrer and a condenser and put under vigorous stirring for 30 min at room temperature. The reaction system was saturated with argon and the flask was then placed in a bath at 50 °C when a solution of BHMF (0.120 mol, 15.4 g) in THF (120 mL) was added dropwise. The reaction mixture was reacted

for 2 h and subsequently poured into 600 mL of an ice/water mix. Then the mixture was extracted two times with 600 mL of EA and the organic phase was washed with water, dehydrated with $MgSO_4$, filtered and dried with a rotatory evaporator. To remove the ECH excess, the crude product was washed three times with hexane and dried again. The total yield of the synthesis is 85%. The obtained product (BOMF) was an amber colored viscous liquid at room temperature, with a viscosity (η) at 30 °C of 0.032 Pa*s and an equivalent epoxy weight (EEW) of 129 g/eq, calculated according to the procedure proposed by F. G. Garcia et al.[2]. The chemical structure of the furan bis-epoxide was confirmed by ^{1}H NMR analysis.
^{1}H NMR (400 MHz, CDCl3) 6.27 (s, 2H), 4.48 (q, J = 12.8 Hz, 4H), 3.74 (dd, J = 11.5, 3.1 Hz, 1H), 3.40 (dd, J = 11.5, 5.9 Hz, 1H), 3.13 (td, J = 6.2, 2.9 Hz, 2H), 2.76 (dd, J = 6.8, 2.3 Hz, 1H), 2.58 (dd, J = 5.0, 2.7 Hz, 1H).
By analyzing NMR spectra performed on crude products, after that an appropriate extraction with water an ethyl acetate was performed, no by-products were noticed. In some cases, only the presence of some residual epichlorohydrin, remained entrapped in the viscous BOMF and that could not be extracted with rotatory evaporator, was detected. Thus the purification by chromatography resulted unnecessary and was replaced by a repeated extraction with hexane. Hexane, being mixable with ECH insoluble with BOMF, when vigorously mixed with the reaction product was able to extract efficiently all the ECH excess. The absence of a chromatography purification step was of great advantage, allowing the use of reduced amounts of solvent and reaction time, keeping a high yield of reaction.
By ^{1}H NMR analysis it was possible to detect the characteristic peaks of furanic proton at 6.28 ppm, a quartet at 4.48 ppm associated to the two methylene protons on the ether carbon bonded with the furan moiety. Peaks of glycidyl moieties are present as the two double doublets at 3.74 and 3.43, due to protons of methylene linked to the ether group, a sextet at 3.14 ppm due to methyne proton of oxirane ring and two double doublets, at 2.76 and 2.59 ppm, due to protons of methylene on oxirane. The spectrum reported in **Fig. 2.1** is in agreement with the one reported by Hu et al.[3].

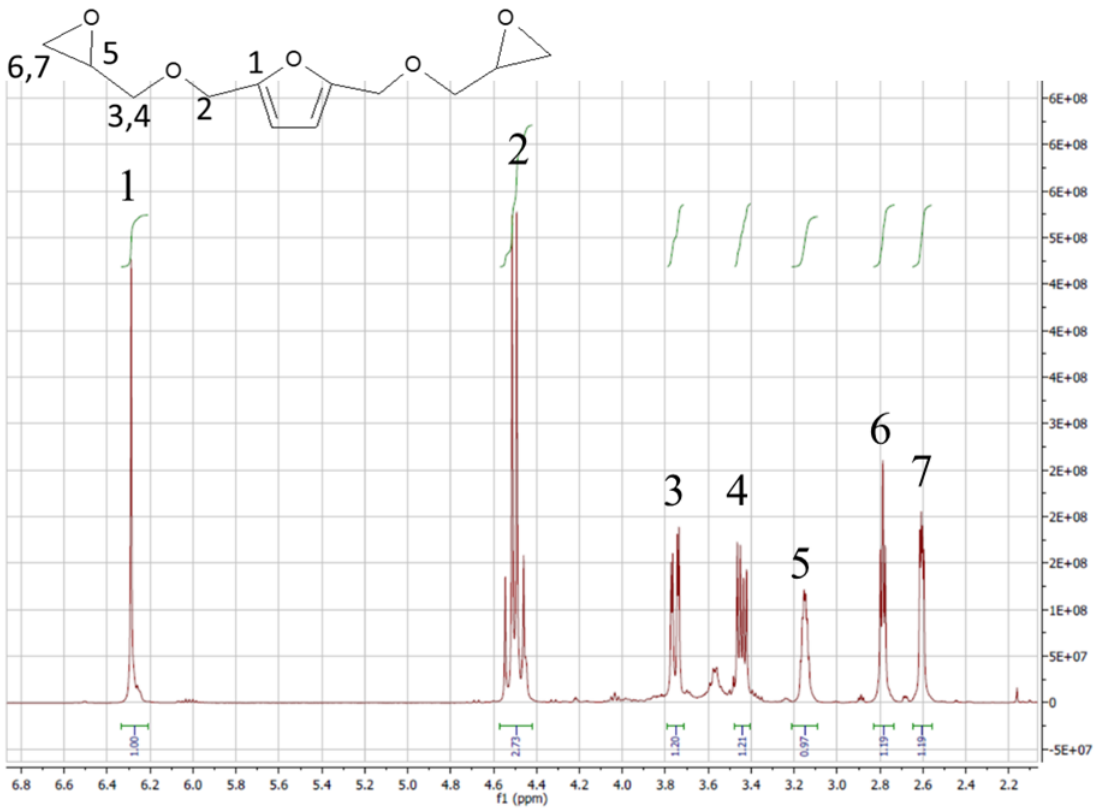

Fig. 2.1 ^{1}H-NMR spectrum of BOMF

The so-obtained BOMF was fully characterized by FTIR-ATR analysis.

As can be noticed in **Fig. 2.2** the band at 3500 - 3000 cm^{-1} characteristic of BHMF disappeared, due to the formation of a new ester bond, associated to C-O stretching band at 1075 cm^{-1}, and the epoxy band between 900 and 700 cm^{-1} appeared in BOMF spectrum.

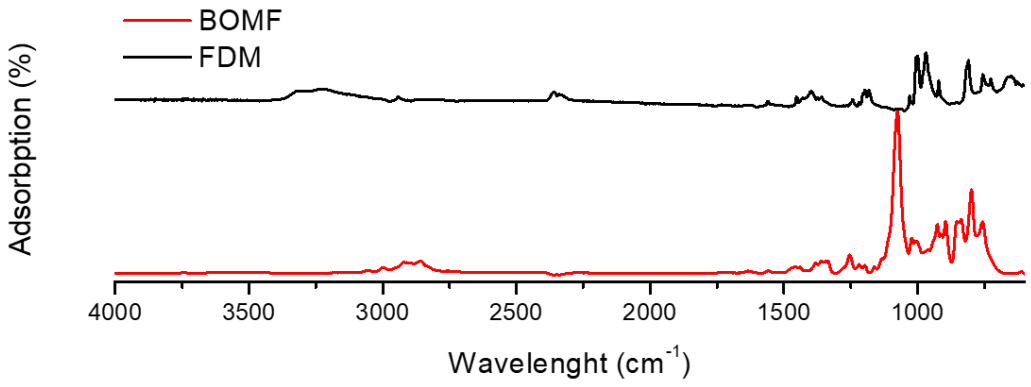

Fig. 2.2 FTIR spectra of BOMF and FDM

2.3 Characterization techniques

2.3.1 Processing and characterization methods of BOMF/MA adhesive system

A TA Instrument DSC Q2000, equipped with refrigerator cooling system (RCS), was used for calorimetric analysis (DSC), under inert nitrogen flux (50mL min^{-1}). Dynamic measurements from 25 to 250°C at 10°C/min heating rates and isothermal analysis at 120°C, 150°C, for 120 minutes were performed to evaluate the enthalpy of the curing process (ΔH_{tot}). A cooling scan at 10°C/min to -30°C and a second heating scan a 10°C/min to 250°C were performed on all the samples to detect the T_g of the cured resins and the potential occurrence of a post-cure. Numerical analysis was performed using Origin software.

Kinetic studies on the polymerization processes of BOMF/MA and DGEBA/MA blends were conducted from DSC data. The heat flux (dH/dt) detected during the analysis was considered directly proportional to the conversion rate (dα/dt) through the Equation 1:

$$\frac{d\alpha}{dt} = \frac{1}{\Delta H_{tot}} \frac{dH}{dt} \quad (1)$$

where ΔH_{tot} is the heat needed to complete the reaction, evaluated by the DSC dynamic analysis.

Consequently, the relationship between the degree of conversion (α) and the ΔHt heat developed during the chemical reaction is given by Equation 2:

$$\alpha = \frac{\Delta H_t}{\Delta H_{tot}} \quad (2)$$

A MARS III rheometer, interfaced with a iN20 Nicolet FT-IR spectrophotometer by a Rheonaut temperature controller, was used to performed combined rheological and infrared analysis. Chemo-rheological tests were performed on plate-plate geometries (20 mm diameter and 0.6 mm gap) at a fixed

frequency (ω) of 10 rad/s and deformation (γ) in auto-strain mode of 15% ± 15%. Measurements were performed in isothermal analysis at 150 °C for the system BOMF/MA.

Simultaneously to the rheological measurements, FT-IR analysis was carried out on the reacting mixtures. Spectroscopic analysis was performed in ATR mode. Spectra were acquired as single beam spectra in the range of 4000-400 cm^1 with a resolution of 4 cm^{-1} and 8 scans; before each analysis, different background spectra were collected at different temperatures in the above-mentioned temperature range. Data were first processed with Omnic software to subtract the appropriate background, then spectra were exported to the PerkinElmer TimeBase software to perform the time-dependent analysis (**Fig. 2.3**).

Fig. 2.3 Rheometer MARS III, iN20 Nicolet FT-IR spectrophotometer

Thermogravimetric analysis (TGA) was performed by using a TA Instrument TGA 500. Tests were carried out from 25°C to 750°C at a heating rate of 10°C/min; different measurements were performed under a 60mL min^{-1} nitrogen.

Tensile tests on bulk materials were performed by using an INSTRON 5564 with 1kN dynamometer. Three specimens for BOMF/MA and DGEBA/MA

systems were tested with 2 mm/min crosshead speed in environmental conditions of 23 °C and 60% humidity.

Three 'dog-bone' specimens were prepared per formulation with a width of 4 mm and a useful length L_0 of 25 mm, as shown in **Fig. 2.4**.

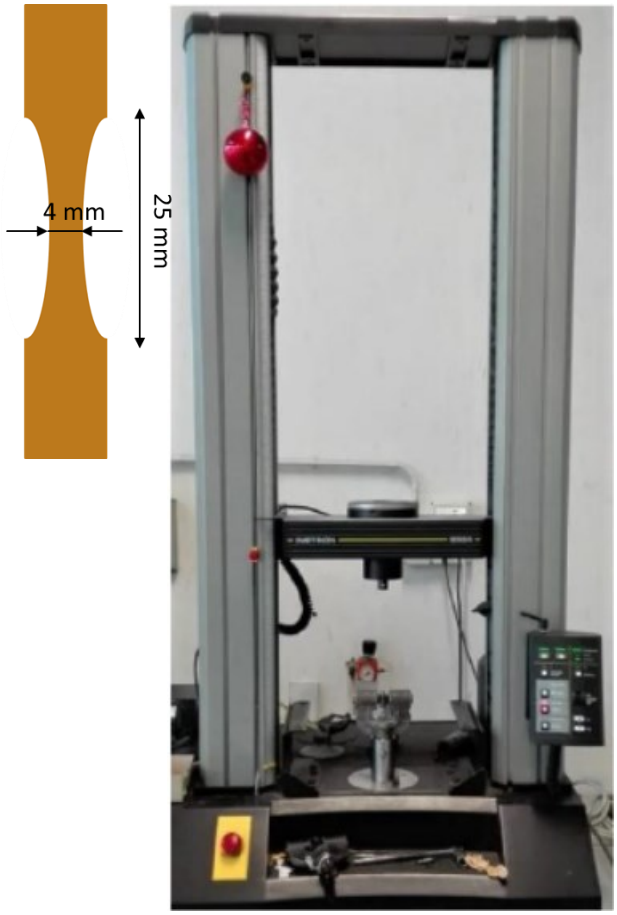

Fig. 2.4 Dog-bone specimen and Instron Machine 5564

The above BOMF/MA mixture containing 0.5 wt% of 2-MI was also used to prepare specimens for single lap-shear tests. For this purpose, joints of epoxy-based CFRP substrates were bonded with the BOMF/MA mixture. CFRP plates, 3 mm thick, were cut to obtain samples with length 100 mm and width 16 mm. To improve the wetting of the substrate with the resin mixture, the plates were mechanically sandblasted. Three drops of the resin mixture (about 73 mg) were applied on the end part of one plate, and

distributed over an area of 16x16 mm^2. The second plate was then applied. The adhesive thickness between the two adherends was about 0.2 mm. The joint specimens were cured in oven applying the same curing program used for bulk samples and no pressure was applied on the overlapped area of the plates to prevent leakage of the liquid non-crosslinked resin. Samples for single lap-shear tests were prepared with the same procedure using the DGEBA/MA mixture as adhesive.

Single lap shear tests of adhesive were performed according to ASTM D1002 using an Instron 4505 dynamometer equipped with 100 kN loading cell. Three specimens for both systems BOMF/MA and DGEBA/MA were testes with 1.3 mm/min crosshead speed in environmental conditions of 25°C and 50% humidity. The joints were 16x100 mm^2 in size and were adhered in an area of 16x16 mm^2, as shown in **Fig. 2.5.**

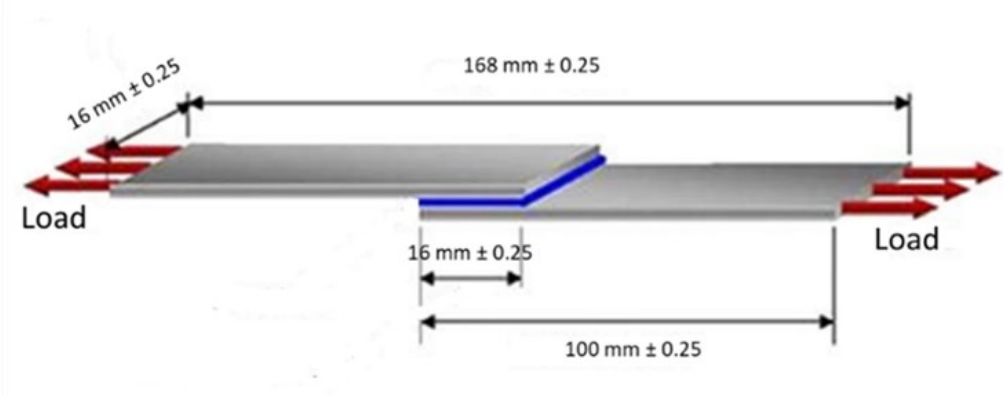

Fig. 2.5 Lap shar test specimen

Scanning electron microscopy (SEM) by means of a FEI Quanta 200 FEG SEM in high vacuum mode was carried out on the samples after lap shear tests.

To evaluate the failure surfaces of three specimens for both systems BOMF/MA and DGEBA/MA after lap shear tests a Lynx EVO stereomicroscope (Vision Engineering Ltd, Milan, Italy) was used.

2.3.2 Processing and characterization methods of BOMF/MA nanofiber systems

BOMF/MA system characterized as described in Section 2.3.1, has been used to obtain electrospun nanofibers.

PLA was chosen as the 'sacrificial polymer' to obtain a core-shell nanofibers.

The epoxy resin mixture was electrospun without solvents, while 20 wt.% PLA was dissolved in chloroform ($CHCl_3$) and dimethylformamide (DMF).

Electrospun fibres were obtained with an NF103 electrospinning equipment from MECC Co. (Fukuoka, Japan) using a coaxial nozzle and plate collector. After optimisation of the process parameters, illustrated below, the flow rate was set at 0.4 mLh^{-1} for the epoxy resin and 1 mLh^{-1} for the PLA solution. The applied voltage and the distance between the nozzle and the collector, covered by aluminum foil, were adjusted to 30 kV and 30 cm, respectively, in order to obtain defect-free fibres for further characterization. Electrospinning was conducted at room temperature and 10% relative humidity. With the collector stationary, randomly oriented mats of in-plane fibres were observed.

The fibres obtained were cross-linked in oven for 2h at 140 °C and then washed in chloroform for 3h, at room temperature, under magnetic stirring.

The three systems: PLA/epoxy uncured, PLA/epoxy cured and PLA/epoxy washed fibres were thermally characterized by differential scanning calorimetry (DSC) and thermogravimetric analysis (TGA).

Dynamic measurements from -30 to 200°C at 5°C/min heating rates. A cooling scan at 5°C/min to -30°C and a second heating scan a 5°C/min to 200°C were performed on all the samples to detect the T_g of the cured resins and the potential occurrence of a post-cure.

Thermogravimetric tests (TGA) were carried out from 25°C to 700°C at a heating rate of 10°C/min; different measurements were performed under a 60mL min^{-1} nitrogen.

The morphology of all systems was observed by scanning electron microscopy (SEM).

Fourier transform infrared spectroscopy (FTIR) analysis was performed in ATR (Attenuated total reflection) modality with a Perkin-Elmer Spectrum 100 spectrometer (Waltham, MA, USA). Spectroscopic manipulation was done with OMNIC 9 software (Thermo Fisher Scientific, Inc, Waltham, MA, USA).

Static contact angles (CA) of water on different substrates were measured by the sessile drop method with the help of FTA 1000B (First Ten Ångstroms) instrument. Measurements were performed at room temperature depositing distilled water drops of 5μL and evaluations of the contact angle were performed directly with the FTA32 Video 2.1 software.

2.3.3 Processing and characterization methods of conductive BOMF/IPD bulk and nanocomposites samples

BOMF/IPD mixtures at different BOMF/IPD molar ratio (1:1, 1.5:1 and 2:1 molar ratio) were thermally characterized by differential scanning calorimetry (DSC) in the same conditions described in Section 2.3.1.

Oven-cured BOMF/IPD bulk samples were analyzed by DSC to evaluate the T_g of the materials. DSC measurements were carried out from 0 °C to 250 °C, at heating rate of 10 °C/min under 30 mL min^{-1} nitrogen flow.

Bulk samples were also characterized by thermogravimetric analysis (TGA) by using a TA Instrument TGA 500. TGA tests were carried out from 25 to 750 °C at a heating rate of 10 °C/min, under a 60 mL min−1 nitrogen flow.

Tensile tests on bulk materials were performed by using an Instron 5564 dynamometer equipped with a 1 kN loading cell on specimens 40 x 10 x 1 mm3. Three specimens were tested for each sample. Tests were performed at 2 mm/min crosshead speed, at 23 °C and 50% relative humidity.

Nanocomposite samples at variable CNT loadings (1.0, 2.5, 5.0, 7.5 phr) were prepared as follows. Suitable amount of CNT were dispersed in chloroform (BOMF/chloroform ratio about 1 g/ 20 ml) by sonication with a Sonics Vibracell ultrasonic processor (Newton, USA) (500 W, 20 kHz), at 25% of amplitude for 20 min, with 10 s/20 s on/off cycles. Then, the chloroform was evaporated and the

suitable amount of IPD corresponding to the selected formulation was added. The specifications of the MWCNTs used and the sonication test conditions are shown in **Fig. 2.6**.

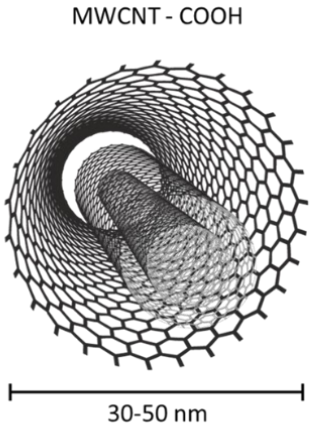

Outer Diameter	30-50 nm
Insider Diameter	5-10 nm
Ash	<1.5 wt.%
Purity	>95 wt.%
Functional content	0.70 wt.%
Length	10-20 µm
Specific Surface Area	60 m^2/g
Electrical Conductivity	>100 S/cm

Time	**Cycles ON/OFF**	**Amplitude**
20 min	10 s ON/20 s OFF	25%

Fig. 2.6 Specifications of the MWCNTs used and the sonication test conditions

Thin films (thickness about 0.2 mm) were obtained by applying the mixtures on a polytetrafluoroethylene substrate and curing them for 2h at 80°C with a post-cure step at 160 °C for further 2 h.

First, the films were used to evaluate the electrical percolation threshold of CNT. Volume conductivity measurements were carried out by a Keithley Electrometer/High resistance meter Model 6517A coupled with the Resistivity Test Fixture Model 8009 (**Fig. 2.7**). Circular disks (6 cm diameter) were placed between the test fixture electrodes and the conductivity was measured using an alternating voltage between -100 V and +100 V, switching from positive to

negative potential every 30 s. The conductivity was measured 8 times for each sample discarding the highest and the lowest measures.

Fig. 2.7 Keithley Electrometer/High resistance meter Model 6517A coupled with the Resistivity Test Fixture Model 8009

The morphology of nanocomposite films was analyzed by scanning electron microscopy (SEM) in high vacuum mode on the samples using a SEM FEI Quanta 200 FEG operating at 10 kV acceleration voltage and using a secondary electron detector. Before SEM observations, samples were mounted on aluminum SEM stubs and sputter coated with gold/palladium (about 10 nm thickness). By comparison, the neat resin was also analyzed in the same conditions.

Joule heating tests were performed on nanocomposite films by a Keithley 2450 multimeter operating at different voltages (3, 5, 10, 20 V), monitoring the temperature of the samples with an infrared thermal camera (FLIR Systems, Thermo Vision A40M). Copper tapes were applied to the ends of the samples to ensure good electrical contact. The size of the tested samples was about 5 x 5 cm^2 and the distance between the clamps was 4 cm. A region of area 1 cm^2 equidistant from the two clamps was observed and the average temperature was monitored. Each voltage was applied and maintained for a time of 5 minutes until the temperature plateau was reached. After that the voltage was lowered to the

immediately previous voltage value and kept for 5 minutes until the plateau temperature was reached.

2.3.4 Processing and characterization methods of conductive BOMF/IPD coated cotton fabrics

Cotton fabrics specimens (about 6 × 6 cm^2) were dip-coated with epoxy resin precursors/CNT dispersions in chloroform at 2.5 and 5 phr CNT loading prepared as detailed in Section 2.3.3.

By comparison, the BOMF/IPD solution was applied using the same conditions. For these applications, the dry content of the dispersions (CNT + BOMF + IPD or BOMF + IPD) was fixed at 5 wt%. Three subsequent impregnations were carried out for each composition. Each dipping treatment was prolonged for about 1 min until, then the sample was blotted on filter paper and then the solvent was let to evaporate. The impregnated cotton samples were then treated in oven at 80 °C for 2 h and 160 °C for further 2 h, in order to promote the curing of the epoxy resin (**Fig. 2.8**).

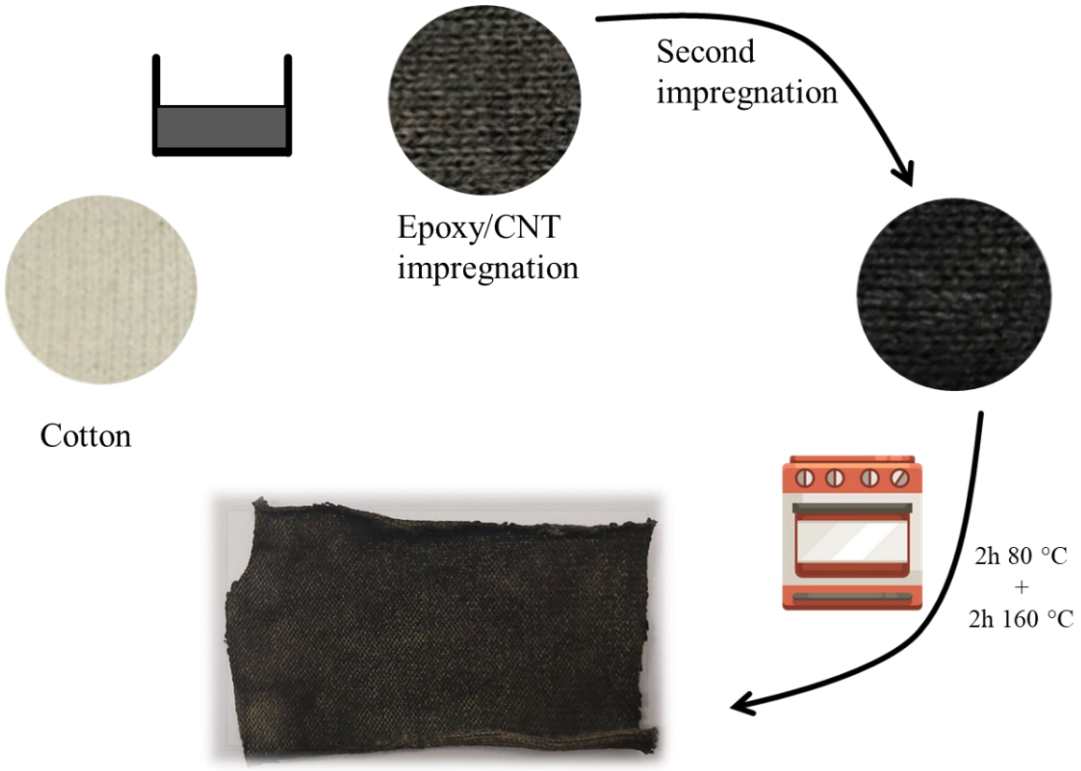

Fig. 2.8 Procedure for obtaining cotton impregnated with epoxy resin/CNT

The morphology of coated cotton fabrics after the curing of the neat resin was observed by SEM under the same conditions used to analyze the neat resin and nanocomposite samples.

To assess the wettability of treated and untreated fabrics, measurements of static contact angles (CA) of coated cotton fabrics were measured by the sessile drop method with a First Ten Ångstroms 1000B instrument. Measurements were performed at room temperature, and evaluations of the contact angle were performed directly with the FTA32 Video 2.1 software. For the measurements, distilled water drops of 10 μL were deposited on the cotton surfaces.

Breathability tests were performed on cotton, pristine-coated cotton, 2.5phrCNT resin-coated cotton and 5phrCNT resin-coated cotton using the ASTM E96 vertical cup standard at 25 °C and 50% RH.

Joule heating tests on coated fabrics were performed under the same conditions used for nanocomposite films. The dimensions of the samples analyzed were 5 x 5 cm^2.

The temperature change response of cotton fabric impregnated with 5phrCNT was observed by cyclically applying a voltage of 20V with an on/off ratio of 5 minutes for 10 cycles, in order to highlight the repeatability of the fabric heating process.

Finally, a thermochromic ink was applied to the surface of the coated cotton fabric to obtain a visual demonstration of the Joule heating behaviour of the samples.

References

1. Cho JK, Lee JS, Jeong J, et al. Synthesis of carbohydrate biomass-based furanic compounds bearing epoxide end group(s) and evaluation of their feasibility as adhesives. *J Adhes Sci Technol* 2013; 27: 2127–2138.

2. Garcia FG, Soares BG. Determination of the epoxide equivalent weight of epoxy resins based on dig...: UDiscover. *Polym Test* 2003; 22: 51–57.

3. Hu F, La Scala JJ, Sadler JM, et al. Synthesis and characterization of thermosetting furan-based epoxy systems. *Macromolecules* 2014; 47: 3332–3342.

Chapter

3 Bio-based Furan/Maleic Anhydride Epoxy Resins with Enhanced Adhesive Properties

3.1 Introduction

As discussed in Chapter 1, in recent decades, the interest towards the development of high performance polymers obtained from biomasses has significantly grown with the aim of progressively replacing materials obtained from non-renewable resources [1] and reducing their eco-toxicity. A particular concern is devoted to Bisphenol A (BPA) that is the most used precursors for the synthesis of epoxy resins thanks to its molecular rigid structure [2]. Epoxy resins based on BPA are extremely resistant to corrosion, moisture and chemicals, have good adhesive strength toward most materials and exhibit low shrinkage upon curing, which is a strict requirement for composite industries. For these reasons, BPA-based epoxies are used for protective coatings [3], as thermosetting matrices in composites for boating, wind turbines, and aircrafts [4], as well as structural adhesives [5]. In this latter field, epoxies represent the largest share in all those applications where high strength bonds are required [6]. However, BPA has serious toxic effects on human health, therefore, the necessity to find non-toxic and sustainable building blocks to replace BPA in the production of epoxy resins results mandatory. Therefore, the pivotal challenge is to develop suitable safe bio-based compounds, which also meet the high technical and safety requirements of downstream applications. In the specific field of biobased epoxy resins for structural adhesives, few example have appeared in literature. For example, Li et al. synthesized an epoxy resin starting from liquefied banana stem cured with a polyamide, to get an adhesive for wood materials. The joint had a shear strength comparable to that of diglycidyl ether of BPA (DGEBA)-based epoxy resins, and excellent resistance to organic agents and acid and alkaline environments [7]. Aziz et al. synthesized a bio-based epoxy reinforced with cellulose nanocrystals (CNC). The presence of native CNCs greatly improved the tensile modulus and the bonding performance of the bio-based epoxy resin in the interface area [8]. In another work, a bio-based triglycidylamine was synthetized and reacted hyper-branched aminated polysaccharide to create a new sustainable adhesive for plywood manufacturing [9], while the only example of the use of a sustainable epoxide adhesive for bonding

carbon fiber reinforced polymer (CFRP) has been recently reported by Tomić et al. who synthesized a renewable epoxy from tannic acid [10].

In the last years, furan-based epoxy compounds obtained from carbohydrates are regarded as alternatives to petroleum-based formulations for adhesive applications. This is the case of 2,5-bis[(oxiran-2-ylmethoxy)methyl]furan (BOMF), a compound derived from 5-hydroxymethylfurfural (HMF), which is one the most important platform molecules produced from sugars via biological or chemical conversions. As an example, BOMF-derived epoxy resins have been used for bonding polycarbonate substrates, exhibiting a tensile-shear strength higher than that of a petrochemical-based phenyl glycidyl ether [11].

In one of our previous works, BOMF has been cured with methyl nadic anhydride (MNA). Curing behaviour and physical properties were tuned by varying the reacting mixture formulations [12]. Moreover, by the inclusion of selected percentages of titanium oxide, it was possible to develop functional coatings for metallic substrates with improved corrosion resistance [13].

In the present Chapter, as a further step to address challenges of sustainability in the production of bio-sourced epoxy resins, we report the preparation of a bioepoxy system by curing BOMF with maleic anhydride (MA). The latter is also easily derived from HMF [14], via oxidative C–C bond cleavage of 5-hydroxymethylfurfural, by using homogeneous and heterogeneous catalytic systems working under green conditions [15].

BOMF and MA were cured in the presence of 2-methylimidazole as catalyst. The crosslinking process was monitored by differential scanning calorimetry (DSC) and chemo-rheological analysis. On crosslinked samples thermal, mechanical and adhesives properties in carbon fiber-reinforced thermoset (CFRP) joints were evaluated and compared to those of a BPA-based system. The remarkable adhesion properties of BOMF/MA towards CFRP joints highlighted the potential of furan-based epoxy resins as structural adhesives.

3.2 Formulation and preparation of BOMF/MA samples

BOMF was synthesized according to a modified procedure described in a previous work [11,12]. The total yield of the synthesis was 85%. At room temperature the obtained product was an amber-colored viscous liquid.

Epoxy/anhydride reaction mixture was prepared by mixing BOMF epoxy monomer and maleic anhydride in a stoichiometric ratio R=1, where R denotes the ratio between the number of moles of the epoxy monomer (BOMF) and the crosslinking agent (MA), with 2-MI used as initiator (0.5 wt% with respect to the total weight of the epoxy and anhydride mixture). The reaction mixture was labelled as BOMF/MA.

As a general procedure, a mixture containing the proper amounts of epoxy monomer and 2-MI was prepared at room temperature under magnetic stirring. After about 25 minutes, when the mixture of epoxy and 2-MI was homogeneous, the proper amount of MA was added to the system under magnetic stirring until homogeneous dispersion of MA in the viscous mixture. With the same procedure, DGEBA/MA mixtures were realized for comparison.

Starting from the above BOMF/MA mixture containing 2-MI as initiator, samples of bulk material (dimension about 70 mm x 60 mm x 1 mm) were obtained for mechanical tests and thermal analysis. A cure program consisting of heating at 120 °C for 20 min and post-cure at 150°C for further 2 h was applied. DGEBA/MA bulk samples were realized for comparison.

3.3 Kinetic studies

Using the equations (1) and (2), which were applied to data acquired by DSC, the curing reactions of BOMF/MA and DGEBA/MA blends were investigated.

Crosslinking of epoxies with anhydrides typically includes an initiation step consisting in the nucleophilic attack of the secondary nitrogen of the initiator to the anhydride (**Scheme 3.1**), which leads to the formation of an intermediate zwitterion containing a quaternary nitrogen cation and a carboxylate [16,17]. Subsequently, in the propagation step, the carboxylate reacts with the epoxy ring to form ester groups and an alkoxide anion. The latter propagates the chain growth

through an alternating anionic polyesterification mechanism. The development of the crosslinked structure also involves the etherification reactions of the hydroxyl group generated by the epoxy ring opening and the unreacted epoxy [18,19,20].

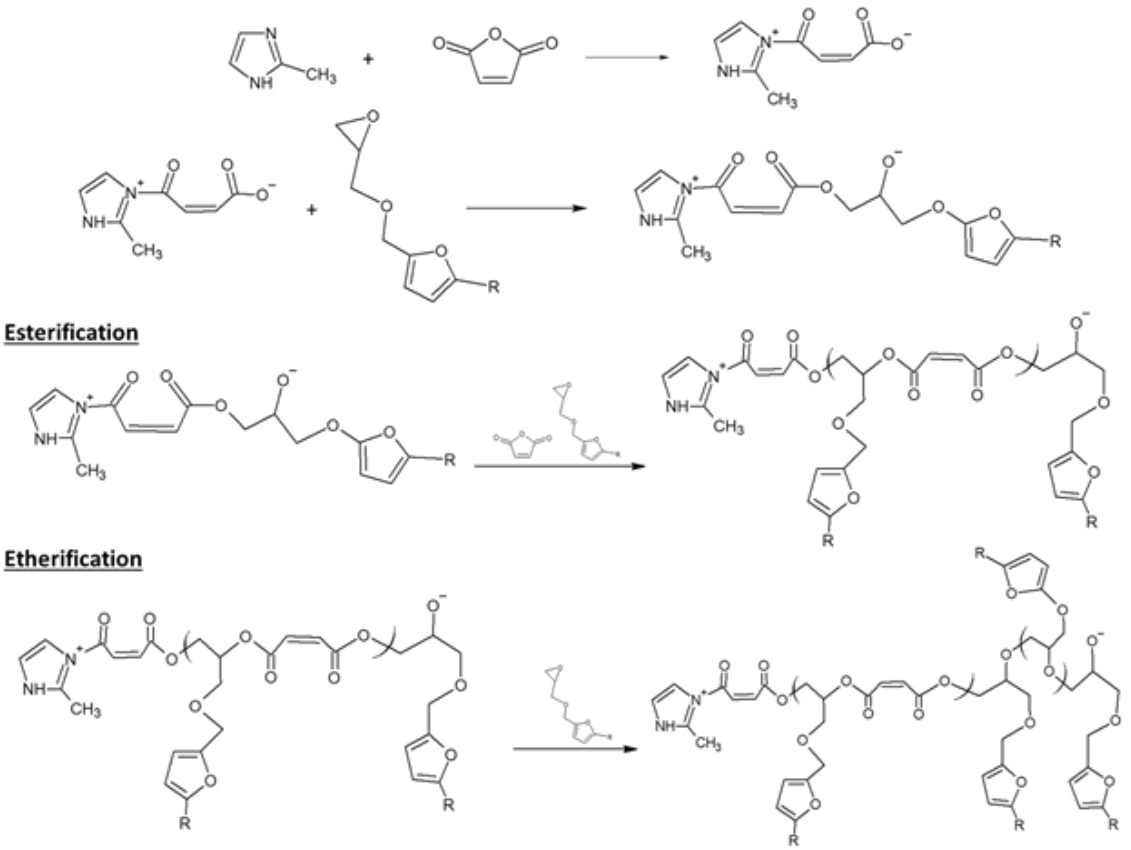

Scheme 3.1. Mechanism of epoxy−anhydride polymerization reactions initiated by tertiary amines.

The curing behavior of BOMF/MA was first studied by DSC under non-isothermal conditions to select the suitable temperature condition to polymerize the bulk materials. DGEBA/MA was selected as reference system. **Table 3.1** reports the temperature values of the onset (T_{onset}) and the maximum (T_p) of the exothermic curves and the reaction enthalpy (ΔH_{tot}) associated to the curing process, as well as the glass transition (T_g) temperatures for both systems [21]. The first heating scan (**Fig. 3.1a**) exhibited a single peak for DGEBA/MA at 145 °C, whereas BOMF/MA displayed an exothermic curve with a maximum at 143 °C and a higher temperature shoulder at 163 °C (labeled as P1 and P2), attributed to esterification and etherification reactions, respectively [18]. The lower T_{onset} value for the BOMF-

based system suggests a higher reactivity towards MA in comparison to the DGEBA counterpart. From the second heating ramp glass transition values were calculated (**Table 3.1**), and the occurrence of a residual cure was ruled out.

Table 3.1. Curing reaction data inferred from DSC under non-isothermal conditions.

	ΔH_{tot} [J/g]	T_{onset} [°C]	T_P [°C]	T_g [°C]
BOMF/MA	326	113	143-163	39
DGEBA/MA	265	124	145	55

A higher value of ΔH_{tot} was noticed for BOMF/MA, due to the higher number of epoxy groups per mass unit in BOMF compared to DGEBA. Nonetheless, the T_g value of the cured BOMF/MA resin was about 15 °C lower than that of DGEBA/MA, likely due to the higher chain stiffness of the latter [13].

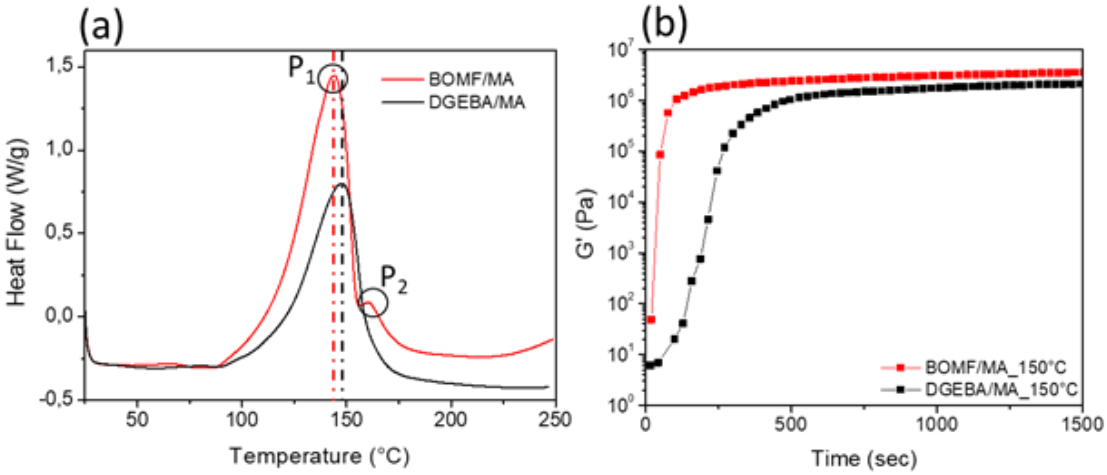

Fig. 3.1. a) Non-isothermal DSC thermograms at a heating rate of 10 °C/min of BOMF/MA and DGEBA/MA; b) Rheological tests on BOMF/MA and DGEBA/MA at 150 °C

3.4 Rheological behavior

On the basis of the above reported results, T = 150 °C was chosen as the temperature for isothermal rheological tests, performed to get further insight on the development of the viscous epoxy networks. The evaluation of the storage

modulus G' reported in **Fig. 3.1b** demonstrated a faster evolution of the viscoelastic properties for BOMF/MA, and the attainment of a plateau value of about 106 Pa in the early five minutes. In comparison, DGEBA/MA required about 10 minutes for G' to reach comparable values, confirming a slower reactivity of this system.

Rheological results were complemented by the data gained through FTIR-ATR spectroscopy performed on samples undergoing rheological measurements. The absorbance variation of characteristic peaks belonging to functional groups involved in the curing reaction were monitored as a function of time.

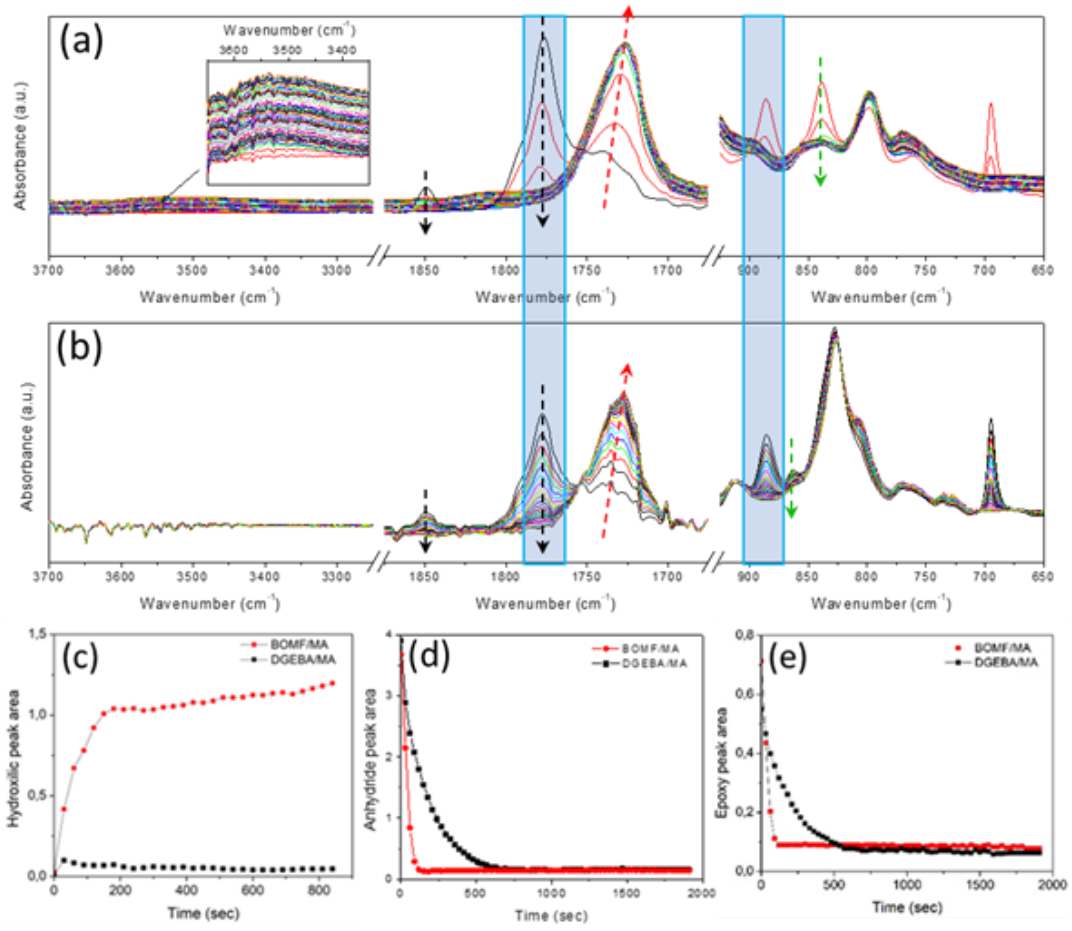

Fig. 3.2. Time evolution of FTIR-ATR spectra of BOMF/MA (a) and DGEBA/MA (b) systems in the wavenumber regions between 3700−3200 cm^{-1}, 1900−1650 cm^{-1} and 900−650 cm^{-1}; areas of hydroxyl groups peak (c), anhydride carbonyl group (d), and epoxy groups (e), as evaluated from ATR FT-IR spectra collected during the rheological measurements at 150 °C.

In **Figs. 3.2a,b** the presence of anhydride in the reacting systems is identified by the peaks at 1849 and 1777 cm^{-1} (see black arrows). These peaks were used to follow the curing process, as they gradually disappeared over time due to the reaction between epoxy and anhydride, which led to the formation of ester groups associated to the increasing peak at 1731 cm^{-1} (indicated by the red arrow). From **Fig. 3.2a** is noted that the peak area increase was accompanied by a shift to lower wavenumbers, indicating the progressive increase of polar interactions between ester carbonyl groups and hydroxyl groups formed upon epoxide ring opening [22]. Moreover, in the spectral region between 950 cm^{-1} and 650 cm^{-1}, two peaks at 838 cm^{-1} and 862 cm^{-1} (see green arrows) were followed to monitor the consumption of the epoxy groups in BOMF and DGEBA, respectively.

The change of anhydride and epoxy group peak areas over time are reported in **Figs. 3.2d,e**. Notably the disappearance rate the two groups was similar, further corroborating the validity of the hypothesized alternating copolymerization mechanism [23]. The conversion rate of anhydride and epoxy groups in DGEBA/MA was significantly slower than that of BOMF/MA. In the latter case, both groups completely converted in less than two minutes, while DGEBA/MA required about ten minutes to achieve reacting groups conversion. This result confirmed the higher reactivity of the BOMF/MA mixture already observed by DSC and rotational rheometry. As expected, the two systems show different reaction rates, as the carbonyl formation of BOMF/MA was faster than that of DGEBA/MA.

An even more different trend was observed as concerns the evolution of hydroxyl groups (**Figs. 3.2a,c**). In particular, in the early two minutes the BOMF/MA system exhibited an increasing absorption in the 3700-3300 cm^{-1} wavelength range as a function of time, characteristic of the formation of hydrogen bonded hydroxyl groups. Interestingly, the spectrum of the DGEBA/MA system did not show any peak in this range. This result suggests that a larger number of growing chains was present in the BOMF/MA mixture, likely due to a more efficient initiation process. A similar finding has been reported by Shen et al., who observed that when BOMF was cured with diamines, a greater amount of hydroxyl groups formed in comparison with those formed upon curing of phenyl-based epoxy counterparts [20].

This result was attributed to the presence of oxygen atoms on the furan ring, which act as efficient proton acceptors, thereby favoring –OH hydrogen bonding.

The difference in reactivity between the two systems was further confirmed by non-isothermal rheological tests from 35 to 200°C, at 3°C/min and 1 Hz frequency. The elastic moduli G' evaluated on bulk samples at the temperature of 150 °C were 10010 Pa for BOMF/MA and 13220 Pa for DGEBA/MA. This means that BOMF/MA resin has a lower degree of crosslinking, so once the hydroxyl groups are formed, their further reaction is hindered.

3.5 Thermal and mechanical properties of BOMF/MA thermosetting resin

Based on the information gained from DSC, the following curing conditions were selected for the preparation of the bulk resin samples: a 20 min pre-polymerization step at 120 °C, which was very close to the DSC onset temperature, was performed to increase the viscosity of the resin and preventing MA evaporation and associated bubbles formation within the bulk. Afterwards, the temperature was maintained for two hours at 150 °C to complete curing. The so cured samples were then characterized in their thermal and mechanical properties. **Table 3.3** summarizes the results gathered through DSC, TGA and tensile tests.

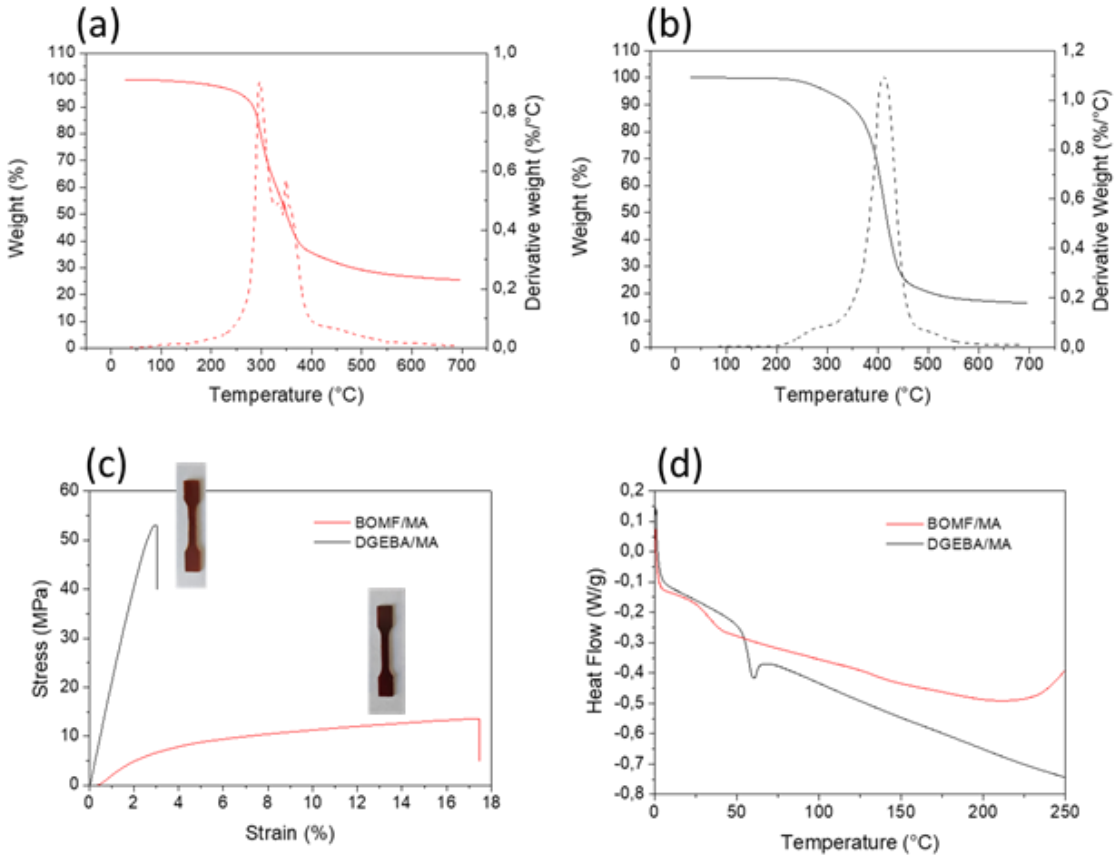

Fig. 3.3. Thermal and mechanical characterization of the cured samples. TGA thermograms of: a) BOMF/MA, b) DGEBA/MA, c) stress-strain curves of bulk materials, and d) second heating DSC scans performed on the bulk BOMF/MA and DGEBA/MA samples

The thermogravimetric curves obtained in nitrogen are reported in **Figs. 3.3 a,b**, For BOMF/MA, the derivative curve of weight (%) showed two steps of degradation peaked (T_p in **Table 3.3**) at 295 and 350°C, with weight losses of 50% and 20%, respectively (**Fig. 3.3a**). DGEBA/MA degraded in a single step, with a T_p of 415 °C, corresponding to a weight loss of about 50% (**Fig. 3.3b**). A comparison of the temperatures at 5% weight loss ($T_{5\%}$) values confirmed the lower thermal stability of BOMF/MA [24], which however, did not preclude its application at temperatures about 200 °C. Interestingly, BOMF/MA exhibited a higher char yield at 700 °C ($Char_{700}$), suggesting that it could perform better as far as flame retardant properties are concerned.

The glass transition temperatures were determined from the second heating DSC scan performed on the oven-cured samples, and DSC analysis did not show residual reaction (**Fig. 3.3d**). As expected, the graph shows the absence of residual exotherms, while the calculated T_g values were comparable the those obtained from non-isothermal DSC curing.

To evaluate the mechanical properties of the cured resins, tensile test experiments were carried out. Typical stress-strain curves of the thermosets are reported in **Fig. 3.3c**. From the experimental stress-strain curves, Young's modulus, stress and strain at peak were determined (**Table 3.3**). Compared to the DGEBA-based sample, BOMF/MA appeared rubbery, with a lower Young's modulus and ultimate strength but a quite higher ultimate strain value. Tensile test results indicate that BOMF/MA system is not suitable to replace the traditional DGEBA/MA system in those applications (such as composites) where high stiffness and strength are required, but can be used as an adhesive for applications requiring flexible substrates [25].

Table 3.3 Degradation temperatures at 5% ($T_{5\%}$) and 50% ($T_{50\%}$) weight loss, char yield at 700°C ($Char_{700}$), Young's Modulus (E'), stress (σ) and strain (ε) at peak of DGEBA/MA and BOMF/MA-based thermosets.

SAMPLES	T_g [°C]	$T_{5\%}$ [°C]	$T_{50\%}$ [°C]	$Char_{700}$ [%]	E' [MPa]	σ [MPa]	ε [%]
BOMF/MA	34	255	349	26	382±58	14±1	17±2
DGEBA/MA	56	200	416	16	2187±125	51±14	3±1

3.6 Adhesive tests (Lap shear test)

BOMF/MA and DGEBA/MA resins were applied on CFRP substrates at room temperature to prepare adhesive joints. The latter were cured in the oven for twenty minutes at 120 °C followed by two hours at 150 °C, using the same curing conditions used to prepare bulk samples. The adhesive properties were evaluated by lap shear test. **Fig. 3.4a** shows a schematic representation of the single lap joints (SLJ) prepared. As shown in **Fig. 3.4b**, the lap shear tests carried out on the BOMF/MA adhesive joint showed a maximum load of about 3100 N. At this value,

corresponding to a deformation of about 0.6 mm, the failure of the adhesive occurred. The maximum load showed by the BOMF/MA adhesive was dramatically higher than the value recorded for the DGEBA/MA, whose failure occurred at about 0.2 mm deformation, with a maximum load of about 750 N. Stress and strain-to-failure values of the analyzed formulations, listed in **Table 3.4**, are comparable with those reported in the literature [26,27].

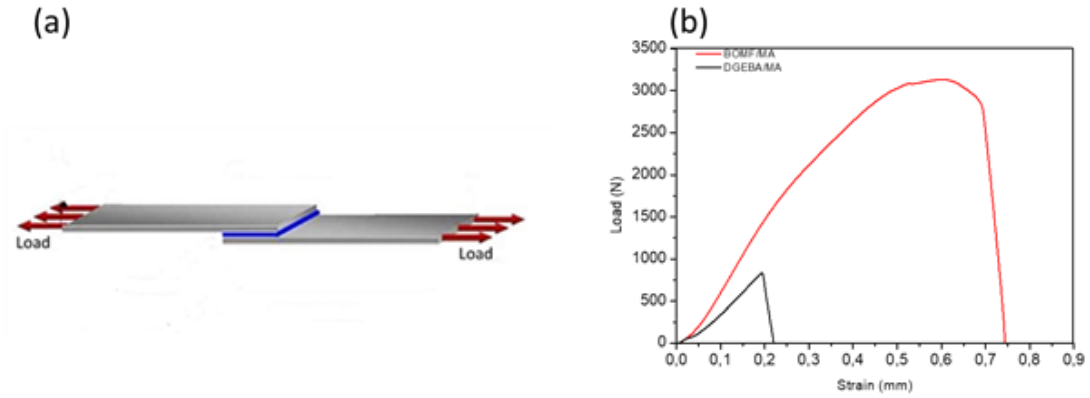

Fig. 3.4. a) Geometry (mm) of single-lap joints tested, b) Load-Strain curves obtained after lap-shear tests of BOMF/MA and DGEBA/MA.

Table 3.4 Summary of strain and stress at break for both sets of adhesive/CFRP specimens

Adhesive mixtures	Strain at break [mm]	Stress at break [MPa]
BOMF/MA	0.7 ± 0.2	13.3 ± 4.5
DGEBA/MA	0.2 ± 0.1	4.3 ± 1.7

3.7 Morphological analysis (SEM)

To explain the different behavior showed by BOMF/MA and DGEBA/MA systems, the morphology of the failure surfaces of the SLJ plates after lap shear tests were investigated by optical microscopy and SEM (**Fig. 3.5**).

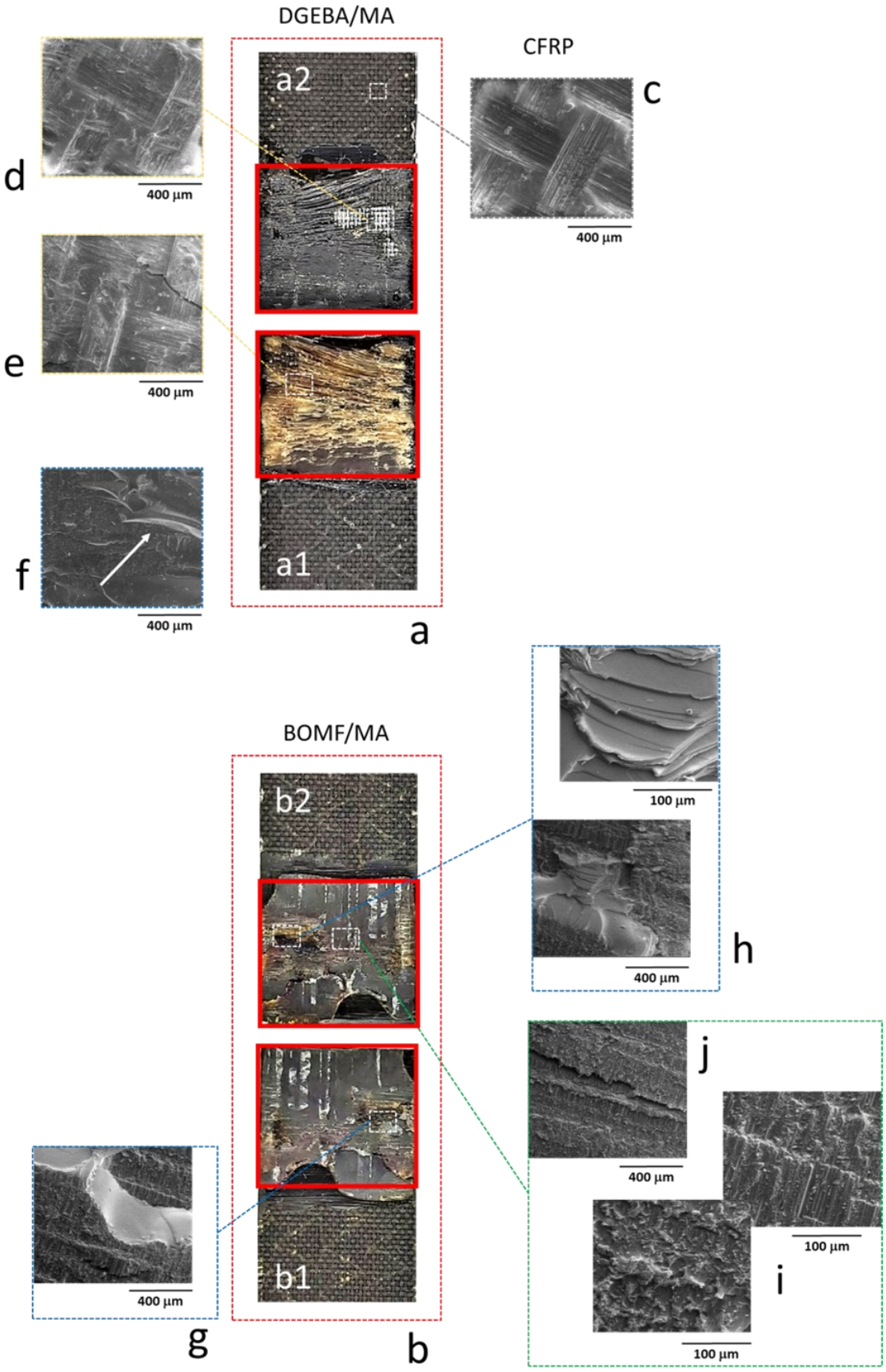
DGEBA/MA
CFRP
a2
a1
a
c
d
e
f
400 µm
BOMF/MA
b2
b1
b
g
h
i
j
100 µm

Fig. 3.5. Optical microscopy images (in red rectangles) of plates after lap shear tests on CFRP joints realized with DGEBA/MA (a) and BOMF/MA (b) adhesives. SEM images of the untreated CFRP surface (c); the plates surface after lap shear tests on CFRP joints realized with DGEBA/MA (d, e, f); the plates surface of the plates after lap shear tests on CFRP joints realized with BOMF/MA (g, h, i, j).

Fig. 3.5a and **b** show the optical images of the two plates of a SLJ realized by the DGEBA/MA adhesive and the BOMF/MA adhesive, respectively.

As shown, for the joint realized with DGEBA/MA (**Fig. 3.5a**) brown/yellow adhesive residues are mainly found on the adherend plate reported in the bottom image (a1), whereas the presence of adhesive residues is less evident on the other plate (a2). This is typical of an adhesive failure mechanism, for which the failure mainly occurs at one interface between the adhesive and the substrate. SEM analysis confirmed the prevalent adhesive failure mechanism for the SLJ realized with the DGEBA/MA adhesive. Indeed, **Fig. 3.5d** well shows the original composite texture on one of the plates after the DGEBA/MA adhesive detachment (see the original composite structure in **Fig. 3.5c** for comparison). On the other plate (**Fig. 3.5e**), the adhesive surface is evidenced, still adhered to the plate, showing the imprint of the composite texture after the failure. For this specimen, evidences of a cohesive failure mechanism of the DGEBA/MA adhesive are only noted in small regions, as SEM shows a brittle fracture occurring within the adhesive layer, evidenced with an arrow in **Fig. 3.5f**.

As for the SLJ realized with the BOMF/MA adhesive, the optical image (**Fig. 3.5b**) shows adhesive residues almost equally distributed on both adherends (b1 and b2) of the SLJ after the test, suggesting a predominant cohesive failure mechanism, typical of an adhesive well adhered on the substrates, whose failure occurs within the adhesive layer. SEM images confirmed this predominant mechanism, as both SLJ plates evidenced brittle fractures occurred within the adhesive layers (**Figs. 3.5g,h**). In addition, SEM images also showed some areas where the inner part of the CFRP substrate was visible, with carbon fibers protruding from the surface after the test (**Fig. 3.5i**) or pulled out from the substrate (**Fig. 3.5j**), indicating the

occurrence of adherend failure of the substrate in these regions [28]. Summarizing, a cohesive failure mechanism of the adhesive was predominant in BOMF/MA SLJ, with evidences of a cohesive failure of the substrate in some regions. This mechanism must be compared to the DGEBA/MA adhesive, whose failure mainly occurred through an adhesive failure mechanism. The behavior evidenced by microscopy clearly indicates a highly enhanced adhesion of the BOMF-based adhesive to the CFRP substrate that well explains the results of the lap shear test. The better adhesion of the BOMF/MA resin to the CFRP substrate is attributed to the larger number of hydroxyl groups formed upon curing of the BOMF/MA system, as evidenced by combined rheological and FT-IR tests (see **Fig. 3.2**). The increased interaction by the resin hydroxyl groups and the CFRP adherend substrate resulted in a remarkably higher failure strength, further confirming the key role of hydrogen bonding as a main adhesion mechanism to enhance the adhesion performance of epoxy based adhesives [10,29].

3.8 Conclusions

In the present work, a new fully bio-based epoxy resin was synthesized from a furan based epoxy monomer, namely 2,5-bis[(oxiran-2ylmethoxy)methyl]furan (BOMF) cured with maleic anhydride (MA). The curing behavior of the resin was investigated by thermal and chemo-rheological analysis, and the curing process of the system was optimized to obtain sheets. In comparison to traditional DGEBA-based epoxy monomer cured with the same anhydride, the BOMF/MA samples have a lower glass transition temperature, Young's modulus and ultimate tensile strength, but a higher ultimate strain. Thus, the BOMF/MA system is not suitable to replace the corresponding DGEBA/MA system in those applications (such as composites) where high stiffness and strength are required, but can be used for applications requiring more flexible materials.

Very interesting results were obtained when the BOMF/MA system was tested as an adhesive for fiber reinforced polymer composites. In this application, the BOMF/MA system shows highly enhanced properties in comparison to the traditional epoxy system based on DGEBA, with stress and strain-to-failure values

more than 3 times higher. These remarkable adhesive properties are well explained by the observation of the failure mechanism. Indeed, while the DGEBA/MA adhesive shows a predominant adhesive failure mechanism, with the failure mainly occurs at the interface between the adhesive and the substrate, the failure of the BOMF/MA adhesive mainly occurs through a cohesive failure mechanism, typical of an adhesive well adhered on the substrates. This highly improved adhesion of the BOMF/MA adhesive towards the epoxy based CFRP is explained by the presence of hydroxyl groups, formed during the curing of the BOMF/MA system and stabilized by the presence of the furan ring, able to strongly interact with the CFRP epoxy substrate.

References

1. Meier MAR, Metzger JO, Schubert US. Plant oil renewable resources as green alternatives in polymer science. *Chem Soc Rev* 2007; 36: 1788–1802.

2. Flint S, Markle T, Thompson S, et al. Bisphenol A exposure, effects, and policy: A wildlife perspective. *J Environ Manage* 2012; 104: 19–34.

3. Sørensen PA, Kiil S. Anticorrosive coatings : a review. 2009; 6: 135–176.

4. Jacob GC, Hoevel B, Pham HQ, et al. Technical advances in epoxy technology for wind turbine blade composite fabrication. *Int SAMPE Tech Conf*.

5. Kneafsey B. *Structural adhesives*. 2005. Epub ahead of print 2005. DOI: 10.1002/0470014229.ch17.

6. Prolongo SG, Del Rosario G, Ureña A. Comparative study on the adhesive properties of different epoxy resins. *Int J Adhes Adhes* 2006; 26: 125–132.

7. Li R, Li W, Zheng F, et al. Versatile bio-based epoxy resin: From banana waste to applied materials. *J Appl Polym Sci* 2019; 136: 1–8.

8. Aziz T, Fan H, Zhang X, et al. Adhesive properties of bio-based epoxy resin reinforced by cellulose nanocrystal additives. *J Polym Eng* 2020; 40: 314–320.

9. Zhang Y, Chen M, Zhang J, et al. A High-Performance Bio-Adhesive Using Hyperbranched Aminated Soybean Polysaccharide and Bio-Based Epoxide. *Adv Mater Interfaces* 2020; 7: 1–12.

10. Tomić NZ, Saleh MN, de Freitas ST, et al. Enhanced interface adhesion by novel eco-epoxy adhesives based on the modified tannic acid on al and CFRP adherends. *Polymers (Basel)*; 12. Epub ahead of print 2020. DOI: 10.3390/polym12071541.

11. Cho JK, Lee JS, Jeong J, et al. Synthesis of carbohydrate biomass-based furanic compounds bearing epoxide end group(s) and evaluation of their

feasibility as adhesives. *J Adhes Sci Technol* 2013; 27: 2127–2138.

12. Marotta A, Faggio N, Ambrogi V, et al. Curing Behavior and Properties of Sustainable Furan-Based Epoxy/Anhydride Resins. *Biomacromolecules* 2019; 20: 3831–3841.

13. Marotta A, Faggio N, Ambrogi V, et al. Biobased furan-based epoxy/TiO2 nanocomposites for the preparation of coatings with improved chemical resistance. *Chem Eng J* 2021; 406: 127107.

14. Wojcieszak R, Santarelli F, Paul S, et al. Recent developments in maleic acid synthesis from bio-based chemicals. *Sustain Chem Process* 2015; 3: 1–11.

15. Thiyagarajan S, Franciolus D, Bisselink RJM, et al. Selective Production of Maleic Acid from Furfural via a Cascade Approach Combining Photochemistry and Electro- or Biochemistry. *ACS Sustain Chem Eng* 2020; 8: 10626–10632.

16. Kumar S, Samal SK, Mohanty S, et al. Epoxidized Soybean Oil-Based Epoxy Blend Cured with Anhydride-Based Cross-Linker: Thermal and Mechanical Characterization. *Ind Eng Chem Res* 2017; 56: 687–698.

17. Kumar S, Samal SK, Mohanty S, et al. Study of curing kinetics of anhydride cured petroleum-based (DGEBA) epoxy resin and renewable resource based epoxidized soybean oil (ESO) systems catalyzed by 2-methylimidazole. *Thermochim Acta* 2017; 654: 112–120.

18. Park WH, Lee JK, Kwon KJ. Cure behavior of an epoxy-anhydride-imidazole system. *Polym J* 1996; 28: 407–411.

19. Xu L, Schlup JR. Resin / Amine Cure : An In Situ Study Using Near-Infrared Spectroscopy. *J Appl Polym Sci* 1997; 895–901.

20. Paramarta A, Webster DC. Bio-based high performance epoxy-anhydride thermosets for structural composites: The effect of composition variables. *React Funct Polym* 2016; 105: 140–149.

21. Park WH, Lee JK. A study on isothermal cure behavior of an epoxy-rich/anhydride system by differential scanning calorimetry. *J Appl Polym Sci* 1998; 67: 1101–1108.

22. Antoon MK, Koenig JL. Crosslinking Mechanism of an Anhydride-Cured Epoxy Resin As Studied By Fourier Transform Infrared Spectroscopy. *J Polym Sci A1* 1981; 19: 549–570.

23. Matejka L, Lovy J, Pokorny S, et al. Curing Epoxy Resins With Anhydrides. Model Reactions and Reaction Mechanism. *J Polym Sci A1* 1983; 21: 2873–2885.

24. Sammani A, Arabia S, Al-muaikel NS. Thermal properties of epoxy (DGEBA)/ phenolic resin (NOVOLAC) blends THERMAL PROPERTIES OF EPOXY (DGEBA)/ PHENOLIC RESIN (NOVOLAC) BLENDS.

25. Meredith HJ, Wilker JJ. The Interplay of Modulus, Strength, and Ductility in Adhesive Design Using Biomimetic Polymer Chemistry. *Adv Funct Mater* 2015; 25: 5057–5065.

26. Kadioglu F, Puskul H. Effects of Different Fiber Orientations on the Shear Strength Performance of Composite Adhesive Joints. *Int J Mater Metall Eng* 2016; 10: 65–68.

27. Liu S, Cheng X, Zhang Q, et al. An investigation of hygrothermal effects on adhesive materials and double lap shear joints of CFRP composite laminates. *Compos Part B Eng* 2016; 91: 431–440.

28. Nagoshi T, Harada Y, Nakasumi S, et al. Inherent cohesive failure of epoxy adhesive in carbon-fiber-reinforced plastic composites revealed by micro-tensile testing and finite element analysis. *Compos Part B Eng* 2022; 242: 110059.

29. Nakamura S, Tsuji Y, Yoshizawa K. Role of Hydrogen-Bonding and OH-πInteractions in the Adhesion of Epoxy Resin on Hydrophilic Surfaces. *ACS Omega* 2020; 5: 26211–26219.

Chapter

4 Electrospun Nanofibers based on Furan-based Epoxy/Maleic Anhydride Resins

4.1 Introduction

Polymer fibers can be obtained by dry spinning, wet spinning, melt spinning, gel spinning and electrospinning[1].

Dry spinning entails the ejection of fibers from a polymer solution, which undergoes solidification as the solvent evaporates [2], while wet spinning consists of removing the solvent by chemical means [3].

In melt spinning, temperature is used to melt the polymer to a viscosity suitable for extrusion from a spinneret, then the fibers solidify with cooling [4].

Gel spinning is a preparation method for high-strength, high-modulus fibers. After extrusion, the plasticized gel is cooled in solvent before elongation, so that an ultra-high modulus gel fiber is obtained [5]. All the techniques described above allow fibers with diameters of 10-100μm to be obtained, while the sub-micron scale remains difficult to achieve.

Electrospinning is a commonly employed manufacturing technique used to produce polymer-based fibers, featuring diameters spanning from a few micrometers to several tens of nanometers by means of a strong electrostatic field applied to stretch a polymer solution travelling from a reservoir (syringe) to a metallic collector [6,7]

Determining the optimal parameters for electrospinning is a necessary step that has to consider first of all solution parameters i.e. dielectric properties of solvent, that makes the solution electroresponsive, polymer molecular weight and concentration[8]. As well, equipment parameters have to be optimized as voltage, needle-to-collector distance and solution feed rate.

Thermoplastics are the most common polymer family used in electrospinning. In the case of thermosetting polymers such as epoxy resins, the electrospinning technique has not yet been widely used. The reason for this is the high reactivity of epoxy systems, which leads to rapid cross-linking and the consequent formation of a rigid 3D network and the fragility of these fibers.

Wang et al. in 2012 proposed a strategy to obtain epoxy resin nanofibers via a core-shell technique by coaxial electrospinning, using PVP as a polymer for the shell [9]. The core-shell morphology was used as a microreactor: due to the confinement

effect, hot polymerization took place in the core generating epoxy nanofibers with a diameter of 210 ± 60 nm. ATR-FTIR analysis revealed that the epoxy nanofibers showed no obvious differences to the casting film from the core solutions.

In a recent work [10], electrospun epoxy based fibers with diameters up to 3μm were obtained. The DGEBA epoxy system cross-linked with a primary amine was dissolved in methyl ethyl ketone (MEK) solvent. After that, during heating and mixing, the viscosity of the solution gradually increased because of crosslinking. until reaching the gelation point. When the solution started to show haziness, they considered the solution ready to electrospin.

A similar procedure was developed by Aliahmad et al. who produced submicron epoxy carbon nanotube (CNT) based filaments. In this case, to achieve a viscosity suitable for the electrospinning process and to maintain the shape of the fiber, partial polymerization of the epoxy is enhanced through mixing with the hardener at high temperature, without the addition of plasticizers[11]. The addition of CNT to the epoxy improved the mechanical modulus of the fibers by 49% and reduced the porosity of the manufactured filaments by up to 25%.

A hybrid multi-scale self-healing polymer matrix composite was developed by integrating co-electrophilic dicyclopentadiene (DCPD)/polyacrylonitrile (PAN) core-shell nanofibers at the laminate interfaces[12]. A 10wt.% PAN in DMF solution was prepared to generate the shell and a 10 wt % DCPD in DMF solution was prepared to generate the liquid core as healing agent. Once nanofiber breaks due to crack-opening, fiber stretching and pull-out induced breakage, the liquid healant stored in the core network is released. Thanks to the action of capillary force, it moves to crack fronts resulting in interfacial self-healing effect, and stiffness/strength recovery

In this chapter, the furan-based epoxy system BOMF/MA - characterized in Chapter 3 - was used for the fabrication of nanofibers by electrospinning. Due to the low viscosity and high reactivity of the BOMF/MA mixture, it was very difficult to obtain plain fibers by controlling the pre-polymerization step. Therefore, a core-shell morphology was investigated by using PLA as template

polymer: the PLA shell acts as mould to allow the confinement and polymerization of BOMF/MA core and then removed to obtain furan-based epoxy fibers.

4.2 Thermal analysis of electrospun core-shell PLA/epoxy fibers

Thermal properties of electrospun nanofibers performed by means of DSC analysis were evaluated to determine: the phase transitions of PLA/r uncured after electrospinning; the temperature of crosslinking of PLA/r cured in oven; the absence of residual curing of PLA/r washed fibers (after removal of the PLA shell by chloroform washing); the complete removal of the 'sacrificial' PLA shell.

During electrospinning, the PLA did not have time to crystallize completely; however, the high stretching level of polymer jet causes a high molecules alignment. Therefore, crystallization is enhanced during a subsequent heating step as it occurs in the DSC furnace. In fact, a cold crystallization peak is evident in the first run at 87°C for PLA fibers (**Fig. 4.1a)** whereas it disappears in the third run (**Fig. 4.1b)**. The annealing treatment at 140°C facilitated the crystallization of the PLA; DSC analysis corroborates this statement in fact, the curve of PLA treated no longer shows any typical characteristic of amorphous phase: both T_g and cold crystallization peaks were not detected in the first run (**Fig. 4.1a**).

This result is confirmed also by TGA analysis where both $T_{5\%}$ and $T_{50\%}$ values increase for annealed fibers (**Table 4.1)**. It is reported that an increase in thermal stability could be ascribed to high crystallization levels and more perfect crystals [13].

PLA/r uncured fibers exhibited a similar behaviour, as they went through cold crystallization during the first heating run in the DSC furnace. On the other hand, when the fibers underwent the annealing/curing process, the cold crystallization peak was no longer evident. However, the amorphous phase is still evident probably because the resin hindered the complete crystallization of the polymer. Also for the washed fibers the T_g and thus a residual amorphous phase is still present while the melting peak disappears indicating that the PLA phase had been successfully removed (**Fig. 4.1c**).

The presence of the thermosetting resin in the PLA/r uncured fibers, affecting the crystalline phase of the PLA, led to a lower degradation temperatures $T_{5\%}$ and $T_{50\%}$ respect to pure PLA fibers. However, degradation temperatures increased for both cured and washed PLA/r fibers probably because of high crystallization levels (as recorded for PLA cured sample) and the removal of less perfect crystals by chloroform washing (**Table 4.1**).

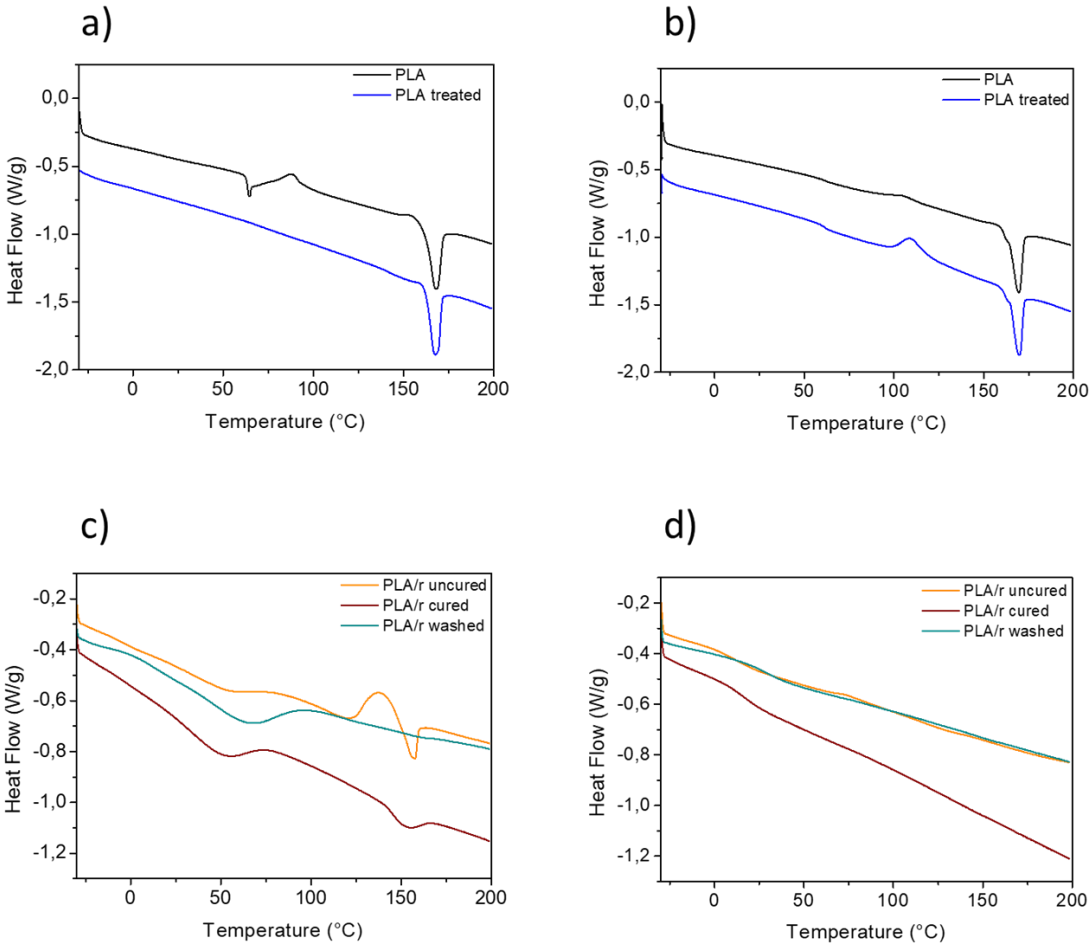

Fig. 4.1 DSC first heating scan thermograms of (a,c) PLA fibers and core-shell PLA/epoxy and DSC third heating scan thermograms of (b,d) PLA fibers and core-shell PLA/epoxy

Table 4.1 Degradation temperatures at 5% ($T_{5\%}$) and 50% ($T_{50\%}$) weight loss, Char yield at 700 °C ($Char_{700}$), Glass transition temperature (T_g)

Samples	$T_{5\%}$ [°C]	$T_{50\%}$ [°C]	$Char_{700}$ [%]	T_g[°C]
PLA uncured	290	328	2	61
PLA cured	301	340	1	61
PLA/r uncured	185	317	15	12
PLA/r cured	201	314	13	16
PLA/r washed	219	333	16	28

4.3 Spectroscopic characterization of electrospun PLA/epoxy resin fibres

To assess the effectiveness of the cross-linking process and washing in chloroform, FT-IR spectroscopic analyses of electrospun PLA/epoxy resin fibers were performed.

The spectra of the PLA and PLA/r cured fibers (**Fig. 4.2a**) are very similar, probably because the IR analysis was performed in ATR (Attenuated Total Reflection) mode so the PLA/r cured spectrum can be mainly associated to the PLA shell. Both curves show the PLA characteristics peaks: the most intense band is at 1750 cm^{-1} and is associated with the stretching of the C=O double bond, while the stretching and bending movements of the CH and CH_3 groups appear in the 1300-1450 cm^{-1} and 2800-3000 cm^{-1} range, respectively[14].

As regard PLA/r washed fibers, the related spectrum was compared to the bulk epoxy resin one (**Fig. 4.2b**). Both BOMF/MA bulk and PLA/r washed showed increasing absorption in the wavelength range 3700-3300 cm^{-1} as a function of time, which is characteristic of the formation of hydroxyl groups bound to hydrogen. Furthermore, the presence of carbonyl peaks at 1732 cm^{-1} confirms the formation of polyester linkages in the fibers.

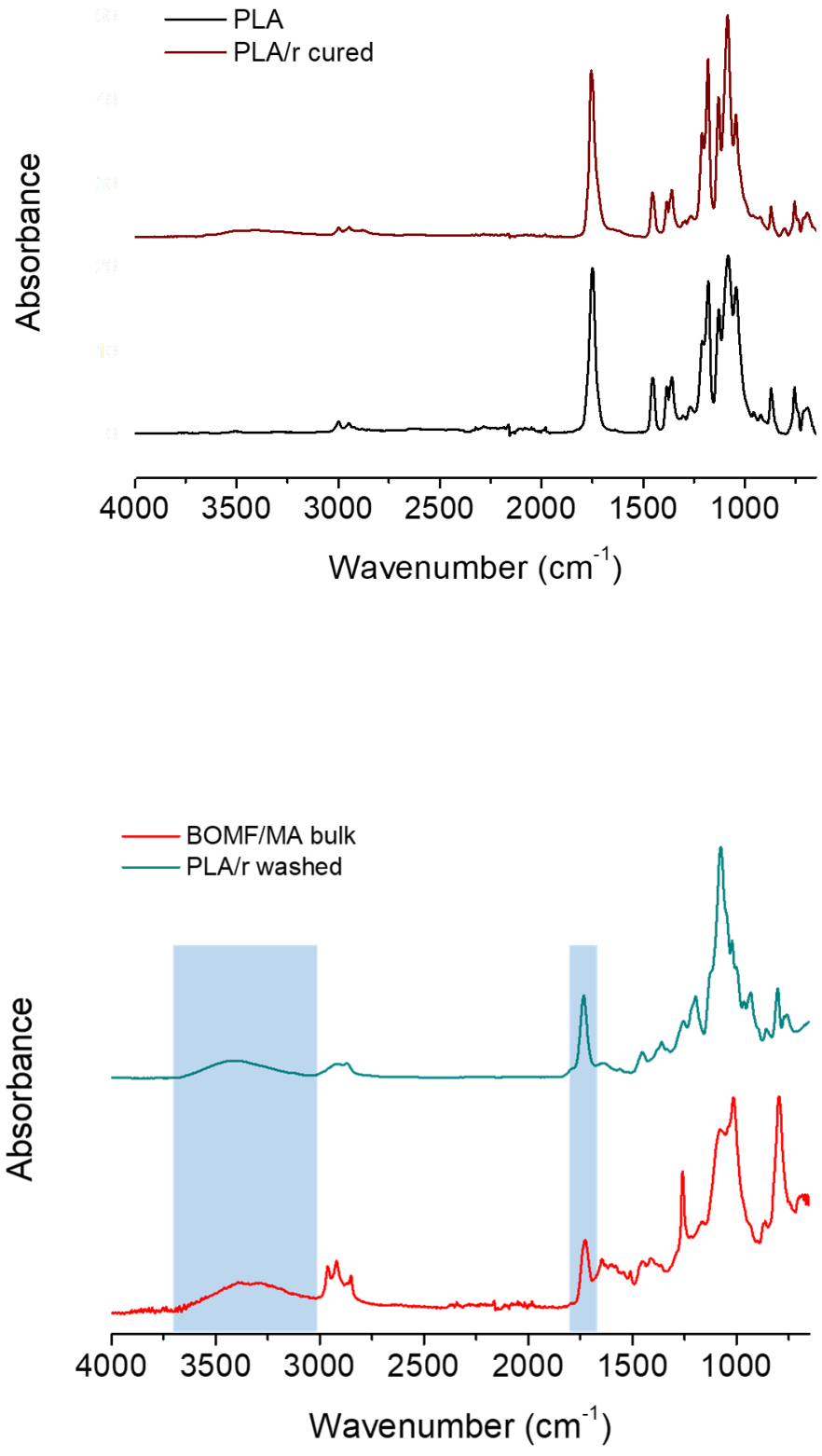

Fig. 4.2 FT-IR spectra of a) PLA and PLA/r cured, b) BOMF/MA bulk and PLA/r washed

4.4 Morphological analysis (SEM) and wettability of electrospun core-shell nanofibers

The morphology of electrospun nanofibers was investigated by optical and SEM analysis.

The PLA mat (**Fig. 4.3a)** showed uniform regular structure, defect-free fibers with homogenous diameters. The average diameter calculated from micrographs (by using ImageJ software) is 0.786±0.124μm. In contrast, PLA fibers after thermal treatment (**Fig. 4.3b**) were physically welded but without severe structural modification, and the surface texture is not so smooth. The average diameter calculated from micrographs is 0.738±0.183μm, diameters distribution is larger respect to uncured PLA fibers. All these variations are due to slight melting of fiber surface[15]. The morphology of the PLA/r uncured fibers **(Fig. 4.3c)** reveal a regular quite homogenous structure; some welded areas are noticeable and they could be ascribed to the presence of resin that is still fluid when fibers landed on the collector thus causing collapse of fibers. The average diameter calculated from micrographs is 1.441±0.399μm. Fibers are bigger respect to the neat PLA ones confirming the presence of two components; however, some smaller fibers are evident due to likely some mono-component (PLA) fibers. The PLA/r cured fibers (**Fig. 4.3d)** presented a more uniform and homogenous surface, some welded areas are evident displaying an overall more cohesive structure. The average diameter calculated from micrographs is 1.602±0.301μm; this increase respect to the uncured ones is due to the thermal treatment. Finally, fibers after thermal treatment and chloroform washing (**Fig. 4.3e)** appeared still uniform, without defects and with homogeneous dimensions. The average diameter calculated from micrographs is 1.676±0.378μm; it is not possible to detect a huge difference in the diameter values before and after washing more likely because the chloroform washing step led to fibers swelling[16].

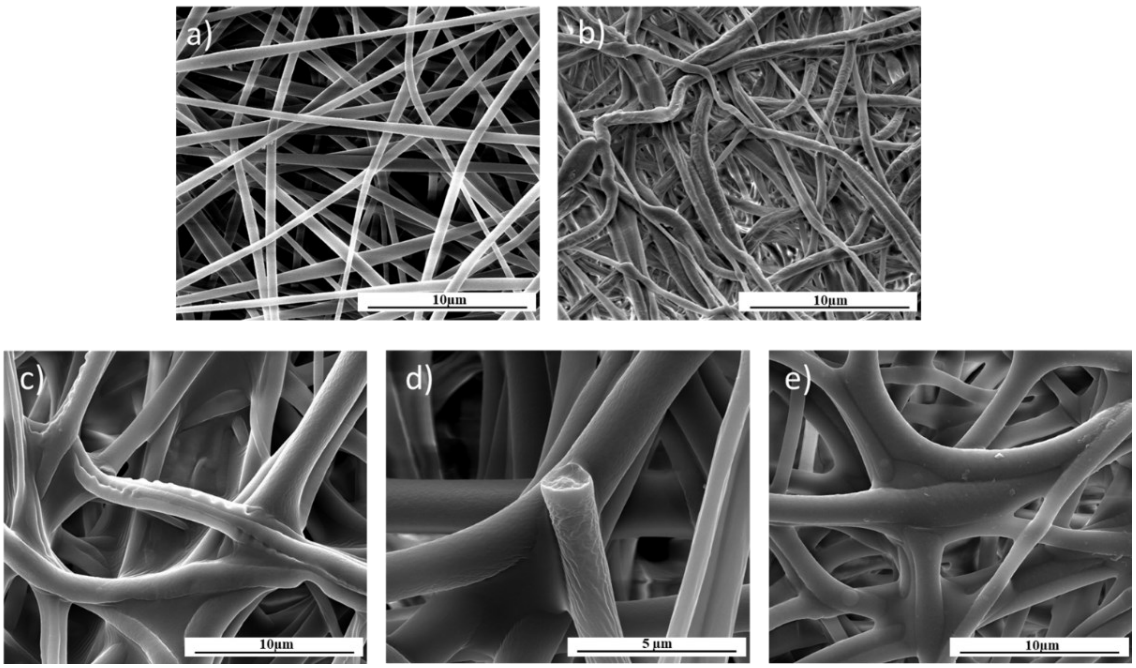

Fig. 4.3. Scanning electron microscopy (SEM) of a) PLA, b) PLA thermal treated, c) PLA/r uncured, d) PLA/r cured and e) PLA/r washed electrospun nanofibers

The obtained BOMF/MA resin nanofibers exhibit good and uniform morphology as reported in **Fig. 4.4a,b**, however, they do not have sufficient strength to be used as stand-alone filters, as evidenced by the results of the thermal and mechanical analysis of the bulk resin, discussed in Chapter 3.

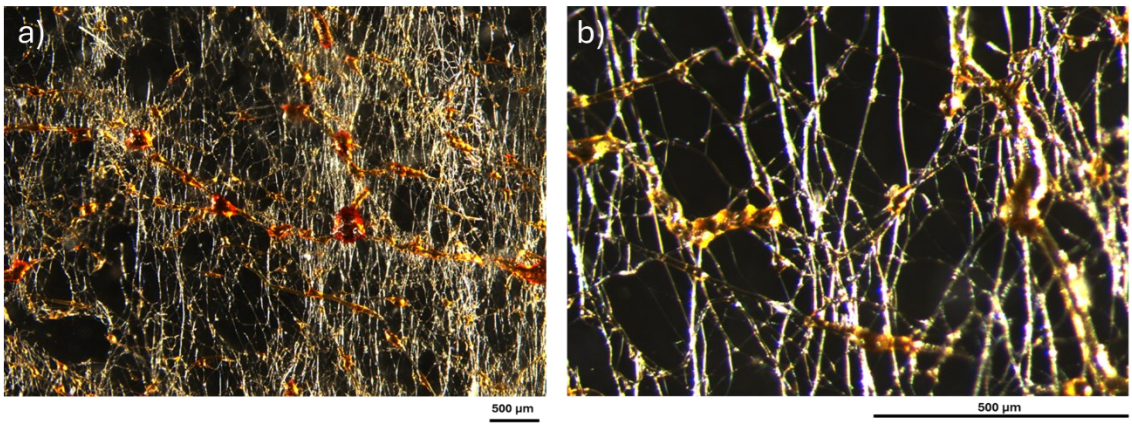

Fig. 4.4 Optical images of the BOMF/MA electrospun nanofibers

Attempts to address the aforementioned drawbacks have been made by fabricating multi-layered filtration materials, in which one of the layers is made up of epoxy resin based nanofibers. It is well known that in multi-layered filtration materials, the nanofibrous layer improves filtration efficiency, while the non-woven layers provided support and strength. In particular, the fabrication of a multi-layered filtration material using a commercial CA non-woven as substrate and epoxy BOMF/MA nanofibers as functional layer was investigated.

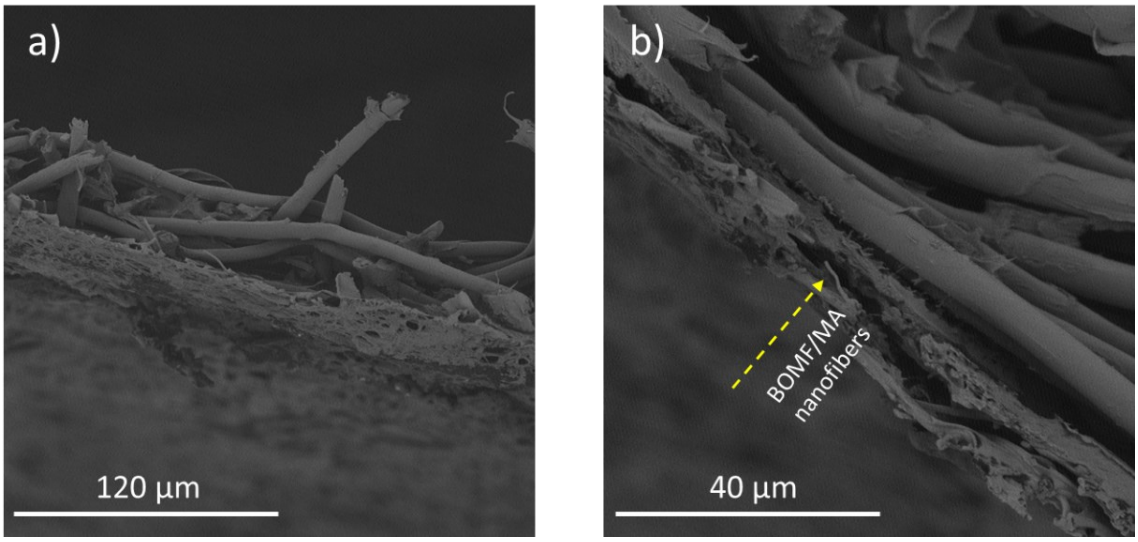

Fig. 4.5 Cross-sectional SEM images of the BOMF/MA modified CA membrane

The successful fabrication of the epoxy/CA membrane by direct electrospinning of BOMF/MA on the CA membrane and subsequent thermal treatment and chloroform washing was confirmed by the cross-sectional SEM micrographs (**Figs. 4.5a,b)**. In fact, the CA membrane is completely covered by a dense and homogenous layer of electrospun fibers.

Surface porosity was analyzed by using the SEM micrographs and ImageJ software.

For the neat CA substrate a mean pore area of 17.586 μm^2 and porosity of 3% was calculated; whereas for the multi-layered sample a mean pore area of 3.486 μm^2 and porosity of 10% was measured. Thanks to the presence of electrospun fibers, it was possible to combine layers with different characteristics (an upper layer that is very thin for filtration and the underlying layer that is a nonwoven textile) to

allow high efficiency and long filter life, which occurs with the lowest increase in pressure drop.

The addition of epoxy layer does not modify the hydrophilicity of the CA membranes as it was evident from WCA measurement (56° for pure and by-layer membrane).

As a further activity, BOMF/MA nanofibers combined with the nonwoven material CA will be analyzed.

4.5 Conclusions

Electrospinning of standalone epoxy fibers has not been possible so far due to the high viscosity and reactivity of the epoxy and the brittleness of the fibers. This study introduces electrospinning as a promising route to produce nanoscale BOMF/MA furan-based epoxy fibers. Due to the low viscosity and high reactivity of the BOMF/MA mixture, it is very difficult to control the system by means of pre-polymerization. Therefore, PLA was chosen as 'sacrificial polymer' to realize a core-shell morphology by coaxial electrospinning: the PLA shell acts as a mould to allow the epoxy nanofibers to polymerize inside and then removed by chloroform washing. The obtained electrospun epoxy nanofibers are homogenous and defect-free, with an average diameter of 1.676μm. Bilayer membranes were successfully fabricated by depositing electrospun epoxy nanofibers on non-woven cellulose acetate fabric; a variable porosity was measured suitable for different applications in the field of fluids filtration.

References

1. Greiner A, Wendorff JH. Electrospinning: A fascinating method for the preparation of ultrathin fibers. *Angew Chemie - Int Ed* 2007; 46: 5670–5703.

2. Luo CJ, Stoyanov SD, Stride E, et al. Electrospinning versus fibre production methods: From specifics to technological convergence. *Chem Soc Rev* 2012; 41: 4708–4735.

3. Dos Santos DM, Correa DS, Medeiros ES, et al. Advances in Functional Polymer Nanofibers: From Spinning Fabrication Techniques to Recent Biomedical Applications. *ACS Appl Mater Interfaces* 2020; 12: 45673–45701.

4. Costantini M, Colosi C, Święszkowski W, et al. Co-axial wet-spinning in 3D bioprinting: State of the art and future perspective of microfluidic integration. *Biofabrication*; 11. Epub ahead of print 2019. DOI: 10.1088/1758-5090/aae605.

5. Hufenus R, Yan Y, Dauner M, et al. Melt-spun fibers for textile applications. *Materials (Basel)* 2020; 13: 1–32.

6. Rodriguez M, Kluge JA, Smoot D, et al. Fabricating mechanically improved silk-based vascular grafts by solution control of the gel-spinning process. *Biomaterials* 2020; 230: 119567.

7. Jian S, Zhu J, Jiang S, et al. Nanofibers with diameter below one nanometer from electrospinning†. *RSC Adv* 2018; 8: 4794–4802.

8. Greenfeld I, Sui X, Wagner HD. Stiffness, Strength, and Toughness of Electrospun Nanofibers: Effect of Flow-Induced Molecular Orientation. *Macromolecules* 2016; 49: 6518–6530.

9. Wang X, Zhang WJ, Yu DG, et al. Epoxy resin nanofibers prepared using electrospun core/sheath nanofibers as templates. *Macromol Mater Eng* 2013; 298: 664–669.

10. Shneider M, Sui XM, Greenfeld I, et al. Electrospinning of epoxy fibers.

Polymer (Guildf) 2021; 235: 124307.

11. Aliahmad N, Biswas PK, Wable V, et al. Electrospun Thermosetting Carbon Nanotube-Epoxy Nanofibers. *ACS Appl Polym Mater* 2021; 3: 610–619.

12. Wu XF, Rahman A, Zhou Z, et al. Electrospinning core-shell nanofibers for interfacial toughening and self-healing of carbon-fiber/epoxy composites. *J Appl Polym Sci* 2013; 129: 1383–1393.

13. Fambri L, Migliaresi C. Crystallization and thermal properties. Poly (Lactic Acid) Synthesis, Structures, Properties, Processing, Applications, and End of Life. 2022 Aug 10:135-51.

14. Siriprom W, Sangwaranatee N, Chantarasunthon K, Teanchai K, Chamchoi N. Characterization and analyzation of the poly (L-lactic acid)(PLA) films. Materials Today: Proceedings. 2018 Jan 1;5(7):14803-6.

15. You Y, Lee SW, Jin Lee S, et al. Thermal interfiber bonding of electrospun poly(L-lactic acid) nanofibers. Mater Lett 2006; 60: 1331–1333.

16. Khan A, Hadano Y, Takehara H, et al. Effects of physico-chemical treatments on PLGA 50:50 electrospun nanofibers. Polymer (Guildf) 2022; 261: 125400.

Chapter

5 Bio-based Epoxy/CNT Coatings for Smart Wearables on Cotton Fabrics

5.1 Introduction

The development of bio-based epoxy resins well aligns with global sustainability goals, offering significant benefits such as reduced carbon emissions, improved biodegradability, and decreased toxicity [1].

Among lignocellulose-derived platform chemicals for bio-epoxies, furanic compounds are very promising alternatives to petro-sourced chemicals, also thanks to their aromatic characteristics, which enhance the mechanical properties [2,3,4,5].

Furans derived from cellulose and hemicellulose are promising candidates for replacement of fossil based epoxies. Furan-based polymers have higher glass transition temperatures and modulus than their phenyl analogues [6]. They have been already validated as coatings for food metal packaging [7] and in structural applications such as adhesives for carbon fibre composites [8], representing a sustainable alternative to traditional systems based on DGEBA.

Moreover, several works have been carried out over the years to modify epoxy resins by adding different kind of nanofillers [9,10,11] to realize epoxy nanocomposites with specific functional properties. Amongst epoxy-based nanocomposites, epoxy resins loaded with carbon nanotubes (CNTs) have garnered significant attention due to their unique combination of electrical and mechanical performances and the potential they hold for various applications, such as actuators or sensors [12]. Recent progress in bio-based epoxy resins, combined with the incorporation of carbon nanotubes, has resulted in environmentally sustainable nanocomposites with improved properties [13].

In this work, a new bio-epoxy resin based on the furan epoxy monomer 2,5-bis[oxiran-2-ylmethoxy)methyl]furan (BOMF) was synthesized by curing BOMF with isophorone diamine (IPD). IPD was chosen as curing agent due to its high reactivity, excellent thermal and chemical resistance, low viscosity and high transparency [14]. In addition, it is known by various trade names that IPD is extensively used in industrial applications; for example, Vestamine IPD, commercialized by Evonik. Herein, the curing process and thermal stability of the BOMF/IPD system were studied by thermal analysis, to determine the best

performing formulation in terms of epoxy/IPD molar ratio and curing conditions. Then, the BOMF/IPD system was used as a polymer matrix for the realization of electrically conductive bio-epoxy nanocomposites, by in situ polymerization of the resin in presence of multiwalled CNTs. Morphological properties, electrical and mechanical behaviour of the epoxy/CNT nanocomposite were investigated to identify the best formulation to be used as a biobased multifunctional coating on a cotton fabric, to develop breathable and flexible smart wearable systems [15,16], endowed with pronounced hydrophobicity, electrical conductivity and Joule heating effect.

5.2 Curing behavior of BOMF/IPD systems

In the epoxy-amine reaction, a primary amine reacts with an epoxy group, yielding a secondary amine, which subsequently further reacts with epoxy rings leading to a crosslinked structure. The reaction mechanism between BOMF and IPD reported in **Scheme 1** [17].

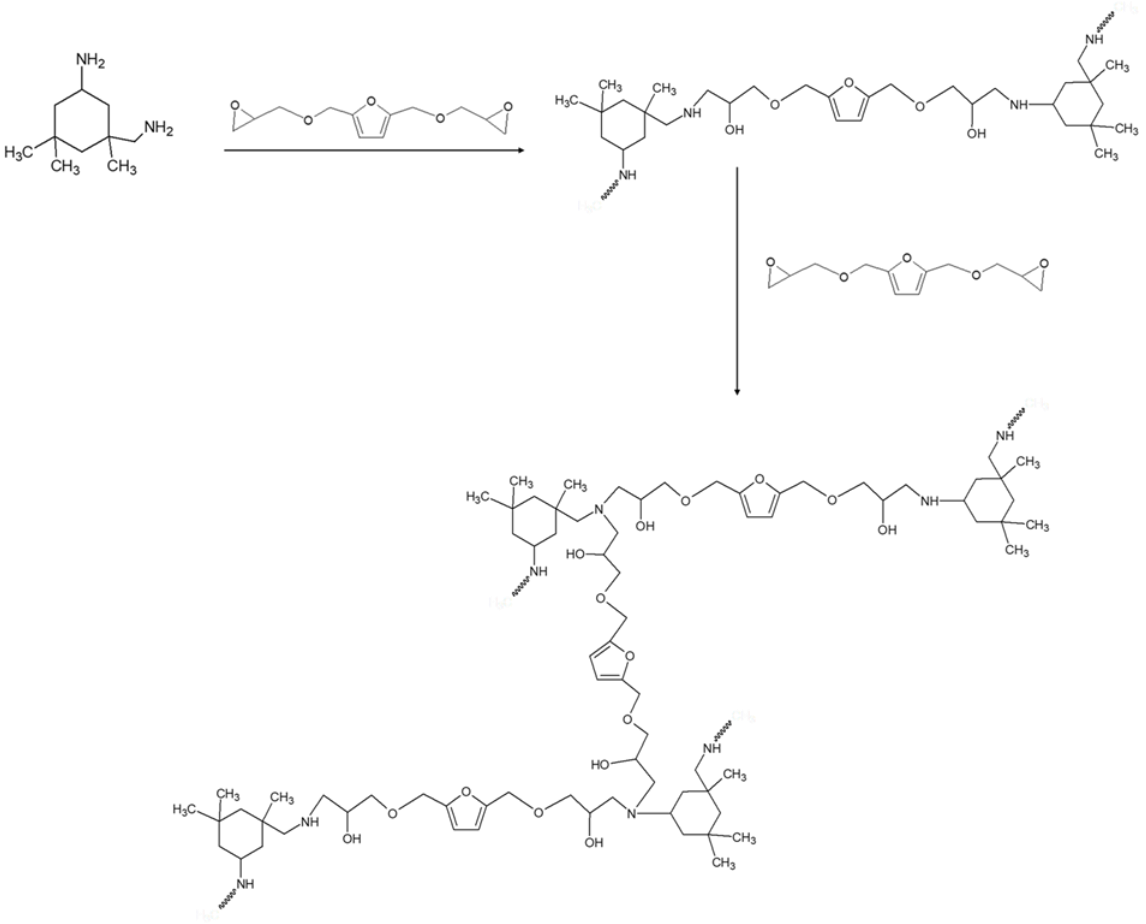

Scheme 1. Cross-linking reaction mechanism between BOMF and IPD.

DSC dynamic measurements thermograms reported in **Fig. 5.1a** shows that all the epoxy systems exhibited a single exothermal peak with a maximum between 107-109 °C, associated to the curing reaction. However, the shape of the peaks becomes broader as the relative amount of epoxy groups increases, suggesting the activation of a reaction occurring at higher temperature (about 150 °C) involving the epoxy excess. This evidence can be discussed considering that BOMF functionality is 2, while IPD although being a tetrafunctional monomer, bears two different kinds of primary amine groups. In particular, aliphatic amines are considered more reactive than the alictclic counterpartes [18]. By deconvoluting the cross-linking peak relative to the BOMF/IPD 2:1 system, it can be seen that the ΔH relative to the reaction of aliphatic amines is 431.7 J/g, while that relative to the reaction of alicyclic amines is 86.3 J/g. Therefore, in the equimolar BOMF/IPD mixture, where a twofold excess of equivalent amines is present, the reaction between BOMF and IPD mainly occurs by the involvement of aliphatic amines, until epoxide consumption. On the other hand, for 1.5:1 and 2:1 molar ratios of BOMF to IPD, the excess epoxy groups are involved in the reaction with the alicyclic amines, as indicated by the high temperature shoulder peak [19]. In **Table 5.1** the total heat of the reaction (ΔH_{tot}), the maximum peak temperature (T_p), the peak onset temperature (T_{onset}) and the glass transition temperature (T_g) are reported.

The peak temperature T_p during curing is slightly lower for the samples obtained at 1.5:1 and 2:1 BOMF/IPD ratios (both 107 °C) than for the sample obtained at 1:1 ratio (109 °C). On the other hand, ΔH_{tot} increases from 447 J/g and (1:1 BOMF/IPD ratio) to 518 J/g (1.5:1 and 2:1 ratios), due to the higher reactivity of the systems containing a molar excess of epoxy groups. Furthermore the T_g values of the 1.5:1 and 2:1 BOMF/IPD samples are significantly higher than that of BOMF/IPD, confirming the trend observed for the ΔH_{tot}. Interestingly, 1.5:1 BOMF/IPD sample exhibits the same ΔH_{tot} value as the 2:1 sample alongside the highest glass transition temperature, suggesting that at the 1.5:1 ratio the system has reached cross-linking saturation, as it is likely that the vitrification of the

system affects the mobility of the growing macromolecular units (**Figure 5.1b** and **Table 5.1**).

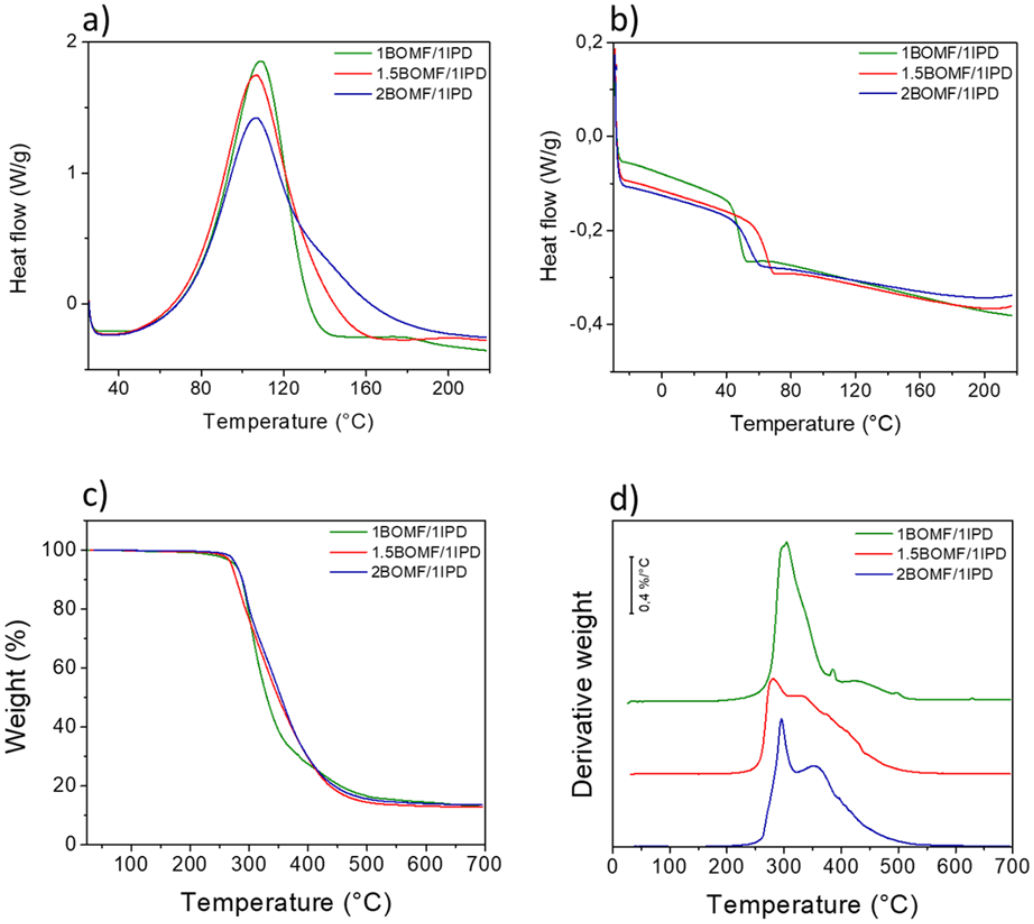

Fig 5.1. DSC thermograms a) exothermic peaks and b) glass transition temperatures, c) TGA thermograms in nitrogen, d) derivative weight of 1BOMF/1IPD, 1.5BOMF/1IPD and 2BOMF/1IPD systems

Table 5.1. Total heat of reaction (ΔH_{tot}), onset temperature (T_{onset}) from DSC, peak temperature (T_p), glass transition temperature (T_g) of samples cured at DSC and of bulk samples 1BOMF/1IPD, 1.5BOMF/1IPD and 2BOMF/1IPD and nanocomposites systems cured at 10 °C/min.

	ΔH_{tot}[J/g]	**T_{onset}[°C]**	**T_P[°C]**	**T_g[°C]**	**T_g[°C]_bulk**
1BOMF/1IPD	447	76	109	49	47
1.5BOMF/IPD	518	73	107	65	70
2BOMF/1IPD	518	73	107	55	65

5.3 Characterization of bulk bio-epoxy resin samples

The T_g values of bulk, oven-cured samples (**Table 5.1**) are very close to those recorded by the second DSC heating run performed on samples cured by the dynamic DSC experiment, confirming the efficiency of the selected oven-curing conditions. For all epoxy systems, TGA analysis showed a multi-step degradation behavior (**Fig.s 5.1c,d**), with a maximum degradation rate at 304 °C (27 wt% loss) for the 1:1 BOMF/IPD sample, 281 °C (12 wt% loss) for the 1.5:1 BOMF/IPD sample and 296 °C (16 wt% loss) for the 2:1 BOMF/IPD sample.

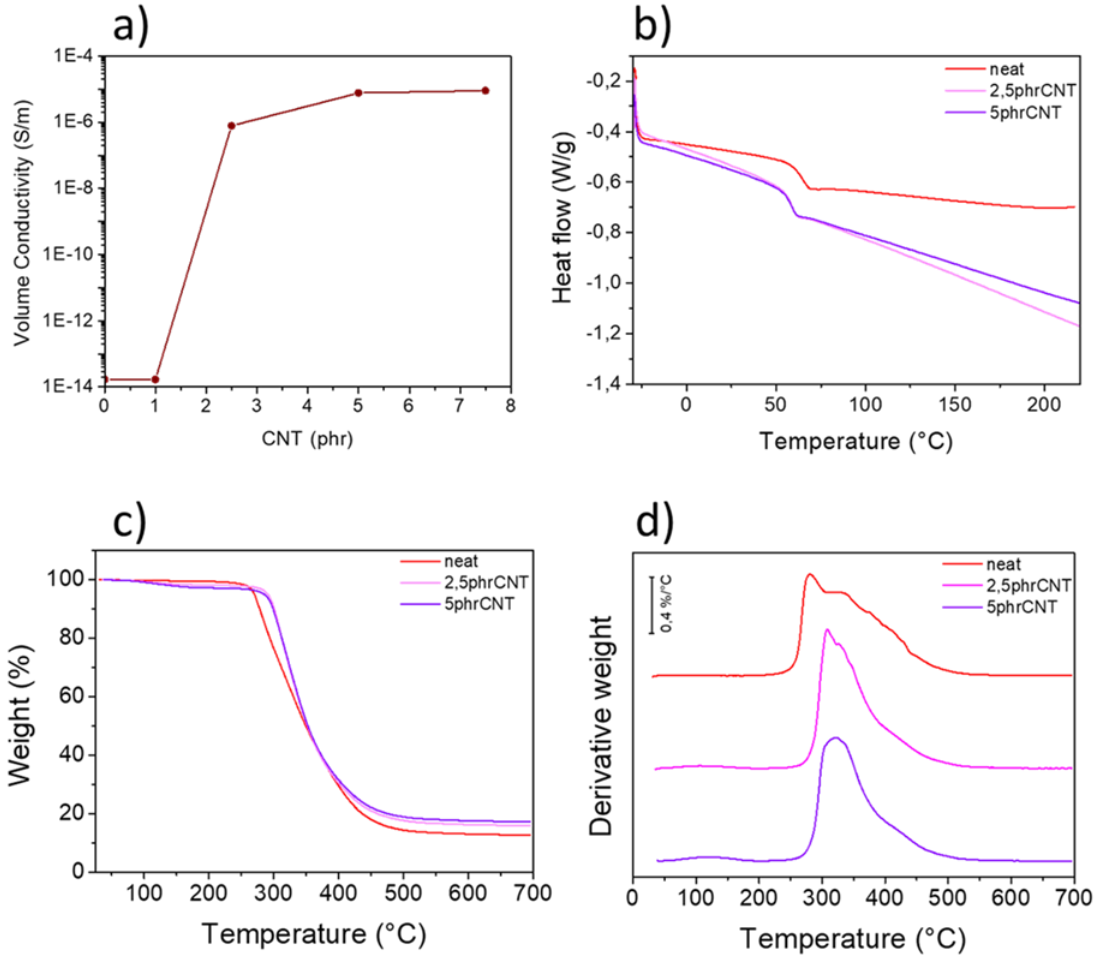

Fig 5.2. a) Percolation threshold of CNT/epoxy nanocomposites, b) Glass transition temperatures, c) TGA thermograms in nitrogen and d) derivative weight thermograms of nanocomposites bulk samples compared to neat bulk resin 1.5BOMF/1IPD

Results of tensile tests on neat epoxy resins at various BOMF/IPD ratio are reported in **Table 5.2.** As shown, the resin obtained at 1:1 BOMF/IPD ratio is characterized by a high modulus, but it also presents a relatively low breaking strength and elongation capacity. Better results were obtained for the system realized using the 1.5:1 BOMF/IPD ratio, which shows a comparable modulus but a significantly increased tensile strength and elongation capacity. Finally, for the resin obtained at 2:1 BOMF/IPD ratio, the modulus is practically unchanged in comparison to previous samples, the strain at break value is comparable to that recorded for the system at 1.5:1 BOMF/IPD ratio, while a slightly lower ductility is recorded.

Overall, tensile test results indicate that 1.5:1 BOMF/IPD evidences the best mechanical performances.

5.4 Characterization of bio-epoxy/CNT nanocomposites

The preparation and characterization techniques of BOMF/IPD/CNT bulk and nanocompsites samples are described in detail in Section 2.3.3 of Chapter 2. Based on the results obtained on neat resins, the 1.5:1 BOMF/IPD formulation, which exhibits the highest T_g and better mechanical properties, was selected for the realization of nanocomposites with carbon nanotubes (CNTs).

As can be seen in **Fig. 5.2a**, the addition of 1 phr of CNTs was not able to modify the electrical conductivity of the neat resin. Instead, already with the 2.5 phr of filler, the conductivity increased by 7 orders of magnitude (10^{-7} S/m) compared to pure resin (10^{-14} S/m) and achieved 10^{-6} S/m by doubling the carbon nanotube content to 5 phr. This CNT content represents the electrical percolation threshold for the bio-epoxy nanocomposites, since no changes in electrical conductivity were moticed by further increasing the CNT amount to 7.5 phr.

For this reason, films and bulk samples containing 2.5 and 5 phr of CNTs were prepared and characterized in comparison to the neat resin.

Fig. 5.2b shows DSC curves of bulk nanocomposites and neat resin. It can be seen that by adding CNTs, the T_g slightly decreases from 70°C to 58°C for the system containing 2.5 and 5 phr. This can be explained considering that CNT could

partially hinder the curing reaction of the bio-epoxy system. Previous works [20] already reported that nanocomposites containing dispersed CNTs showed a huge depression of their glass transition temperature, compared to pure cross-linked epoxy. Indeed, the mobility of the active groups in the epoxy and the curing agent may be hindered by carbon nanotubes, which dramatically impact the viscosity of the mixture, resulting in a reduced degrees of curing [21,22].

TGA results (**Table 5.2** and **Fig. 5.2c**) indicate that the two epoxy nanocomposite samples show an initial 5% weight loss at similar temperatures, as can be seen from the data in the **Table 5.2**, suggesting that the presence of carbon nanotubes, irrespectively on their amount, induce a slight increase of the onset of the degradation in comparison to the neat epoxy resin. Moreover, a slight difference in the residue at 700°C of the epoxy nanocomposites in comparison to the neat resin can be attributed to a thermal stabilization effect and higher char formation of CNT. Derivative weight thermograms in **Fig. 5.2d** showed one step of degradation for nanocomposite samples with maximum rates of degradation located at 309 °C (17 wt% loss) and 322 °C (27 wt% loss), for 2.5phr and 5phr CNT, which are significantly higher than that of neat epoxy resin (281 °C).

Table 5.2. Stress (σ) and strain (ε) at peak, Young's Modulus (E′), degradation temperatures at 5% ($T_{5\%}$) and 50% ($T_{50\%}$) weight loss, char yield at 700 °C ($Char_{700}$), of 1BOMF/1IPD, 1.5BOMF/1IPD, 2BOMF/1IPD-based and nanocomposites thermosets

	$T_{5\%}$ [°C]	**T_P [°C]**	**$Char_{700}$ [%]**	**Stress at break [MPa]**	**Strain at break [%]**	**Young's Modulus [MPa]**
1BOMF/1IPD	276	304	13	20.0 ± 1.5	2.5 ± 0.7	1141.7 ± 57.1
1,5BOMF/1IPD	270	281	13	52.2 ± 4.0	8.2 ± 0.7	1150.6 ± 113.2
2BOMF/1IPD	278	296	14	41.8 ± 3.3	7.1 ± 0.5	1108.1 ± 64.8
2.5phrCNT	291	309	16	43.4 ± 8.3	5.7 ±0.8	1142.0 ± 131.6
5phrCNT	285	322	17	31.1 ± 0.2	4.0 ± 0.7	1114.5 ± 84.4

Tensile test results on CNT-reinforced epoxy nanocomposite samples indicate that the addition of 2.5 phr of CNT induces a slight reduction of the tensile strength in comparison to the pure resin sample. Young's modulus remains high, indicating good overall stiffness. The addition of 5 phr of CNT further reduces strain and stress at break compared to the sample with 2.5 phr of CNT and the neat resin. However, both nanocomposite samples still shows good strength and acceptable deformation capacity. The Young's modulus is comparable to the other samples. The absence of changes in the Young's modulus of nanocomposites in comparison to the neat bio-epoxy was already observed for CNT/epoxy systems [20], and was explained with a non-optimal interfacial interactions in the nanocomposites, resulting in and ineffective stress-transfer mechanism with a non-appreciable increase of the modulus despite the presence of the rigid filler.

The morphology of the film cross-sections of nanocomposites was investigated by SEM. Neat epoxy resin was also analyzed by comparison. Concerning the pure resin film (**Fig.s 5.3a,b**), it is evident a fragile fracture mechanism. For the nanocomposite samples, both formulations show a homogenous distribution and a good dispersion of the nanotubes within the bio-epoxy matrix, as illustrated in **Fig.s 5.3d** and **f.** Absence of debonding phenomena at the filler/epoxy interfaces indicate a satisfactory interfacial adhesion.

Joule effect behaviour of nanocomposites was investigated by applying and subsequent removal of different voltage on the films. The better results were obtained applying 20 V voltage, which induces a temperature increase of more than 1 °C to the nanocomposite containing 2.5 phr CNT. Doubling the amount of CNT to 5 phr and applying the same voltage, an increase of temperature of approximately 13 °C is observed. For both samples, by lowering the voltage to 10 V, thermal dissipation occurrs in about one minute (**Figs. 5.3g,h**). Comparable behaviours, with lower temperature increases, were recorded with experiments at lower voltages.

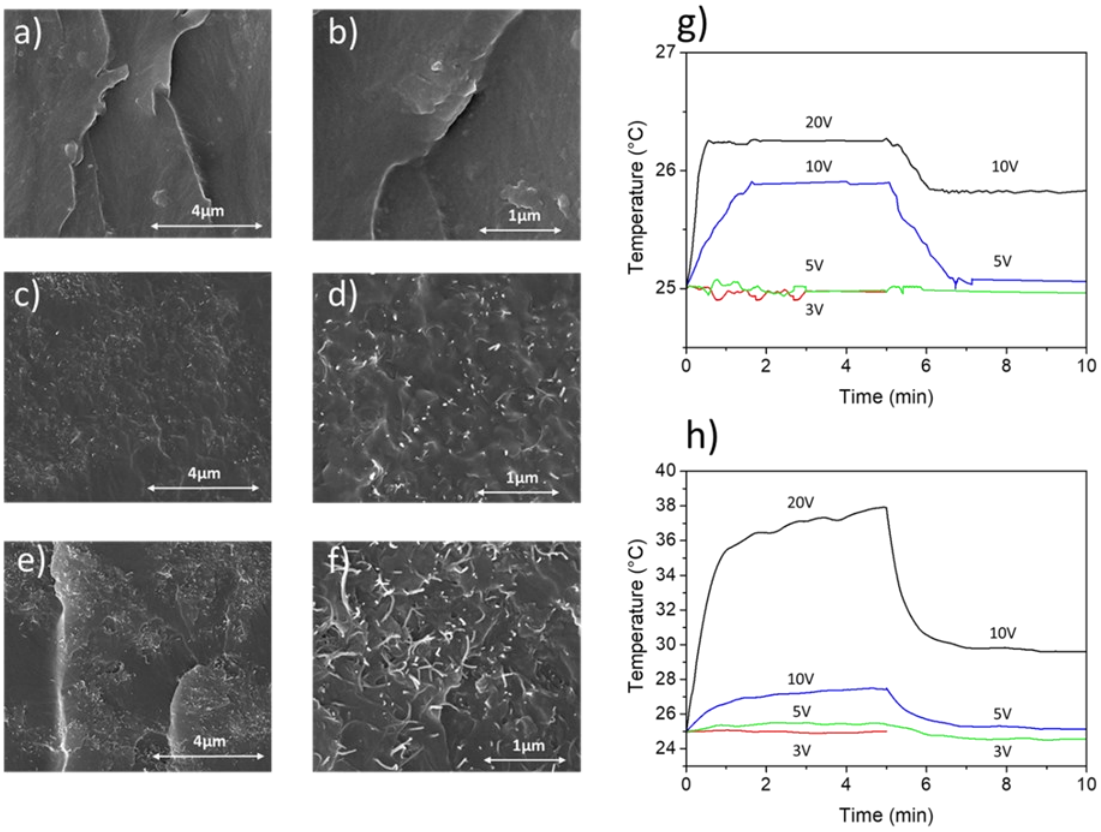

Fig 5.3. SEM images of (a,b) 1.5BOMF/1IPD sample, (c,d) 1.5BOMF/1IPD/2.5phrCNT sample and (e,f) 1.5BOMF/1IPD/5phrCNT sample and electrothermal behaviour of nanocomposite films under different applied voltages of (g) 1.5BOMF/1IPD/2.5phrCNT and (h) 1.5BOMF/1IPD/5phrCNT

5.5 Coated cotton fabrics characterization

Based on the results obtained from the characterization (described in Sections 2.3.3 and 2.3.4 of Chapter 2) of CNT/epoxy nanocomposites, the formulations containing 2.5 and 5 phr of CNT were applied as coatings on cotton fabrics. By comparison, a neat resin coating was also applied on cotton.

SEM micrographs of untreated and treated cotton samples are illustrated in **Fig. 5.4.** The surface of the pristine cotton fabric is reported in **Figs. 5.4a,b**, evidencing typical features of cotton fibers, with characteristic flat and twisted morphology. For the cotton impregnated with the neat resin, it can be seen that the cotton fibers are well covered by the epoxy, which forms a continuous film embedding in some cases adjacent cotton fibers (**Figs. 5.4c,d**). A similar finding was observed for samples coated with the 2.5 phr CNT/epoxy nanocomposite (**Figs. 5.4e,f**),

indicating good impregnation of the fabric. When the CNT content was increased to 5 phr, the good coverage of the fibers by the nanocomposite coating was confirmed, but agglomerates of filler/resins become more evident (**Figs. 5.4g,h**), due to the presence of high amounts of CNTs with respect to the resins since the dry content of the mixtures, as already reported in Section 2.4, was fixed at 5 wt%. To assess the water wettability of cotton coated with carbon nanotube-reinforced epoxy, static contact angle measurements were carried out. Pure cotton showed a contact angle value of 48° (**Fig. 5.4i**), which indicates the hydrophilicity of the cotton substrate, while the contact angle values measured on the coated cotton fabric substrates were between 122° and 129° (**Figs. 5.4l,m,n**) for impregnated cotton, regardless the addition of CNTs, demonstrating that the application of the furanic bio-epoxy coating is able to confer pronounced hydrophobicity to the substrate. Once confirmed the hydrophobic effect of the coating, the breathability of resin/CNT-coated cotton was also evaluated. Interestingly, water permeability values were very close for all samples, namely 1.21 ± 0.06 kg/(24h•m^2) for the untreated cotton, 1.15 ± 0.06 kg/(24h•m^2) for the cotton impregnated only with pure resin, 1.02 ± 0.03 kg/(24h•m^2) and 1.09 ± 0.06 kg/(24h•m^2) for the fabric impregnated with resin and 2.5phrCNT and resin and 5phrCNT respectively. This result confirmed a good breathability of the cotton substrates, potentially employable for wearable comfortable applications; this is explained taking into account the results of SEM analysis, that show the presence of the epoxy coatings onto the cotton fibers without obstructing the structure of the untreated fabric.

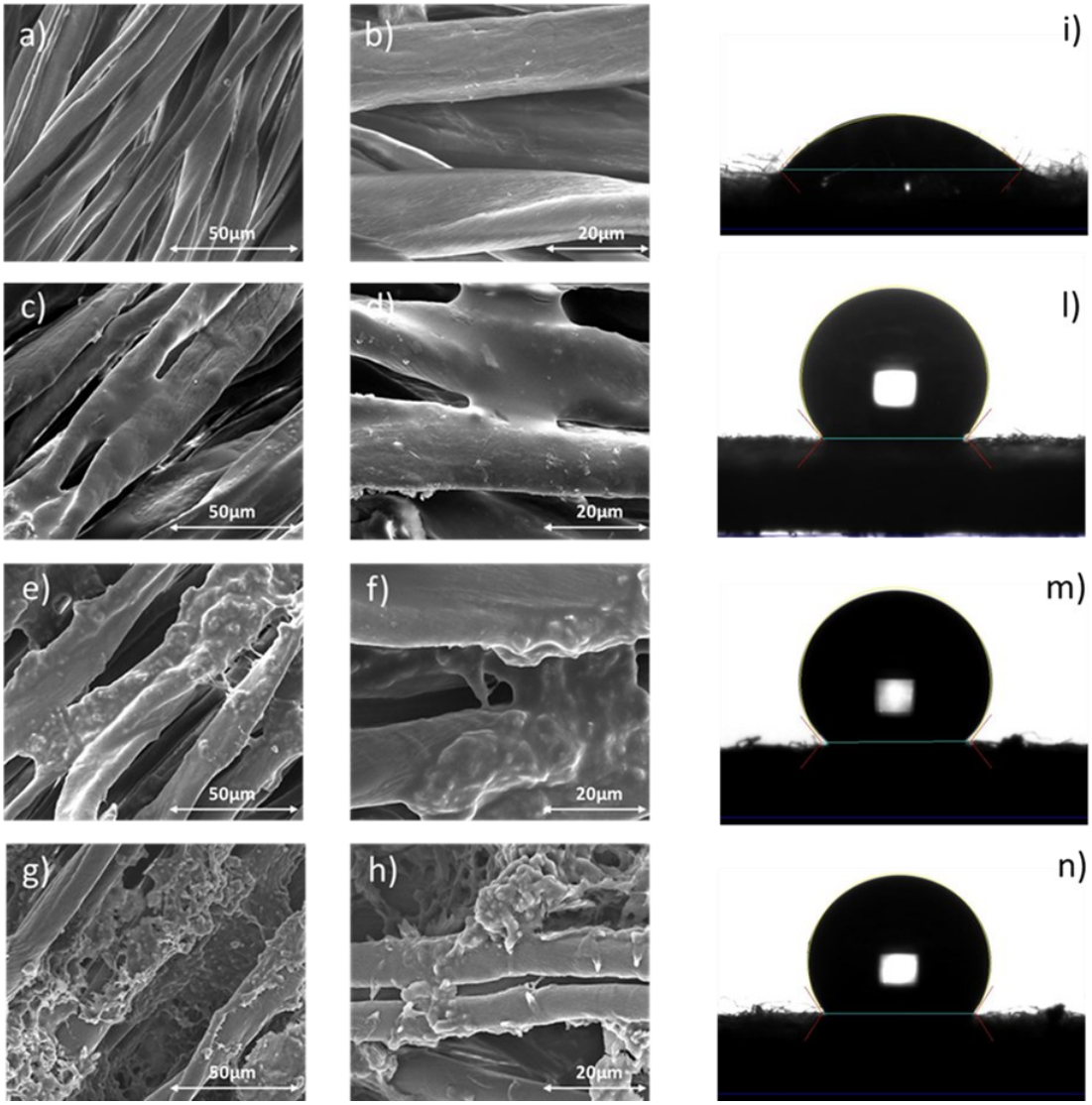

Fig. 5.4. SEM images of (a,b) cotton, (c,d) coated cotton with pure resin, (e,f) coated cotton of epoxy resin reinforced with 2.5phrCNT and (g,h) coated cotton of epoxy resin reinforced with 5phrCNT, and static contact angles on cotton (i), coated cotton with pure resin (l), coated cotton of epoxy resin reinforced with 2.5phrCNT (m) and coated cotton of epoxy resin reinforced with 5phrCNT (n)

Finally, **Figs. 5.5a** and **b** show the electrothermal behaviour of fabrics impregnated with the functionalized epoxy resin. Tests were performed by applying increasing input voltages of 3, 5, 10 and 20 V.

The temperature increase occurred very rapidly, especially when the voltage of 20 V was applied. In the case of the sample impregnated with epoxy resin loaded with 2.5phrCNT, an increase of 1 °C was recorded at the highest voltage, while doubling

the CNT content resulted in a temperature increase of about 8 °C. For each applied voltage, once the plateau temperature was reached, the voltage was lowered to the immediately preceding value. As seen for nanocomposite films, also for coated cotton fabrics, lowering the voltage decreases the temperature to a plateau value in 5 minutes.

Fig. 5.5c shows the temperature change response of the cotton fabric impregnated with 5phrCNT by cyclically applying a voltage of 20V with an on/off ratio of 5 minutes.

During this test, the gained temperature by applying the voltage is approximately 8 °C and the temperature at each cycle reaches the same value in 5 minutes. The absence of any significant change in temperature or decrease in heating performance shows the high stability of the fabric heater. The good conductivity, lightness, flexibility and stability characteristics found in the present epoxy/CNTs resin-based fabric heaters strongly suggest their potential applications in wearable heating/electronic devices. In order to visualize the temperature variation on the surface of the coated fabric, an X symbol was drawn on the fabric with a thermochromic ink which changed colour from blue to neon green at 28 °C. **Fig. 5.5d**, shows the colour transition by applying a voltage of 20 V. Furthermore, the colour change process is reversible and repeatable when the voltage is repeatedly switched on and off cycles. The uniform discoloration of the thermochromic ink emphasizes the homogeneous distribution of CNTs over the cotton fabric surface [23].

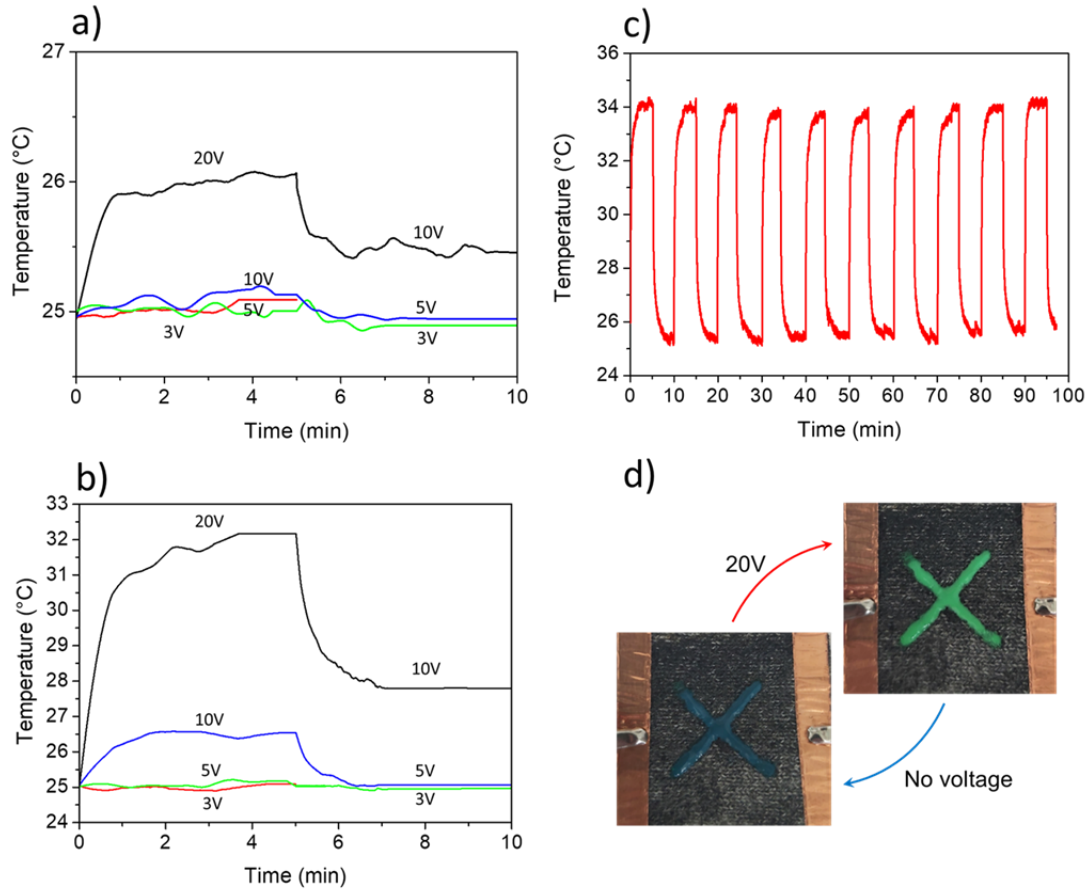

Figure 5.5. Electrothermal behaviour of coated cotton fabrics under different applied voltages of (a) BOMF/IPD/2.5phrCNT and (b) BOMF/IPD/5phrCNT, (c) temperature response of BOMF/IPD/5phrCNT coated fabrics during subsequent voltage (20 V) application and removal cycles, (d) optical images of cotton fabric coated with BOMF/IPD/5phrCNT marked with thermochromic ink under 20V applied voltage.

5.6 Conclusions

New sustainable epoxy resins were obtained by crosslinking a furan-based epoxy monomer (BOMF) with isophorone diamine (IPD) at varying molar ratios. The resins were thermally and mechanically characterized. DSC analysis showed T_g values spanning from 50 to 70 °C, while tensile tests evidenced elastic moduli of about 1 GPa and strain at break values up to 8%. In order to impart an electrical functionality to the resin, suitable amounts of CNTs were subsequently added as fillers. The nanocomposites obtained exhibited electrical conductivity values in the order of 10^{-6} S/m, showing Joule heating behaviour.

Considering their ductility, the functional CNTs/epoxy nanocomposites were then used to impregnate a natural cotton fabric, with the aim of developing thermo-responsive wearable textiles. Breathability tests showed that the CNTs/resin coating does not reduce the breathability of the cotton fabric. Wettability tests showed an increase in the hydrophobicity of the covered fabrics, which additionally maintained good flexibility. Finally, the thermoelectrical functionality of the textiles was thoroughly evaluated by means of Joule heating test. The temperatures achieved applying a voltage of 20V (around 34 °C), and the robust and reproducible behavior under cyclic heating tests demonstrated the potential for use as wearable heating textiles and for biomedical devices.

References

1. Mattar N, Langlois V, Renard E, et al. Fully Bio-Based Epoxy-Amine Thermosets Reinforced with Recycled Carbon Fibers as a Low Carbon-Footprint Composite Alternative. *ACS Appl Polym Mater* 2021; 3: 426–435.
2. Gandini A, M. Lacerda T. Furan Polymers: State of the Art and Perspectives. *Macromol Mater Eng* 2022; 307: 1–17.
3. Eid N, Ameduri B, Boutevin B. Synthesis and Properties of Furan Derivatives for Epoxy Resins. *ACS Sustain Chem Eng* 2021; 9: 8018–8031.
4. Janvier M, Hollande L, Jaufurally AS, et al. Syringaresinol: A Renewable and Safer Alternative to Bisphenol A for Epoxy-Amine Resins. *ChemSusChem* 2017; 10: 738–746.
5. Memon H, Liu H, Rashid MA, et al. Vanillin-Based Epoxy Vitrimer with High Performance and Closed-Loop Recyclability. *Macromolecules* 2020; 53: 621–630.
6. Hu F, La Scala JJ, Sadler JM, et al. Synthesis and characterization of thermosetting furan-based epoxy systems. *Macromolecules* 2014; 47: 3332–3342.
7. Marotta A, Faggio N, Ambrogi V, et al. Biobased furan-based epoxy/TiO2 nanocomposites for the preparation of coatings with improved chemical resistance. *Chem Eng J* 2021; 406: 127107.
8. Faggio N, Marotta A, Ambrogi V, et al. Fully bio-based furan/maleic anhydride epoxy resin with enhanced adhesive properties. *J Mater Sci* 2023; 58: 7195–7208.
9. Gonçalves FAMM, Santos M, Cernadas T, et al. Influence of fillers on epoxy resins properties: a review. *J Mater Sci* 2022; 57: 15183–15212.
10. Marotta A, Faggio N, Ambrogi V, et al. Biobased furan-based epoxy/TiO2 nanocomposites for the preparation of coatings with improved chemical

resistance. *Chem Eng J* 2021; 406: 127107.

11. Xian G, Walter R, Haupert F. Friction and wear of epoxy/TiO2 nanocomposites: Influence of additional short carbon fibers, Aramid and PTFE particles. *Compos Sci Technol* 2006; 66: 3199–3209.

12. Babahan-Bircan I, Demirkaya I, Hasan SOH, et al. Comparison of new bio-based epoxide-amine coatings with their nanocomposite coating derivatives (graphene, CNT, and fullerene) as replacements for BPA. *Prog Org Coatings* 2022; 165: 106714.

13. Lorwanishpaisarn N, Srikhao N, Jetsrisuparb K, et al. Self-healing Ability of Epoxy Vitrimer Nanocomposites Containing Bio-Based Curing Agents and Carbon Nanotubes for Corrosion Protection. *J Polym Environ* 2022; 30: 472–482.

14. Tkachuk AI, Zagora AG, Terekhov I V., et al. Isophorone Diamine—A Curing Agent for Epoxy Resins: Production, Application, Prospects. A Review. *Polym Sci - Ser D* 2022; 15: 171–176.

15. Krifa M. Electrically Conductive Textile Materials—Application in Flexible Sensors and Antennas. *Textiles* 2021; 1: 239–257.

16. Olivieri F, Rollo G, De Falco F, et al. Reduced graphene oxide/polyurethane coatings for wash-durable wearable piezoresistive sensors. *Cellulose* 2023; 30: 2667–2686.

17. Mora AS, Tayouo R, Boutevin B, et al. A perspective approach on the amine reactivity and the hydrogen bonds effect on epoxy-amine systems. *Eur Polym J* 2020; 123: 109460.

18. Núñez L, Fraga López F, Fraga Grueiro L, et al. Activation energies and rate constants for an epoxy/cure agent reaction: Variation in peak exotherm temperature. *J Therm Anal* 1996; 47: 743–750.

19. Zhao X, Huang Z, Song P, et al. Curing kinetics and mechanical properties of epoxy resin/1-benzyl-2-methylimidazole/isophorone diamine system.

Thermochim Acta 2020; 690: 178657.

20. Khare KS, Khare R. Effect of carbon nanotube dispersion on glass transition in cross-linked epoxy-carbon nanotube nanocomposites: Role of interfacial interactions. *J Phys Chem B* 2013; 117: 7444–7454.

21. Tao K, Yang S, Grunlan JC, et al. Effects of carbon nanotube fillers on the curing processes of epoxy resin-based composites. *J Appl Polym Sci* 2006; 102: 5248–5254.

22. Allaoui A, El Bounia N. How carbon nanotubes affect the cure kinetics and glass transition temperature of their epoxy composites? - A review. *Express Polym Lett* 2009; 3: 588–594.

23. Yang M, Pan J, Luo L, et al. CNT / cotton composite yarn for electro-thermochromic textiles. *Smart Mater Struct*; 28.

Chapter

6 General conclusions and future outlook

6.1 General conclusions

In recent decades, interest in the development of high-performance polymers made from biomass has grown significantly with the aim of progressively replacing materials made from non-renewable resources and reducing their ecotoxicity.

The work presented was aimed to the developing of new bio-based epoxy resins, starting from the synthesis of 2,5-bis[(ossiran-2-ilmetossi)methyl]furan, a furan-based epoxy monomer named BOMF, which was cross-linked by the suitable choice of green curing agents.

The choice was made to use maleic anhydride (MA), which can be obtained from vegetable raw materials, resulting in a fully biobased epoxy resin. By using maleic anhydride as a hardener, it is possible to obtain fully polymerized materials with a renewable content of more than 60 wt%, which is an environmentally interesting value.

The BOMF/MA epoxy resin's curing behavior was examined through thermal and chemo-rheological analyses, and the curing process of the system was fine-tuned to produce sheets. When compared to a traditional epoxy monomer based on DGEBA cured with the same anhydride, the BOMF/MA samples exhibit a lower glass transition temperature, Young's modulus, and ultimate tensile strength, but a higher ultimate strain. As a result, the BOMF/MA system is unsuitable for replacing the corresponding DGEBA/MA system in applications requiring high stiffness and strength, such as composites. However, it proves suitable for applications necessitating more flexible materials.

Notably, when the BOMF/MA system was tested as an adhesive for fiber-reinforced polymer composites, it demonstrated significantly enhanced properties compared to the traditional epoxy system based on DGEBA. Stress and strain-to-failure values were more than three times higher. The exceptional adhesive properties were elucidated by the observation of the failure mechanism. While the DGEBA/MA adhesive primarily exhibited an adhesive failure mechanism, with failure mainly occurring at the interface between the adhesive and the substrate, the BOMF/MA adhesive predominantly failed cohesively. This cohesive failure

mechanism, characteristic of well-adhered adhesives, contributed to the substantially improved adhesion of the BOMF/MA adhesive to the epoxy-based CFRP. This improvement is attributed to the presence of hydroxyl groups formed during the curing of the BOMF/MA system, stabilized by the furan ring, allowing strong interaction with the CFRP epoxy substrate.

The same system has been used to make nanofibers by electrospinning. Due to the challenging control of the BOMF/MA mixture's low viscosity and high reactivity through pre-polymerization, PLA was selected as a 'sacrificial polymer' to achieve a core-shell structure via coaxial electrospinning. The PLA shell serves as a mold, facilitating the polymerization of epoxy nanofibers within. Characterization by DSC and SEM analysis confirmed the successful production of epoxy nanofibers The obtained fibers exhibited uniformity, lacked defects, and withstood chloroform washing to remove the PLA shell. Bilayer membranes were effectively created by depositing electrospun epoxy nanofibers onto non-woven cellulose acetate (CeA) fabric, resulting in two-component filters with adjustable porosity suitable for applications in fluid filtration.

In order to improve the mechanical properties of the resin in terms of glass transition temperature, isophorone diamine (IPD), a cycloaliphatic amine, was chosen as the cross-linking agent. It exhibits enhanced weathering, chemical and UV resistance, low viscosity at room temperature and does not require the use of catalysts.

Therefore, sustainable epoxy resins were developed by crosslinking BOMF with isophorone diamine (IPD) at varying molar ratios. Thermal and mechanical properties of the resins were characterized, revealing T_g values between 50 and 70 °C through DSC analysis. Tensile tests indicated elastic moduli of approximately 1 GPa and strain at break values up to 8%. To introduce electrical functionality, controlled amounts of CNTs were incorporated as fillers, resulting in nanocomposites with electrical conductivity around 10^{-6} S/m, exhibiting Joule heating behavior.

Leveraging their ductility, the functional CNT/epoxy nanocomposites were employed to impregnate natural cotton fabric, aiming to create thermo-responsive wearable textiles. Breathability tests demonstrated that the CNT/resin coating maintain fabric breathability, comparable to pure cotton. Wettability tests revealed an increased hydrophobicity without compromising flexibility. Subsequently, the thermoelectrical functionality of the textiles was extensively assessed through Joule heating tests. The achieved temperatures under a 20V voltage (around 34 °C) and the robust, reproducible behavior in cyclic heating tests highlighted the potential for application in wearable heating textiles and biomedical devices